

ENCLOSURE 2

MFN 09-637

Marathon-5S Control Rod Assembly, NEDO-33284-A Revision 2,
October 2009

Non-Proprietary Information

IMPORTANT NOTICE

Enclosure 2 is a non-proprietary version of the Marathon-5S Control Rod Assembly, NEDE-33284P-A Revision 2, October 2009 from Enclosure 1, which has the proprietary information removed. Portions that have been removed are indicated by open and closed double brackets as shown here [[]].



HITACHI

GE Hitachi Nuclear Energy

NEDO-33284-A

Revision 2

Class I

DRFSection 0000-0056-6788 R2

October 2009

Non-Proprietary Information

Licensing Topical Report

MARATHON-5S CONTROL ROD ASSEMBLY

Copyright 2009 GE-Hitachi Nuclear Energy Americas LLC

All Rights Reserved

INFORMATION NOTICE

This is a non-proprietary version of the document NEDE-33284P-A, Revision 2, which has the proprietary information removed. Portions of the document that have been removed are indicated by an open and closed bracket as shown here [[]].

The non-proprietary version of the NRC's SE, which is enclosed in NEDO-33284-A, Revision 2, has the proprietary information removed. Portions of the document that have been removed are indicated by an open and closed bracket as shown here [].

IMPORTANT NOTICE REGARDING THE CONTENTS OF THIS REPORT

Please Read Carefully

The information contained in this document is furnished **for the purpose of obtaining NRC approval for the use of the Marathon-5S control rod in Boiling Water Reactors**. The only undertakings of GE Hitachi Nuclear Energy respecting information in this document are contained in the contracts between GE Hitachi Nuclear Energy and the participating utilities in effect at the time this report is issued, and nothing contained in this document shall be construed as changing those contracts. The use of information by anyone other than that for which it is intended is not authorized; and with respect to **any unauthorized use**, GE Hitachi Nuclear Energy makes no representation or warranty, and assumes no liability as to the completeness, accuracy, or usefulness of the information contained in this document.

NEDO-33284-A Revision 2
Non-Proprietary Information

June 29, 2009

Mr. Jerald G. Head
Senior Vice President, Regulatory Affairs
GE-Hitachi Nuclear Energy Americas LLC
P. O. Box 780, M/C A-18
Wilmington, NC 28401

SUBJECT: FINAL SAFETY EVALUATION FOR GE HITACHI NUCLEAR ENERGY AMERICAS, LLC, LICENSING TOPICAL REPORT NEDE-33284P, REVISION 1, "MARATHON-5S CONTROL ROD ASSEMBLY" (TAC NO. MD8758)

Dear Mr. Head:

By letter dated November 19, 2007, GE Hitachi Nuclear Energy Americas, LLC (GEH) submitted Licensing Topical Report (LTR) NEDE-33284P, Revision 1, "Marathon-5S Control Rod Assembly" to the U.S. Nuclear Regulatory Commission (NRC) staff. By letter dated May 11, 2009, an NRC draft safety evaluation (SE) regarding our approval of NEDE-33284P, Revision 1 was provided for your review and comment. By letter dated June 11, 2009, GEH commented on the draft SE. The NRC staff's disposition of GEH's comments on the draft SE are discussed in the attachment to the final SE enclosed with this letter.

The NRC staff has found that NEDE-33284P, Revision 1 is acceptable for referencing in licensing applications for GE-designed boiling water reactors to the extent specified and under the limitations delineated in the LTR and in the enclosed final SE. The final SE defines the basis for our acceptance of the LTR.

Our acceptance applies only to material provided in the subject LTR. We do not intend to repeat our review of the acceptable material described in the LTR. When the LTR appears as a reference in license applications, our review will ensure that the material presented applies to the specific plant involved. License amendment requests that deviate from this LTR will be subject to a plant-specific review in accordance with applicable review standards.

In accordance with the guidance provided on the NRC website, we request that GEH publish accepted proprietary and non-proprietary versions of this LTR within three months of receipt of this letter. The accepted versions shall incorporate this letter and the enclosed final SE after the title page. Also, they must contain historical review information, including NRC requests for additional information and your responses. The accepted versions shall include an "-A" (designating accepted) following the LTR identification symbol.

NEDO-33284-A Revision 2
Non-Proprietary Information

J. Head

- 2 -

If future changes to the NRC's regulatory requirements affect the acceptability of this LTR, GEH and/or licensees referencing it will be expected to revise the LTR appropriately, or justify its continued applicability for subsequent referencing.

Sincerely,

/RA/

Thomas B. Blount, Deputy Director
Division of Policy and Rulemaking
Office of Nuclear Reactor Regulation

Project No. 710

Enclosures:

1. Non-Proprietary Version of Final SE
2. Proprietary Version of Final SE

cc w/encl 1 only: See next page

NEDO-33284-A Revision 2
Non-Proprietary Information

J. Head

- 2 -

If future changes to the NRC's regulatory requirements affect the acceptability of this LTR, GEH and/or licensees referencing it will be expected to revise the LTR appropriately, or justify its continued applicability for subsequent referencing.

Sincerely,

/RA/

Thomas B. Blount, Deputy Director
Division of Policy and Rulemaking
Office of Nuclear Reactor Regulation

Project No. 710

Enclosures:

1. Non-Proprietary Version of Final SE
2. Proprietary Version of Final SE

cc w/encl 1 only: See next page

DISLTRIBUTION:

PUBLIC

PSPB Reading File

RidsNrrDpr

RidsNrrDprPspb

RidsNrrPMMHoncharik

RidsNrrLADBaxley

RidsOgcMailCenter

RidsAcrsAcnwMailCenter

RidsNrrDss

RidsNrrDssSnpb

Joe Donoghue (NRO)

Chris Van Wert (NRO)

Paul Clifford

SRosenberg (Hardcopy)

ADAMS ACCESSION NOs.:

Package: ML091680760

Cover letter: ML091680386

Non-Prop Final SE: ML091750842

Prop Final SE: ML091680377

NRR-043

| OFFICE | PSPB/PM | PSPB/LA | SNPB/BC | NRO/BC | PSPB/BC | DPR/DD |
|--------|------------|------------------------------|-------------------------|--|------------|---------|
| NAME | MHoncharik | DBaxley (GLappert for) | AMendiola Via e-mail | JDonoghue GThomas via e-mail for | SRosenberg | TBlount |
| DATE | 6/24/09 | 6/25/09 | 6/24/09 | 6/24/09 | 6/29/09 | 6/29/09 |

OFFICIAL RECORD COPY

FINAL SAFETY EVALUATION BY THE OFFICE OF NUCLEAR REACTOR REGULATION

NEDE-33284P, REVISION 1, "MARATHON-5S CONTROL ROD ASSEMBLY"

GE HITACHI NUCLEAR ENERGY AMERICAS, LLC

1.0 INTRODUCTION

By letter dated November 19, 2007 (Reference 1), GE Hitachi Nuclear Energy Americas, LLC (GEH) requested review and approval of NEDE-33284P, Revision 1, entitled, "Marathon-5S Control Rod Assembly." This licensing topical report (LTR) provides design specifications along with mechanical lifetime and nuclear lifetime calculations for the new Marathon-5S control blade (also referred to as "control rod" or "control rod blade"). Revision 1 of NEDE-33284P supersedes NEDE-33284P, Revision 0 (which did not receive U.S. Nuclear Regulatory Commission (NRC) approval).

2.0 REGULATORY EVALUATION

Regulatory guidance for the review of fuel rod cladding materials and fuel system designs and adherence to Title 10 of the *Code of Federal Regulations* (10 CFR) Part 50, Appendix A, General Design Criteria (GDC) for Nuclear Power Plants, GDC-10 "Reactor Design," GDC-27 "Combined Reactivity Control Systems Capability," and GDC-35 "Emergency Core Cooling" is provided in NUREG-0800, "Standard Review Plan [(SRP)] for the Review of Safety Analysis Reports for Nuclear Power Plants," Section 4.2, "Fuel System Design" (Reference 2). In accordance with SRP, Section 4.2, the objectives of the fuel system safety review are to provide assurance that:

- The fuel system is not damaged as a result of normal operation and anticipated operational occurrences,
- Fuel system damage is never so severe as to prevent control rod insertion when it is required,
- The number of fuel rod failures is not underestimated for postulated accidents, and
- Coolability is always maintained.

NEDE-33284P, Revision 1 provides nuclear and mechanical design calculations for the Marathon-5S control blade design. The NRC staff's review of this LTR is to ensure that the Marathon-5S design adequately addresses the regulatory requirements identified in SRP, Section 4.2.

The Marathon-5S control blade design is a derivative of the Marathon design approved in Reference 3. The primary difference between the two control blade designs is the absorber tube geometry. Both designs employ the same materials, including GEH proprietary 304S stainless steel. Section 2 of NEDE-33284P, Revision 1 details the Marathon-5S design specifications and identifies deviations from the original Marathon design. The Marathon-5S design has been evaluated to ensure compliance with the same licensing criteria as the original Marathon design.

As such, the NRC staff's review of the Marathon-5S design will follow the same logic as Reference 3.

3.0 TECHNICAL EVALUATION

The NRC staff's review of NEDE-33284P, Revision 1 is summarized below:

- Verify that the control blade design criteria are consistent with regulatory criteria identified in SRP, Section 4.2.
- Verify that the control blade design criteria are consistent with past reviews (e.g., Marathon, Reference 3).
- Verify that the mechanical design methodology is capable of accurately or conservatively evaluating each component with respect to its applicable design criteria.
- Verify that the nuclear design methodology is capable of accurately or conservatively evaluating boron depletion and blade worth.
- Verify that the Marathon-5S control blade design satisfies regulatory requirements.
- Verify that GEH's experience database supports the mechanical lifetime and nuclear lifetime being requested. If necessary, implement a surveillance program to monitor in-reactor behavior and confirm design calculations.

In addition to reviewing the material presented in NEDE-33284P, Revision 1 and responses to the NRC staff's requests for additional information (RAIs), the NRC staff conducted two separate audits at the GE-Wilmington offices. The scope of these audits is documented in the NRC staff's audit reports (References 4 and 5). Pacific Northwest National Laboratory (PNNL) assisted the NRC staff in the review of the Marathon-5S control blade component structural evaluations and participated in these audits. PNNL's review of the Marathon-5S structural design analyses, documented in the attachment to this safety evaluation (SE), builds off a parallel review of the Finite Element Analysis (FEA) models and methods for the Economic Simplified Boiling Water Reactor (ESBWR) control blade design.

3.1 Marathon-5S Mechanical Design Evaluation

3.1.1 Design Specifications

Section 2 of NEDE-33284P, Revision 1 details the Marathon-5S design specifications and identifies deviations from the original Marathon design. Table 2-1 of NEDE-33284P, Revision 1 provides direct comparisons between the design specifications of the two control blade designs for the different boiling water reactor (BWR) lattice configurations (e.g., C, D, and S lattice).

The NRC staff understands the need for manufacturing flexibility, especially for shop maintenance and improvements. However, changes in design specifications or materials and processing specifications (e.g., alloying elements and thermal processing) may alter the basis for the NRC staff's approval of the Marathon-5S design. As such, changes to the Marathon-5S control blade component design or materials are prohibited. The NRC staff's SE includes a limitation defining the regulatory definition of Marathon-5S as the detailed description, without deviation, provided in Section 2 of NEDE-33284P, Revision 1.

A good example of design flexibility that directly impacts the NRC staff's approval is provided in Section 10 of NEDE-33284P, Revision 1. The hafnium option would allow the introduction of hafnium absorber material within high absorption rate absorber tubes. This optional design feature directly impacts the nuclear lifetime calculations presented in Section 4 of NEDE-33284P, Revision 1 (and potentially the mechanical design analysis). In addition, independent NRC staff calculations did not model the presence of hafnium. As such, the NRC staff's SE included a limitation defining the regulatory definition of Marathon-5S without the hafnium option.

3.1.2 Operating Experience

The Marathon-5S control blade design is similar to the previously approved Marathon design. As part of its approval of the original Marathon design (Reference 3), the NRC staff imposed a surveillance program for GEH to monitor and confirm the control blade performance. Enclosures 2 and 3 of Reference 3 provide details of the Marathon surveillance program. The surveillance program includes the following action statement:

“Should evidence of a problem with the material integrity arise; (1) arrangements will be made to inspect additional Marathon control rods to the extent necessary to identify the root cause and (2) if appropriate, GE shall recommend a revised lifetime limit to the NRC based on the inspections and other applicable information available.”

One weakness in the Marathon surveillance plan was the lack of required periodic reporting to the NRC. This is evident from the first Marathon surveillance program status report transmitted to the NRC, dated February 2007 (Reference 6). During the 15 years between its approval and introduction and the first status report, the Marathon control blade had experienced in-reactor material degradation, specifically, cracking in the control blade handles and absorber tubes.

A second surveillance program status report was received in April 2008 (Reference 7). Both of the status reports described Marathon-5S design features introduced to prevent reoccurrence of the cracking observed in the Marathon design. These design features, as well as the need for a more rigorous surveillance program, will be addressed in the following sections.

3.1.3 Mechanical Design Evaluation

The same licensing criteria used to judge the acceptability of the previous Marathon control blade design (Reference 3) were used for the Marathon-5S design. Specifically,

- 1) The control rod stresses, strains, and cumulative fatigue shall be evaluated to not exceed the ultimate stress or strain of the material.
- 2) The control rod shall be evaluated to be capable of insertion into the core during all modes of plant operation within the limits assumed in the plant analyses.
- 3) The material of the control rod shall be shown to be compatible with the reactor environment.
- 4) The reactivity worth of the control rod shall be included in the plant core analyses.

- 5) Prior to the use of new design features on a production basis, lead surveillance control rods may be used.

As stated in Reference 3, these five general criteria were identified by GEH as the basis used to demonstrate that the Marathon (and now the Marathon-5S) control blade design will operate in a satisfactory manner. The NRC staff agrees with these criteria as being consistent with SRP, Section 4.2 (Reference 2). The first three licensing criteria will be discussed in this section. Section 3.2 addresses the fourth licensing criterion, reactivity worth. Section 3.3 addresses the fifth licensing criterion, which was modified to require a surveillance program for the Marathon-5S design (similar to the approach for Marathon). Also note that Section 3.1.1 limits the introduction of new design features, which curtails the application of licensing criterion number five.

3.1.3.1 Stress, Strain, and Fatigue

Failure or deformation of control blade components may challenge control blade insertion or may result in a loss of reactivity worth (i.e., leaching of B_4C). GEH's licensing criterion is that stresses, strains, and cumulative fatigue shall not exceed the ultimate stress or strain of the material due to normal, abnormal, emergency, and faulted loads. The integrity of the welds under these loading conditions is also part of this criterion. This criterion is consistent with SRP, Section 4.2 and, therefore, is acceptable.

Section 3 of NEDE-33284P, Revision 1 details the structural evaluation for the Marathon-5S control blade components under various loading conditions. Following the same methodology as Reference 3, effective stresses and strains were determined using the distortion energy theory (Von Mises). As discussed in Section 3.1.2 of NEDE-33284P, Revision 1, the structural calculations employ minimal strength properties (unirradiated) and minimal strain properties (irradiated). This approach is consistent with past evaluations (e.g., Reference 3) and conservatively reflects the most limiting time-in-life. Further conservatism is included in the evaluation by limiting stresses to one-half of the ultimate tensile value (see Table 3-2 of NEDE-33284P, Revision 1).

Field inspections of the existing Marathon control blades revealed cracking in the handles near the roller pins. The root cause was determined to be irradiation-assisted stress corrosion cracking (SCC) prompted by chemical remnants (from the manufacturing process) within the roller pin holes. Note that due to its design and geometry, the NRC staff believes that stagnant flow conditions existed in the pin holes. This stagnant condition allowed for the chemical interaction (along with mechanical loading) needed to produce SCC. The Marathon-5S design eliminates the handle roller pins. Figures 2-6 and 2-7 of NEDE-33284P, Revision 1 illustrate the spacer pad and plain extended handle design for the Marathon-5S control blade.

Absorber tube failure due to B_4C swelling and SCC along grain boundaries are the limiting mechanisms for establishing control blade mechanical lifetime. As described in the NRC staff's review of the Marathon design (Section 3.2 of Reference 3), earlier absorber tube failures due to SCC were not due to absorber tube stresses exceeding the ultimate tensile strength (UTS) of the tubing material, but instead due to a decrease in strain capability. The Marathon-5S design, like the Marathon design, employs a high purity 304 stainless steel which has been shown to be less susceptible to SCC. However, absorber tube cracks observed as part of the Marathon surveillance program (References 6 and 7) raise concerns regarding the estimated mechanical lifetime. Specifically, observed cracking may be the result of either (1) under prediction of

swelling in B₄C with irradiation or (2) over prediction of strain capability in absorber tube material with irradiation. The Marathon-5S absorber tube design addresses both of these concerns.

Section 3.6 of NEDE-33284P, Revision 1 details the Marathon-5S absorber tube mechanical design analysis. The Marathon-5S absorber tube design, like the Marathon design, contains boron carbide powder within capsules. Some tubes contain empty capsules to accommodate helium released via the ¹⁰B neutron absorption. Figure 2-4 of NEDE-33284P, Revision 1 provides illustrations of the absorber tube configurations.

Relative to the current Marathon design, the Marathon-5S absorber tube and capsule combination have significantly improved design safety margin. Figure 2-2 of NEDE-33284P, Revision 1 provides an illustration comparing the absorber tube geometry for the two designs. Examination of this figure reveals that the Marathon-5S absorber tube has an increased wall thickness and better geometry for improved strength. In addition, the B₄C capsule-to-absorber tube gap has been increased. Table 3.1.3-1 provides a comparison of the two designs. This table reveals a significant increase in minimal initial gap size for the Marathon-5S design. As a result, [

].

Table 3.1.3-1: Comparison of Absorber Tube and Capsule Dimensions*

| Control Blade Design | Minimum Initial Diametral Capsule-to-Tube Gap (inches) | Local B ₄ C Depletion at Capsule-to-Tube Contact (nominal parameters) |
|---------------------------|--|--|
| Marathon – D/S Lattice | [| |
| Marathon – C Lattice | | |
| Marathon-5S – D/S Lattice | | |
| Marathon-5S – C Lattice | |] |

* Values from Reference 6.

The calculations provided in Table 3.1.3-1, as well as the original Marathon LTR (Reference 3), were based upon the mean of the irradiated B₄C swelling data ([] diametral swelling at 100% local depletion, Table 3-17 of NEDE-33284P, Revision 1). The Marathon-5S design analysis is based upon a +3σ upper bound of the irradiated B₄C swelling data ([] diametral swelling at 100% local depletion) along with worst-case manufacturing tolerances. The Marathon-5S design analysis demonstrates that [

].

Therefore, there is no strain placed on the absorber tube due to B₄C swelling. The Marathon-5S capsule-to-tube design clearance is sufficient to accommodate B₄C swelling, eliminating this potentially limiting strain component.

Using a +3σ upper bound resolves NRC staff concerns related to under predicting B₄C swelling with irradiation. Demonstrating that [] resolves NRC staff concerns related to over predicting the strain capability in absorber tube material with irradiation.

In the absence of B₄C swelling strain, the limiting mechanical lifetime mechanism for the Marathon-5S design is the pressurization of the absorber tubes due to the release of helium gas from the absorption of neutrons by the B₄C powder. Section 3.6.4 of NEDE-33284P, Revision 1 details this design analysis for the Marathon-5S design. FEAs were performed using the ANSYS code, along with worst-case dimensions, maximum expected corrosion and wear, and largest allowable surface defect, to calculate absorber tube pressurization capability. Stress components at the point of maximum stress intensity were analyzed and found to be within the allowable stress value for the 304S tubing. As mentioned above, unirradiated strength properties were employed to bound all times in life. Further conservatism exists in the use of one-half the UTS.

To confirm the finite element results, GEH performed burst pressure tests on multiple tubes welded together (see Figures 3-12 and 3-13 of NEDE-33284P, Revision 1). The results of the burst testing are tabulated with the FEA calculations in Table 3-23 of NEDE-33284P, Revision 1. Examination of this table reveals that the absorber tube burst pressure is significantly higher than the FEA design calculation (worst-case dimensions and surface defects) and slightly higher than the nominal FEA prediction. These tests confirm the accuracy of the FEA calculations.

Section 4.6 of NEDE-33284P, Revision 1 details the control blade mechanical lifetime calculations. The absorber tube mechanical limit is calculated as a function of ¹⁰B depletion for the C, D, and S lattice configurations based upon peak heat generation, temperature, and helium release fractions, using the FEA maximum allowable internal pressure (discussed above). As seen in Tables 4-9 through 4-11 of NEDE-33284P, Revision 1, the allowable ¹⁰B depletion (corresponding to internal pressurization limit) is significantly influenced by the absorber tube configuration (i.e., number of empty plenums) and assumed helium release fraction. Section 3.6.3 of NEDE-33284P, Revision 1 states that "helium release fractions are based on models developed using data from multiple sources." The estimated helium release fractions are listed in Table 3-13 of NEDE-33284P, Revision 1. The NRC staff had concerns with the lack of documentation supporting the helium release model (especially since these release fractions deviated from the original Marathon LTR, Reference 3). In an RAI response (Reference 8), GEH provided a detailed description for the helium release model, the supporting empirical database, and a list of conservative aspects of the methods. Based upon the information provided in Reference 8, the NRC staff finds the helium release fractions employed in the Marathon-5S tube pressurization analysis acceptable.

As shown in Table 4-4 of NEDE-33284P, Revision 1, the end of life ¹⁰B depletion calculations demonstrate that the Marathon-5S design is nuclear lifetime limited for all lattice configurations. In other words, ¹⁰B depletion leads to a loss of 10% cold worth prior to associated helium release yielding internal pressure beyond the allowable limit.

The design criterion to maintain structural integrity during normal, abnormal, emergency, and faulted loads applies to the hundreds of linear feet of welded connections in a single Marathon-5S control blade. The objective of Revision 1 to NEDE-33284P was to incorporate RAI responses. Some of the RAI responses related to weld integrity are not captured in Revision 1. For example, in response to RAI #10 in Reference 1 regarding weld properties, GEH stated that mechanical tests confirmed that the mechanical properties of the weld were higher than the minimum properties of the base metal. As illustrated in the figure on Page 28 of Enclosure 4 to Reference 1 tensile tests confirm that the absorber tube failed prior to the laser weld.

Section 3.8 of NEDE-33284P, Revision 1 details the load combinations and fatigue analyses. PNNL assisted the NRC staff in reviewing the component structural evaluations and FEA models and methods and participated in two audits conducted at the GE-Wilmington offices (References 4 and 5). The attachment to this SE documents PNNL's review of the Marathon-5S control blade design thermal, component and combined loads, and fatigue analyses. PNNL's review of Marathon-5S builds off of the ESBWR control blade review. The NRC staff has reviewed and accepts PNNL's evaluation of the Marathon-5S structural analyses. Based upon the material presented in NEDE-33284P, Revision 1 and PNNL's review, the NRC staff finds the load combinations and fatigue analyses acceptable.

Based upon the information provided above, the NRC staff finds the Marathon-5S mechanical design analyses acceptable.

3.1.3.2 Control Blade Insertion

Failure or deformation of control blade components may challenge control blade insertion. GEH's licensing criterion is that the control blade shall be evaluated to be capable of insertion into the core during all modes of plant operation within the limits assumed in the plant analyses. This criterion is consistent with SRP, Section 4.2 and, therefore, is acceptable.

As illustrated in Figure 2-2 of NEDE-33284P, Revision 1, the thickness of the Marathon-5S wing (i.e., absorber tube cross section) is identical to the current Marathon design. Other envelope dimensions, including those for control blades with plain handles or with spacer pads, are also identical. Therefore, the fit and clearance of the Marathon-5S control blade in the fuel cell is identical to the Marathon control blade, which has many reactor-years of operating experience.

As discussed in Section 3.1.3.1 above, mechanical design analyses demonstrate that the Marathon-5S design is capable of withstanding all normal, abnormal, emergency, and faulted loads without permanent deformation or failure, hence, maintaining the capability of insertion.

Section 3.4 of NEDE-33284P, Revision 1 addresses control blade insertion with respect to seismic conditions and fuel channel bow induced bending. Section 3.4.4 of NEDE-33284P, Revision 1 describes seismic scram testing performed on the Marathon-5S design. The test facility consisted of a simulated pressure vessel and reactor internals, and a control rod drive. Prototype Marathon-5S control blades were installed and the control rod drive was set to simulate D, C, and S lattice operation. GEH's criteria for the seismic testing is (1) control blade insertion within scram time requirements at Operational Basis Earthquake conditions and (2) control blade insertion at Safe Shutdown Earthquake conditions. These criteria satisfy SRP requirements and, therefore, are acceptable. Testing demonstrated that the seismic scram criteria were satisfied for all lattice types.

Based upon results of the engineering calculations and seismic scram testing presented in NEDE-33284P, Revision 1, the NRC staff finds that the Marathon-5S control blade design satisfies the control blade insertion licensing criterion.

3.1.3.3 Control Blade Material

GEH's licensing criterion is that the material of the control blade shall be shown to be compatible with the reactor environment. This criterion is consistent with SRP, Section 4.2 and, therefore, is acceptable.

The Marathon-5S control blade uses the same materials as the current Marathon design. No new material has been introduced. The absorber tubes, while differing in geometry, are made of the same high purity stabilized type 304 stainless steel. One of the top challenges facing operating BWRs is shadow corrosion induced channel bow and resulting control blade interference. Deep control blade insertion programs are sometimes used to hold down excess reactivity in order to achieve longer operating cycles. Extended duration of the type 304 stainless steel blades in close proximity to the zircaloy channel boxes results in shadow corrosion. The industry has developed fuel management programs coupled with augmented surveillance programs to aid in managing channel bow. Changes in channel design and materials are also being introduced to limit control blade interference. At this time, there does not appear to be an easy fix to this phenomenon other than channel replacement; however, there is no evidence that any features of the Marathon-5S design will exacerbate the problem.

Based upon in-reactor service of these materials, the NRC staff finds that the Marathon-5S design has satisfied this licensing criterion.

3.2 Marathon-5S Nuclear Design Evaluation

3.2.1 Design Specifications

Section 4 of Reference 1 details the Marathon-5S nuclear evaluation design criteria and depletion methodology. It is stated in Section 4.1 that “a control rod’s nuclear worth characteristics shall be compatible with reactor operation requirements.” Using precedence from the approved Marathon control blade design (Reference 3), GEH meets these compatibility limits by demonstrating that the initial hot and cold control blade reactivity worths are within $\pm 5\%$ $\Delta k/k$ (defined by $1 - k_{con}/k_{unc}$) of the original equipment design worth.

GEH defines the control blade nuclear lifetime as “the quarter-segment depletion at which the control rod cold worth ($\Delta k/k$) is 10% less than its zero-depletion cold worth.” (Reference 1, Section 4.1) As discussed previously, a new design may have an initial cold worth that differs by up to $\pm 5\%$ of the initial cold worth of the original equipment control blade. The end of nuclear lifetime for the new control blade design is defined as the quarter-segment depletion at which the cold worth is the same as the end of nuclear lifetime cold worth of the original equipment control blade that it is replacing. The NRC staff agrees with this approach with the understanding that a new design is always compared with the original equipment nuclear design (e.g., Duralife) and not the control blade design that is being replaced if multiple control blade design replacements have occurred over the plant’s lifetime, as stated in Reference 1.

During this review, the NRC staff questioned the basis of the nuclear lifetime criterion (i.e., 10% reduction in $\frac{1}{4}$ segment cold worth) and to what extent the ^{10}B depletion should be specifically accounted for in shutdown margin calculations and plant safety analyses. In response (Reference 9), GEH provided the historical basis of the nuclear lifetime criterion. Based on the information presented in Reference 9, the NRC staff finds the nuclear lifetime criterion acceptable.

3.2.2 Nuclear Design Evaluation

3.2.2.1 Methodology

The nuclear lifetime for a particular control blade is calculated by the use of a two-dimensional Monte Carlo analysis applied in a step-wise fashion in order to account for ^{10}B depletion over

time. For each time step, the poison reaction rates are assumed to be constant and the poison inventories are calculated in each discrete area of the blade. The poison number densities are then updated by averaging on a cell by cell basis and the process is repeated until the reduction in cold worth reaches the end-of-nuclear-life criterion.

This process was used and approved previously for the Marathon control blade design (Reference 3). For the Marathon-5S nuclear design evaluations, GEH has replaced the Monte Carlo code, MERIT, used in Reference 3, with a GEH controlled version of MCNP4A. The NRC staff approves this change in methodology.

When using an MCNP-based approach to calculating ^{10}B depletion, NRC staff is concerned about system geometry definitions for the poison region. In order to preclude the appearance of ^{10}B drifting during the averaging of number densities in each region for each time step, the region thicknesses should be on the order of one neutron mean free path. ^{10}B drift was accounted for in Reference 1 by dividing the B_4C column into four equal-area rings, resulting in ring thicknesses that are approximately 1 neutron mean free path or less. The NRC staff finds that by dividing up the B_4C column in this fashion, the averaging of the poison number densities over the cell at each time step is a reasonable approximation.

3.2.2.2 Nuclear Lifetime and Initial Control Blade Worth

NRC staff reviewed the Marathon-5S control blade nuclear lifetime and initial blade worth results for the D, C, and S lattices as calculated by the methodology described in Section 3.2.2.1 of this SE. During audits held at the GE-Wilmington offices (References 4 and 5), NRC staff reviewed sample MCNP decks used in calculating the control blade reactivity worth. The NRC staff determined that the methodology described in Sections 4.1 and 4.2 of Reference 1 (and outlined in Section 3.2.2.1 of this SE) was correctly implemented. Specifically, the NRC staff inspected the MCNP input decks to ensure that (1) the B_4C regions were modeled to handle " ^{10}B drift," (2) material densities were correctly calculated, and (3) the overall geometry matched what was presented in NEDE-33284P, Revision 1.

3.2.2.3 Heat Generation Rates

One major concern when calculating the control blade mechanical lifetime is the calculation of the internal pressure resulting from the release of helium generated after a ^{10}B atom captures a neutron. Helium release is directly impacted by temperature, and therefore the heating rate is critical when calculating mechanical lifetime.

GEH calculates the heat generated by the neutron-control blade interaction as solely a (n,α) interaction resulting in 2.79 MeV of energy deposition for each interaction with a neutron and a ^{10}B atom. NRC staff was concerned about a possible undercounting of the energy deposition because the carbon-neutron scattering and gamma contributions were not being considered. GEH explained that by calculating the μ value (ratio of average absorptions in the control poison to the total fissions in the adjacent bundles) and multiplying by the 2.79 MeV energy deposition, the calculational method used in Reference 1 is bounding. The explanation of this is that this method does not account for gammas that are lost from the control blade during the decay of the excited ^7Li state which results from 94% of the neutron- ^{10}B interactions. These gammas account for 0.48 MeV per interaction (17% of the total 2.79 MeV) and while some deposit their energy within the B_4C , the majority escape.

NRC staff performed a simplified calculation to determine the mean free path of a 0.48 MeV photon traveling through compacted B_4C powder (70% TD). Using a mass attenuation coefficient of $9.55\text{E-}2 \text{ cm}^2/\text{g}$ (based on Carbon, which is more limiting than Boron) and density of 1.76 g/cm^3 , the linear attenuation coefficient is 0.168 cm^{-1} , resulting in a mean free path of approximately 6 cm. Considering the capsule tube thickness of approximately 0.5 cm, the NRC staff agrees that GEH's assumptions in their simplified heating rate calculations are conservative and appropriate.

3.2.2.4 Control Blade Drop Speed

The rate of reactivity insertion during a control rod drop accident (CRDA) depends on the blade worth (which in turn depends on control blade design and poison loading, position of the dropped blade with respect to other inserted blades, fuel management, burnup, and operating conditions) and control blade drop speed (which in turn depends on weight, velocity limiter design, and operating conditions). The Marathon-5S velocity limiter design is illustrated in Figures 2-5 through 2-8 of NEDE-33284P, Revision 1. Section 5.4 of NEDE-33284P, Revision 1 addresses drop speed for the Marathon-5S design. In this section, GEH states that the Marathon-5S control blade drop speed will remain less than speeds assumed in the CRDA analyses-of-record (AOR) at 99.9% confidence. Based upon maintaining the drop speeds less than the current CRDA AORs, the NRC staff finds the Marathon-5S velocity limiter design acceptable.

3.3 Marathon-5S Surveillance Program

During NRC staff audits at GE-Wilmington (References 4 and 5), GEH and NRC staff discussed the need for a more rigorous surveillance program for Marathon-5S control blades. In light of sparse reporting on the Marathon surveillance program (see Section 3.1.2), the Marathon-5S surveillance program would include annual reporting requirements. Further, detailed visual inspections would be required to ensure that Marathon-5S design features were not susceptible to the same material degradation problems observed in the older Marathon control blade design. The surveillance program was designed to detect material degradation due to early-in-life failure mechanisms (e.g., stress corrosion cracking, welding degradation) and validate end-

of-life mechanical design lifetime predictions (e.g., absorber tube failure). In addition, surveillance is required for control blades in each lattice type and from different BWR plants. The Marathon-5S Surveillance Program requirements are detailed in Table 3.3-1.

In the development of the surveillance program and embedded example, the following inputs and assumptions were made.

- The limiting $\frac{1}{4}$ segment, nuclear depletion for Marathon-5S control blades is:
 - [
 -
 -]
- A domestic BWR utility reports that a Marathon-5S control blade in a high duty control cell may accumulate 7% to 13% $\frac{1}{4}$ segment equivalent ^{10}B depletion in one two-year cycle.

Table 3.3-1: Marathon-5S Surveillance Program

| | |
|----|---|
| 1 | A minimum of two (2) Marathon-5S control blades will be inserted in high duty locations in a D, C, or S lattice, domestic or international BWR. |
| 2 | Additional Marathon-5S control blades may be inserted in other domestic BWRs, with the intent that they remain at a lower depletion than the two lead depletion Marathon-5S control blades at the designated BWR. Should other control blades at a domestic or international BWR become the highest depletion in the BWR fleet, they will become the control blades inspected per this surveillance program. |
| 3 | The two lead depletion control blades will be irradiated, achieving as close to end of nuclear design lifetime as practical (target minimum 90% of end-of-life). |
| 4 | During refueling outages in which the depletion of the lead Marathon-5S assemblies are less than 75% of nuclear design lifetime, the two (2) highest depletion Marathon-5S control blades will be visually inspected in-core, with two diagonal fuel bundles removed. This will allow for inspection of four of eight control blade faces, one face from each wing. Alternately, the control blades may be moved and inspected in the spent fuel pool. |
| 5 | The in-core visual inspections shall have sufficient resolution, lighting, and scan rate such that crack indications similar to those observed on Marathon control blades would be seen. |
| 6 | For refueling outages in which the depletion of the lead Marathon-5S assemblies are greater than 75% of nuclear design lifetime, the two (2) highest depletion Marathon-5S control blades will be moved to the spent fuel pool, with a visual inspection of all eight faces of each control blade performed. Lead Marathon-5S control blades may exceed 75% depletion prior to the eight-face inspections planned in the spent fuel pool as long as those inspections are performed before the control blades are utilized in another fuel cycle. |
| 7 | For Marathon-5S control blades inserted in the opposite lattice type as the lead depletion units, two (2) highest depletion control blades shall be visually inspected during refueling outages in which the depletion of the control blades exceeds 75% of nuclear design lifetime. These visual inspections shall consist of an inspection of all eight faces of the control blade. For the purpose of this surveillance program, D and S lattice applications are considered equivalent, since the geometry of the absorber tube and capsule are identical. For example, if the lead depletion control blades are in a D or S lattice plant, inspections of the lead C lattice Marathon-5S control blades shall be performed during outages for which the depletion exceeds 75% of the nuclear design lifetime. Conversely, if the lead depletion Marathon-5S control blades are in a C lattice plant, additional inspections of D or S lattice Marathon-5S control blades shall be performed during outages for which the depletion exceeds 75% of the nuclear design lifetime. |
| 8 | To confirm the end-of-life performance of the Marathon-5S control blade, the first twelve (12) control blades of each lattice type (D/S lattice and C lattice) shall be visually inspected upon discharge, for a total of 24 visual inspections, not to exceed four (4) control blades from any single plant. These visual inspections shall consist of an inspection of all eight faces of each control blade. |
| 9 | Should a material integrity issue be observed, GEH will (1) arrange for additional inspections to determine a root cause and (2) if appropriate, recommend a revised lifetime limit to the NRC based on the inspections and other applicable information available. |
| 10 | GEH will report to NRC the results of all Marathon-5S visual inspections annually. |

EXAMPLE: A sample lead depletion Marathon-5S inspection program meeting these criteria is shown below. This example is for a D or C lattice application, in which the ¼ segment nuclear lifetime is 57% ¼ segment equivalent ¹⁰B depletion.

| | | | | | | |
|---------------------|---|---------|-----------------------|-----------------------|-----------------------|--|
| Nuclear Lifetime | → | 0 | 23% | 45% | 68% | 90% |
| ¼ Segment Depletion | → | 0 | 13% | 26% | 38% | 51% |
| | | | | | | |
| | | Cycle 1 | Cycle 2 | Cycle 3 | Cycle 4 | |
| | | | | | | |
| | | ↑ | ↑ | ↑ | ↑ | ↑ |
| | | Install | In-Core Inspection | In-Core Inspection | In-Core Inspection | Discharge to Fuel Pool and Inspect |

4.0 CONCLUSION

Based upon its review of NEDE-33284P, Revision 1 and the required surveillance program, the NRC staff finds the Marathon-5S control blade design acceptable for licensing applications in BWR/2-4 D lattice, BWR/4-5 C lattice, and BWR/6 S lattice power plants. Licensees referencing this LTR will need to comply with the conditions listed in Section 5 of this SE.

Section 7 of NEDE-33284P, Revision 1 details the impact of the Marathon-5S control blade design on standard plant technical specifications; concluding that there is no effect from the introduction of the Marathon-5S design. Since the details of each plant’s technical specifications may vary, each licensee must determine if the introduction of the Marathon-5S control blade design necessitates a license amendment.

5.0 LIMITATIONS AND CONDITIONS

Licensees referencing NEDE-33284P, Revision 1 must ensure compliance with the following limitations and conditions:

- 1) The Marathon-5S control blade design is restricted to the design specifications provided within Section 2 of NEDE-33284P, Revision 1. Changes in component design, materials, or processing specifications may alter the in-reactor behavior of this design and the basis of the NRC staff’s approval.
- 2) The Marathon-5S control blade design is restricted to the use of B₄C absorber material. The introduction of alternative absorber materials (e.g., hafnium) requires NRC review and approval. Further, enriched B₄C powder (i.e., artificial increase in ¹⁰B isotopic concentration) was not considered in the NRC staff’s review and therefore is not approved by this SE.
- 3) The inspection and reporting requirements in the Marathon-5S Surveillance Program, detailed in Table 3.3-1 must be fulfilled.

6.0 REFERENCES

1. Letter from GEH to USNRC, MFN 07-619, "GE Hitachi Nuclear Energy Licensing Topical Report, NEDE-33284P, Revision 1, 'Marathon-5S Control Rod Assembly,' November 2007 (TAC No. MD3119)," dated November 19, 2007. (ADAMS Accession No. ML073320285)
2. NUREG-0800, "Standard Review Plan for the Review of Safety Analysis Reports for Nuclear Power Plants," Section 4.2, "Fuel System Design," Revision 3, dated March 2007. (ADAMS Accession No. ML070740002)
3. Safety Evaluation by the Office of Nuclear Reactor Regulation for Topical Report NEDE-31758P, "GE Marathon Control Rod Assembly," dated July 1, 1991. (ADAMS Legacy Library Accession No. 9107090009)
4. USNRC Memorandum, "Audit Report for ESBWR GE14E Fuel Assembly Design, ESBWR Marathon Control Blade Design, and Marathon-5S Control Blade Design," dated September 11, 2007. (ADAMS Accession No. ML072550006)
5. USNRC Memorandum, "Audit Report and Summary (2007 & 2008) for Global Nuclear Fuels Control Blade and Fuel Assembly Design," dated December 22, 2008. (ADAMS Accession No. ML083230072)
6. Letter from GEH to USNRC, MFN 07-138, "Marathon Control Rod Assembly Surveillance Program Status," dated February 26, 2007. (ADAMS Accession No. ML070580456)
7. Letter from GEH to USNRC, MFN 08-355, "Marathon Control Rod Assembly Surveillance Program Update," dated April 11, 2008. (ADAMS Accession No. ML081020674)
8. Letter from GEH to USNRC, MFN 09-156, "Request for Additional Information (RAI) Response Regarding the Marathon-5S Control Rod (TAC No. MD8758)," dated March 2, 2009. (ADAMS Accession No. ML090620485)
9. Letter from GEH to USNRC, MFN 09-343, "Draft Safety Evaluation by the Office of Nuclear Reactor Regulation Licensing Topical Report (LTR) NEDE-33284, Revision 1, 'Marathon-5S Control Rod Assembly', "dated June 11, 2009. (ADAMS Accession No. ML091630582)

Attachments:

- 1) Pacific Northwest National Laboratory Audit Reports
- 2) Comment Resolution Table

Principal Contributors: P. Clifford
C. Van Wert

Date: June 29, 2009

Pacific Northwest National Laboratory

Audit Report: GEH Marathon-5S Control Blade

Nick Klymyshyn

PNNL Evaluation of GEH topical report NEDE-33284P, Revision 1 entitled "Marathon-5S Control Rod Assembly"

Introduction

The finite element analyses (FEA) of the Marathon-5S (M-5S) control blade have been reviewed by PNNL staff. This review is largely based on a comparison against the models and methodology employed by GE Hitachi (GEH) in their ESBWR control blade design, NEDE-33244P Rev 1. The ESBWR review included hands-on investigation of GEH's models and methodology, which are fundamentally the same as the M-5S.

Additional model information for this review is also gathered from MFN 08-688, "ESBWR Marathon and Marathon-5S Control Rod Finite Element Analysis Summary." This spreadsheet contains some information about the models that is not included in the LTRs, such as whether material plastic stress-strain curves were based on true stress or engineering stress. In some cases the spreadsheet notes that irradiated material properties were checked when the LTR did not mention it.

Each of the following sections will discuss the Marathon-5S FEA models. The last section is a summary and conclusion of the finite element analysis review.

Thermal Analysis

The M-5S and ESBWR thermal models and methodology are identical, and consider both nominal and worst-case dimensions. There are no problems, issues, or concerns about this model or the results.

Lifting Load

One difference between the two lifting load analyses is that the M-5S was evaluated at 2x control rod weight while the ESBWR was evaluated at 3x control rod weight. In both cases the purpose of increasing the weight load was to artificially account for dynamic load factors. GEH staff explained that the 2x load factor was sufficient for the expected lifting conditions and that 3x was excessive. Either way, scaling the M-5S results by 3/2 to approximate 3x loading still keeps the stress state below the material allowable. This scaling approach is legitimate because the load is linear and the scaled stresses remain in the linear-elastic regime for all cases. The load factor choice was the only issue of concern for this model, and since stresses remain acceptable at 2x or 3x this issue is resolved.

External Pressure + Channel Bow Lateral Load

This case was evaluated slightly differently for the M-5S and ESBWR. The M-5S model geometry consisted of a quarter of an absorber tube cross section while the ESBWR added an adjacent half of an absorber tube. With proper symmetry conditions, the two geometries provide equivalent results.

Another difference between the two evaluations is the choice of material properties. The M-5S was not specifically checked for the effect of irradiated end of life properties. Instead, the models for the D/S and C lattices were run with purely elastic material properties and then checked with plasticity enabled. This implies the reported [] and [] peak stresses were calculated using elastic materials. Since the yield strength of 304S at beginning of life conditions is [], only the D/S lattice exceeded yield, and only by a small margin. Since the irradiated yield strength at 550F is above [], the elastic analyses effectively represent irradiated analyses also.

The differences in model geometry are not a concern. The material property representation is also not a concern because the elastic analysis so closely resembles an irradiated analysis that all material behavior of interest (elastic, plastic, irradiated) is covered by the existing analyses. All issues for this model are resolved.

Internal Burst Pressure Determination

The purpose of this model is to establish a peak operating pressure for the tubes. There is considerable variation between the M-5S and ESBWR approaches. The M-5S considers surface defects, wear, and corrosion while the ESBWR does not. These features contribute to a more conservative maximum pressure determination for the M-5S. The model is loaded with increasing pressure until any point on the absorber tube reaches the ultimate true stress. Then that pressure is halved. This conservatively estimates an operation pressure, which is further tested in a pressurization test model, discussed in the next section.

Experimental burst pressure testing was also carried out to confirm the adequacy of the M-5S burst pressure finite element analyses. It was found that the actual tube burst pressure was 5% higher than the nominal geometry model and 40% higher than the worst case geometry model. The final operating pressure was based on the highly-conservative worst geometry case.

This model was satisfactorily confirmed with experimental testing. There are no remaining issues or concerns.

Pressurization Stress on Absorber Tubes

The previously discussed model was used to estimate a peak operating pressure – this model tests that pressure in an absorber tube model. The worst-case tube dimensions are used. Based on the first paragraph of 3.6.4, it is also assumed that this model accounts for surface defects, wear, and corrosion. The peak stress components are listed, and remain below the $\frac{1}{2}$ UTS design allowable.

The experimental burst testing mentioned in the previous section helps confirm the safety of this design and the adequacy of this analysis. There are no issues, problems or concerns with this

model.

External Pressure + Channel Bow Induced Bending

This case was evaluated differently for the M-5S and ESBWR. The M-5S model consisted of a cross section of a full control blade wing and part of the tie rod, loaded with external pressure and a lateral load on the outermost absorber tube. The ESBWR model consisted of a single tube and half of the tie rod. These are effectively the same because the ESBWR model adds in an artificial moment load while the M-5S model develops the moment naturally, by including the blade geometry all the way to the tie rod.

The M-5S was evaluated for unirradiated materials only, while the ESBWR was checked for irradiated materials as well. The irradiated ESBWR results turned out to be less limiting than the unirradiated case, so that was used as justification by GEH for not checking the M-5S in the irradiated condition. The M-5S is closer to the design limit in terms of stresses, but that does not necessarily mean the M-5S would be more susceptible to problems due to the loss of ductility that comes from irradiation. Instead, the natural stress concentrations found in the ESBWR due to its geometry are expected to make the reduced ductility a bigger concern for the ESBWR than for the M-5S. Given the favorable ESBWR irradiated material results, there was no reason to request an irradiated M-5S evaluation for this load case.

A final difference is that the M-5S was evaluated against engineering stress limits while the ESBWR was evaluated against true stress limits. This should only mean that the plastic stress-strain curves were defined differently in the two analyses: M-5S in terms of engineering values and ESBWR in terms of true values. As long as the plastic curves were treated correctly, there is no problem. The critical difference between engineering and true stress-stain curves is the phenomenon of necking, which happens beyond the material's ultimate tensile strength. Since this analysis remains below the UTS, this is not an issue.

While there were differences in methodology in this analysis, there is no cause for concern. The model geometry is effectively the same, when the added moment load of the ESBWR is considered. Irradiated materials were shown to make no difference from a safety standpoint for the ESBWR, and are expected to be even less important for the M-5S. The choice of using true stress or engineering stress in the model is inconsequential since the stress level remained below the UTS. All issues with this model are fully resolved.

Summary and Conclusions

The M-5S analysis methodology was very similar to the ESBWR methodology, with a few case-by-case variations. None of these variations raise any technical concerns about the accuracy or adequacy of the finite element models. Some of the variations required consideration about their possible effects, but all of those issues were resolved with the available information.

The only caveat about this review is that the M-5S models, input files, and results were not directly investigated. This opens the possibility of modeling errors that might not be apparent in the results. However, considering the design margin demonstrated by the experimental burst testing, it is not likely that any potential modeling error could be so severe as to hide a safety concern.

Pacific Northwest National Laboratory

Audit Report: GEH ESBWR Marathon Control Blade

Nick Klymyshyn

PNNL Evaluation of GE topical report NEDE-33244P, Revision 1 entitled “ESBWR Marathon Control Rod Mechanical Design Report”

1.0 Introduction

This report concludes the PNNL audit of the GE ESBWR control blade finite element analyses (FEA). The goal of this report is to document all the important issues raised and resolved during this review, in a way that also describes the process. Section 2.0 briefly describes the FEA audit history. Section 3 describes the first audit trip, with subsections devoted to the individual models (3.1.1-3.1.7), closed issues (3.2) and open technical issues (3.3). Section 4 discusses the second audit trip, and describes how the open issues were closed at the audit (4.1) and, finally, how the last two issues were closed with RAI responses (4.2). The FEA audit conclusions are presented in Section 5.

2.0 Audit History

PNNL involvement began in 2007 and started with the first version of the licensing topical report (LTR): NEDE-33244P. On the first audit trip in July/Aug of 2007, every finite element model was reviewed interactively. The models were recalculated from their input files and all results databases were available for review. This activity allowed the PNNL reviewer to investigate the results more closely and carefully than would be possible from any prepared report. During this process, certain models were found to have errors and some of the modeling assumptions were questioned. Of the seven models evaluated, two were found to be satisfactory, two had errors, one seemed to violate the Tier One design criteria, and the rest needed further evaluation due to questionable assumptions.

There were also two specific concerns about the absorber tube stainless steel material properties. First was the ductility limit of 304S at end of life properties. Documented GE calculation packages assumed a variety of plastic strain limits, from [] to []. PNNL staff participated in a conference call with GE’s materials experts, and they claimed a [] plastic strain limit was appropriate. PNNL asked for experimental data to provide a reasonable support of those claims.

The second material property issue was the accuracy of the stress-strain curves used to model the post-yield behavior of the 304S stainless steel at beginning and end of life conditions. PNNL asked for experimental test data to compare against the as-modeled curves.

In November of 2007, the LTR was fully rewritten as NEDE-33244P Revision 1. There were changes in the design that reduced the number of FEA models. For example, the design was changed such that absorber swelling would never contact the absorber tube, even under worst-case conditions, so the swelling analysis was no longer necessary. The analyses that were

conducted for the revised LTR addressed all of the PNNL concerns about worst-case assumptions.

In August of 2008, PNNL participated in a second audit trip. The revised models were reviewed and found to be satisfactory. One issue was the observation that the ESBWR evaluation methodology did not always include worst-case geometry, which was a common feature of the Marathon 5S control blade evaluation. GE was asked to perform a worst-case geometry check.

A second issue of this audit trip was the comparison of as-modeled stress-strain curves to actual test data stress-strain curves. When the curves were overlaid for the irradiated 550F case, it was apparent that the curves differed substantially past the yield point. This was not critical for the irradiated case because none of the irradiated analyses were loaded that far, but it raised concerns about the unirradiated cases. GE used the Ramberg-Osgood approximation to generate their stress-strain curves instead of using tensile test data curves. GE was asked to provide plots of their modeled curves overlaid with actual test data to demonstrate that their curves were realistic.

Two RAI's were written to capture those two remaining issues. The response to the worst-case geometry evaluation showed plenty of design margin still remained, so that issue was closed. The response to the material property curve, however, did not adequately cover the concerns of the question. In effect, they used derived data to show that their derived data was correct. A new RAI on the material curve concern was written with more explicit instructions.

GE's response to the final RAI demonstrated that the as-modeled material curves were greatly conservative compared to actual 304S test data. This did not validate GE's Ramberg-Osgood methodology, but it did relieve PNNL's concerns about material representation. With this issue resolved, the last technical concerns about the finite element analyses were laid to rest.

3.0 First Audit: Overview

In general, the finite element analyses of first LTR were found to be unsatisfactory. Some errors were found when the models were closely inspected, and some questionable conclusions were made by the applicant in their LTR. Two of the seven models needed to be fixed and three more needed additional evaluation.

The audit was conducted over three full days. During this time, the reviewers had access to GE's design calculation packages, which document all the finite element analysis assumptions and results in much more detail than was reported in the LTR. In addition, all the input files were made available for review and a workstation was provided to solve the models and interact with the full results databases.

The following sections will detail the findings of the 2007 audit. Each of the individual models will be discussed in the next section. After that, a section will describe the closed issues, technical concerns which were raised but ultimately resolved before the end of the audit. Following that will be a section of open issues, which remained open until the LTR was revised.

3.1 First Audit: Individual Models

3.1.1 Thermal Model

This analysis calculated the temperature of the absorber tube during operation and used a methodology that had been used since 1988. One interesting feature of this model is that it includes a crud layer on the outside of the absorber tube. The source of the crud material data (thermal conduction) was tracked down to a 1966 memo report that is unavailable for review. The crud layer thickness was chosen by the analyst as a “reasonable” 60 year crud buildup. Extrapolating documented data on yearly crud layer buildups estimated a crud layer thickness of [], which was considered excessive. A GE expert in crud buildup stated that a value of [] was more reasonable, and that is what was modeled. Similar models have been calculated dating back at least to 1988, when they used a limited in-house FEA code called ABSTEMP1 instead of ANSYS. Based on all this history, the crud modeling methodology seems reasonable, even though some of the specific parameters of the model were not verifiable.

The only concern about this model was the possibility that the temperature did not match between the mechanical and nuclear LTRs. GE was tasked with comparing the temperatures between the two documents and ensuring they were consistent.

3.1.2 Lifting Load

This model tests the strength of the handle against the expected handling loads. The model has an appropriate mesh, with a fine mesh in high stress regions and coarse mesh in less important regions. The peak stress is well below the material yield strength. This model is a typical linear-elastic structural analysis, with no issues of concern and no action items.

3.1.3 External Pressure

This analysis considered the initial operating pressure of reactor applied to the absorber tube. The model and its evaluation had many problems and needed to be redone. The clearest flaw from a finite element analysis perspective is that the model was run with linear elastic material properties but the calculated stress exceeded the yield strength. That meant that calculated stress state in the absorber tube was incorrect.

Another problem was that the contour plot shown for this stress state in the LTR (Figure 11.2) did not actually match the model results. It appeared that Figure 11.2 matched one of the other contour plots observed in the GE calculation package for a slightly different absorber tube design, but that was not confirmed.

Another problem was their evaluation criteria. Instead of directly comparing node or element stresses from the model results to the material stress allowable they used some kind of averaging approach to determine a representative peak stress. This evaluation approach is suspicious and unjustified when compared to the more direct evaluation used in all their other analyses.

This case was also one of the ones that raised concern over tie rod effects. Most of the

absorber tube models represent one quarter of the cross section of the tube with appropriate quarter-symmetry boundary conditions applied. This model represents one tube within a line of tubes that are all subjected to the same loads and boundary conditions. However, the situation is different for the absorber tube that is welded to the central tie rod. The side that is welded to the tie rod is constrained more heavily than side that is welded to another tube. This extra constraint is expected to cause higher stresses in those absorber tubes adjacent to the tie rod than the same load would cause in all the other tubes in the control blade. The tie rod effects need to be accounted for in any worst-case determination.

To resolve these problems, GE was requested to run the model with plastic material properties and to present plots of stress and strain in the LTR. With the correct results and raw stress and strain data, the reviewers would have enough information to judge whether or not the GE special evaluation method was acceptable or not. In addition, GE was asked to evaluate the absorber tube next to the tie rod to ensure that worst-case conditions are evaluated.

3.1.4 Internal Pressurization Limit

This analysis loads their standard quarter-symmetry absorber tube model with increasing internal pressure until the model fails to converge. The final converged pressure is taken as the burst pressure, and this burst pressure is reduced by half to add a safety factor of two to the peak operating pressure. GE further reduces this peak operating pressure by [], based on experimental observations compared against FEA results of a previous absorber tube design. The reviewer considers this extra [] reduction to be unnecessary, as it was based on a different design and a different FEA model, but the extra conservatism does not hurt the tube's survival.

The two issues with this model have to do with the worst-case assumptions. As stated earlier, the absorber tube next to the tie rod is expected to have a lower burst pressure than the standard tubes because of its connection to the tie rod. The second issue is the assumption of beginning of life properties.

It is well known that end of life material strength is higher than beginning of life due to the strengthening effect of radiation exposure. Because of this fact, it is common for applicants to claim that beginning of life analyses offer the worst case scenarios and the most limiting load cases. However, along with strengthening and a slight stiffening of the elastic modulus, irradiated materials also experience reduced ductility. For example, a stainless steel with an elongation at failure of 30% might instead fail at [] to [] elongation. This loss of ductility is relevant in designs like the ESBWR absorber tube where plastic strains are predicted and there are high stress concentrations due to the geometry. Because of these risk factors, every case should be evaluated at beginning and end of life conditions.

To resolve these two concerns, GE was asked to check the burst pressure determination in the absorber tube adjacent to the tie rod and to reevaluate the analysis with irradiated material properties.

3.1.5 Swelling

This model calculates the strain in the absorber tube due to B₄C swelling. This is another case

where the stress and strain plots were not reported in the LTR. With the opportunity to view the model and its results interactively, the reviewer noted a problem in the stress results. The stresses plotted on the screen exceeded the ultimate tensile strength of the material, even though the strains were within acceptable limits.

This raised a few issues. First, if the model results were correct they violated the Tier One design criteria of ensuring no stresses beyond the ultimate tensile strength. A second possibility was that the stress-strain relationship was somehow flawed in the model – it seemed counter-intuitive that strains would be acceptable when stresses were too high. Another potential problem was that the model was loaded with many different assumptions for B₄C swelling, representing a broad spectrum of possible swelling levels. It was possible the reviewer was inspecting the wrong load case. And finally, one of the absorber tube designers expressed surprise at the audit close-out meeting that swelling was high enough to cause any stress at all. He claimed the tube was designed to ensure a clearance under all conditions. All these issues pointed to some kind of problem with the analysis.

The reviewer's best guess is that the material was loaded beyond the ultimate tensile strength and into the necking region. GE chose to only evaluate the results for strain, so it looked acceptable. Since the model was loaded by displacements it was still stable when the material passed the ultimate tensile stress. But the final solution state was at a point on the downward slope of the material curve, past the ultimate tensile stress and approaching the failure point. The model may have calculated the physically correct stress state for the given load, but that level of stress is not acceptable from a safety standpoint.

To help make sense of the model and the results, GE was asked to reevaluate the swelling model for both stress and strain, and include stress and strain contour plots in their LTR.

3.1.6 Combination Load 1

This model computed the stress state due to pressurization for use in hand calculations. An interesting result of this analysis is that the entire thickness of the absorber tube is expected to experience plastic strain. This suggests that the post-yield stress-strain relationship is an important part of the analysis. It also suggests that the loss of ductility due to irradiation could have a significant effect on the results. When material exceeds yield at a particular point, the change in local stiffness tends to redistribute the load to the neighboring material. The danger with irradiated materials is that the loss of ductility means that the material has less acceptable total strain and thus less load redistribution capacity. It is good policy to check any case with plastic strains in both the beginning and end of life conditions.

GE was asked to recalculate this model with end of life properties to ensure that all the potential worst case conditions were accounted for.

3.1.7 Combination Load 3

This is a model of the absorber tube adjacent to the solid tie rod. It includes internal pressure loading and an applied moment to represent channel bow. A hands-on review of this model revealed faulty mesh connectivity in the weld regions. This problem affects the entire stress state of the model and must be fixed and recalculated.

Without a hands-on inspection of the model, this error would have gone unnoticed. It was not established by the reviewer whether this was a simple mistake or an undocumented assumption. Either way, it is evidence that finite element analyses deserve careful scrutiny in these audits, particularly through investigation of input files and an interactive review of the models and results.

It was requested that the FEA model connectivity be fixed, the model checked with irradiated material properties, and the revised input file be provided for inspection.

3.2 First Audit: Closed Technical Issues

One of the first issues of concern was the modeled geometry of the absorber tubes. The GE models were 2D plane strain representations of the tube cross section. The concern was whether or not that kind of analysis would calculate the worst case stresses. The end caps seemed to be another potential location for high stress, but it was not evaluated in the LTR. This issue was pursued through discussions with GE staff and an investigation of past finite element analyses that did model the end caps. The final closure of this issue came from a review of burst test data that showed bursting failure occurred far away from the ends. This was further supported by the revelation that a significant amount of weld material is added in the end cap vicinity. This extra material could very reasonably counteract any stress concentrations due to the transition of geometry.

Another preliminary concern was GE's [] reduction of peak operating pressure due to experimental burst testing. The reasoning behind this artificial reduction was because an absorber tube pressurization analysis for a previous design predicted a burst pressure that was [] higher than experimental testing demonstrated. The concern of the reviewer was that this reduction factor was based on a geometrically different design – there was no guarantee that a [] reduction would be the same, or enough, in the case of the ESBWR. This issue was finally dropped by the reviewer because the [] reduction was not a critical safety issue. Their method was to calculate a burst pressure, reduce that pressure by [], then cut it in half to arrive at a peak operating pressure. Other models evaluated the stress state at this doubly-reduced pressure, and those models were considered the ones most critical for safety.

3.3 First Audit: Open Technical Issues

The material properties of 304S stainless steel were not fully documented in the LTR and no consistent, conclusive data was provided at the audit. One specific property of interest was the failure strain at end of life conditions. This was considered an important item to document because GE was requested to perform additional analyses at end of life conditions to ensure that they did not represent worst-case conditions.

A second important material property that needed documentation was the stress-strain behavior of 304S over the range of all analyses in the LTR. GE used the Ramberg-Osgood relationship to generate stress-strain curves from a few established material properties, such as yield strength. This method estimates the shape of a stress-strain curve, but a literature search on the topic found evidence that the standard Ramberg-Osgood relationship was not accurate beyond the yield point for stainless steels. Accurate plastic behavior is necessary for the models because most of them are loaded well past yield. A direct comparison of the as-

modeled curves and actual material data was requested.

Another issue that affected many analyses was the consideration of the central tie rod. Most models considered a single absorber tube with symmetry conditions that implied that it was surrounded on both sides by absorber tubes. This situation may be acceptable for analyzing most of the tubes in the blade, but not the one attached to the tie rod. The big difference is that the side of the tube welded to the tie rod experiences more constraint because the solid tie rod does not expand like a pressurized tube. This is expected to create more stresses in that particular tube. However, a competing factor is that pressure is also expected to be lower in that tube. It was requested that GE evaluate some of the analyses for that tube, to ensure that worst-case conditions are considered.

In a similar situation, most of the GE analyses considered only beginning of life material properties. It was claimed that this choice represented the worst case because the yield strength of end of life conditions is considerably higher. However, the geometry of the ESBWR absorber tube causes stress concentrations in certain locations and most of the analyses showed significant levels of plastic strain. Because the ductility of end-of-life materials decreases so much, there was a concern that end of life properties might turn out to be the actual worst case assumption due to localized concentrations of stress. It was requested that GE consider irradiated end of life properties for select cases to ensure all the worst-case conditions were considered.

The thermal model just needed a quick check to ensure that the temperatures were consistent between the structural and nuclear design packages. This was not expected to be a serious issue.

The external pressure model had many issues and needed to be completely redone. It had to be recalculated with plastic properties because stresses exceeded yield. The reporting and design criteria evaluation were also not acceptable because the stress plot included in the LTR was from a different analysis and the design criteria made use of an averaging scheme to report an effective peak stress instead of an actual peak stress taken directly from model results data. These problems made the analysis unacceptable. In addition, it was requested that this model be checked as the absorber tube next to the tie rod to ensure that worst case conditions were considered.

The open issues with the internal pressure limit determination model were related to assuring that the worst case conditions were considered. It was requested that end-of-life properties be considered along with tie rod effects.

The swelling analysis had a problem with the final stress state. It appeared that the stress exceeded the ultimate tensile strength, which should have been considered a design failure. However, GE was only considering the strain results. There were some potential points of confusion in the review of this analysis, so it was not clear how severe the problems with this case really were. GE was asked to re-evaluate this swelling case against both stress and strain criteria, and to present FEA contour plots for both types of results.

Combination Load One, Internal Pressure plus SCRAM, had no problems or major concerns. It was requested, though, that this case be rerun with end-of-life properties to test its worst-case-assumptions.

Combination Load Three, pressure plus bending due to channel bowing, had a mesh connectivity error. Nodes and elements at the welded interface between the tube and tie rod should have been connected, but were not. Physically, this was like modeling cracks in the welds, but this was not discussed in the LTR and GE staff could not provide an explanation during the audit. The model needed to be fixed and recalculated because it had the potential to raise stresses to an unknown level. It was also requested that end-of-life properties be checked to ensure all worst case conditions were evaluated.

3.4 First Audit: Conclusions

GE had a reasonable system in place to collect their FEA and document their analyses. For the purposes of the audit they were able to use their design calculation packages to answer many technical questions about the analyses. However, it should be noted that the LTR did not contain enough information itself to judge the accuracy or adequacy of the finite element analyses on its own.

In fact, three of the FEA problems were invisible until the models were carefully checked. In one case, the model was run with elastic material properties when it clearly exceeded the yield limit. This case was also worrisome because the stress plot that was presented in the LTR did not actually match the results. Even more, the peak stress reported for this case was not taken directly from the model results, like all the other cases in the LTR. Instead, GE used an averaging scheme to arrive at the design criteria value. All of these issues were not recognizable until the models were evaluated by hand.

In a second case, the problem with the model remained invisible because GE chose to report only strain and not stress. This might have made sense from an individual analysis point of view, but from a full design perspective this violated their Tier One design criteria.

In a third and final case, the mesh connectivity problem was not visible in the stress plot. Even a cursory inspection of the model might have missed the problem. It took a close inspection of the model in regions of secondary high stresses to determine that a problem existed.

Separate from these modeling problems is the issue of worst-case determination. GE stated in the LTR that their models evaluated worst case conditions, but they did not support that claim with solid arguments or comparative analyses. This approach invites additional questions and requests for additional analyses during the review process. The additional analyses related to tie rod effects and irradiated material properties represented a relatively small amount of extra work because they involved only minor changes to existing models.

One area where GE's readily available documentation was not sufficient was in regards to the material property data used in their analyses. Instead of referencing experimental data, GE calculation packages referenced previous calculation packages. They used consistent methods to generate their plastic material curves, but there was no indication that they checked the results of those methods against experimental data. This had the potential to invalidate most of the models if the material properties were found to be incorrect.

4.0 Second Audit: Overview

Following the first audit, the LTR was completely rewritten and some of the design features changed. Due to those changes the swelling FEA was no longer necessary. GE investigated the effect of irradiated material properties and absorber tube location to alleviate the concerns of worst case assumptions. The revised LTR was found to be satisfactory, with just two issues remaining open at the end of the two-day audit. Those were closed with additional RAIs.

The next section discusses the resolution of the open issues during the audit trip, and is followed by a section discussing the last remaining open items and how they were eventually closed through follow-up RAIs.

4.1 Second Audit: Resolution of Issues

The tie rod issue was closed by GE's calculation of burst pressure. For that model they tested additional cases to determine a worst case burst pressures. The case with the absorber tube next to the tie rod did have a slightly lower burst pressure than the nominal case, but only by about 2%. This established that, yes, the tie rod did increase peak stresses, but not significantly. The burst pressure was then based on a more conservative situation, a [] reduction in pressure based on prior burst testing.

Irradiated materials were also checked in the burst pressure scenario. Both a single tube and a tube and tie rod model were analyzed at the established conservative burst pressure. Both cases remained below their ultimate strength with a considerable safety margin. This proved that irradiated materials do not represent the worst case during internal pressurization loading. GE also tested irradiated materials in combined loading situations and confirmed that beginning-of-life conditions were the worst case.

All model-specific issues were resolved. The temperatures from the thermal model were compared to the nuclear design package and found to be consistent. The external pressure model was redone to include plastic materials and the contour plots in the LTR were confirmed to match the results. The internal pressure plus channel bow bending case was found to be correctly connected. And finally, the swelling model was dropped from the LTR because the design was changed, such that the B₄C capsule would never expand into contact with the absorber tube wall. With these changes and corrections, the models were all considered to be satisfactory, with only the material property issue remaining as a potential problem.

One of the material concerns was indirectly resolved. The ductility limit of irradiated 304S was never established with documentation, but all of the FEA results for irradiated cases predict strains well below conservative expectations. Regardless of whether the true ductility limit is [] strain, calculated strain intensities under [] are safe under all three limits.

One new issue was raised and resolved. In the previous audit trip GE explained that there were no residual stresses from laser-welding the absorber tubes because the heat involved annealed out all those stresses. However, in the revised LTR they state that some residual stresses are present, but are not of a concern because field cracking has not been observed in the weld region and radiation-induced creep works to reduce the stress. During the audit, additional calculations were presented that showed the maximum expected residual stress was negligible compared to the calculated stress states. Based on their relative magnitude, there is no reason

to include residual stress in the finite element models.

4.2 Second Audit: Final Open Issues and Their Resolution

Two issues remained at the end of the second audit trip. The first was noticed when the ESBWR methodology was compared to the M-5S methodology. For the M-5S, GE typically considered worst-case dimensions due to manufacturing tolerances. The reviewers requested similar worst-case analyses for the ESBWR. GE reported the results of these analyses in an RAI response, and each case was still properly within design limits.

The final issue was the stress-strain relationship of the 304S material used in the finite element models. During the audit it was recognized that the different finite element models used slightly different material curves. One of the irradiated 304S stress-strain curves was compared directly to irradiated 304S test data, and it was found that the modeled curve was significantly different beyond the yield point. It was suspected that the Ramberg-Osgood method was to blame, and it caused concern that the other stress-strain curves could have the same unrealistic behavior. In an RAI, GE was asked to plot actual stress-strain data on the same axes with the as-modeled material curves for all cases.

Their first response was not sufficient to dispel the material concerns. They did provide stress-strain curve comparisons for every modeled condition, but the comparison was against generic 304 stainless steel material data (not 304S) which was scaled to fit the yield strength required of the material vendor. This was not a direct comparison against real, representative material data.

In addition, GE did not plot the curves over the full range of model results, only to the onset of yield. This is not sufficient because the main concern is that the majority of models experience large plastic strains and the plastic behavior needs to be correctly modeled. This is where the Ramberg-Osgood method is suspect, because papers in the open literature indicate that stainless steel tends to depart from the standard Ramberg-Osgood relationship beyond yield.

GE was asked in a more explicit RAI to provide actual material test data for the full range of strains. GE responded with detailed plots that included true test data, FEA model curves, and material specification yield and ultimate strength requirements. The true test data was generated from testing of square absorber tubes, so this is considered highly reliable. This was a satisfactory response that covered all concerns. A couple important points need to be made about this issue.

The test data is significantly stronger than the material specification requirements. This is not uncommon since material vendors create their materials to comfortably exceed the stated requirements. In this case, the actual material used in the absorber tubes is about 15% stronger than the FEA models and the design calculations take credit for. The as-modeled plastic curves are all comfortably below the actual data curves at strains beyond the yield point.

One concern was that the Ramberg-Osgood curve would have an unrealistically high slope beyond the yield point, but a direct comparison of the actual and as-modeled curves showed that was not a problem. In addition, the overall higher strength of the actual data makes concerns over modeling the exact stress-strain behavior trivial. So for all practical purposes, the issue is closed.

However, this conclusion should not be considered an endorsement of GE's Ramberg-Osgood methodology. A real test of their methodology would be to have them generate a curve to mimic the test data. This issue was closed because the data demonstrated the concern was unjustified, not that GE's method was correct. In fact, the comparison of the irradiated plastic curve to the modeled plastic curve is evidence that the Ramberg-Osgood approach is not accurate in end-of-life conditions past the yield point.

4.3 Second Audit: Conclusion

The second audit trip closed nearly all of the open items satisfactorily. Only a couple additional analyses were requested to guarantee conservatism. In addition, the plastic material curve issue took two rounds of additional RAIs to conclude.

5.0 Final ESBWR Control Blade Finite Element Analysis Audit Conclusions

The first audit trip revealed serious flaws in the ESBWR finite element analyses. The second audit trip showed that most issues were satisfactorily resolved. After the second audit trip it took two additional rounds of RAI questions to fully resolve all technical issues.

The issues raised in this review had a few common themes. One was the assumption of worst-case conditions without a thorough check. For example, irradiated materials with reduced ductility should reasonably be considered in a design that is routinely loaded into plastic strain. Another example is the effect of the tie rod on the absorber tube expansion. A hollow, pressurized tube is obviously going to expand differently when it is surrounded by other pressurized tubes than when it is connected to solid bar or steel. It is not obvious in either case if the assumption is going to make a significant difference or not, but GE did not demonstrate much effort in investigating potential worst case scenarios. This seems to be something that must come from the reviewer's side.

Another common theme was a lack of solid documentation to support features of the analysis. For example, the 304S plasticity curves were modeled using the Ramberg-Osgood relationship, but there was no data to support the accuracy of that method. There are more conservative ways of modeling plasticity when good material data is not available. A lot of the issues involving unsupported data were not resolved directly. Like the Ramberg-Osgood issue, or the ductility limit of irradiated 304S, it just became obvious the issues were not worth worrying about from a safety standpoint for this particular case.

A final conclusion is that this audit demonstrates the need for a careful review of finite element analyses. The first audit trip revealed problems with the finite element models that would have otherwise gone unnoticed. This seemed to have an impact on safety, as the design was changed to avoid the swelling load that violated their own design criteria.

Comment Resolution Table
NEDE-33284P, Revision 1, “Marathon-5S Control Rod Assembly”

| Location | GEH Comment | NRC Resolution |
|---|--|--|
| Section 3.2.1 Last Paragraph and Section 5.0 Limitation and Conditions Number 4 | <p>Section 3.2.1 and Section 5.0 Limitation and Condition #4 specify a requirement that is inconsistent with approved nuclear methods and with the requirements specified on all previous control blades. Specifically, accounting for blade depletion directly is not a part of the nuclear analysis methodology.</p> <p>The control blade depletion limit of 10% worth reduction in any axial quarter segment is the lifetime criterion for all approved GE/GEH control blade designs. This limit can be found in the various Safety Evaluation reports for the approved Duralife and Marathon control blade designs. In the GE Marathon Control Blade Assembly Safety Evaluation report (NEDE-31758P-A) it states the control blade end of life to be, “10% reduction in cold reactivity worth in any ¼ axial segment relative to the initial undepleted state of the original equipment control rod”. This 10% worth reduction limit is also documented in Section 4.2.1.1.8 of the US Supplement to GESTAR II (NEDE-24011-P-A-16-US).</p> <p>The shutdown margin (SDM) demonstration requirement in the BWR Technical Specifications specifies that a demonstration be performed after fuel reconfiguration to assure that the core can remain subcritical by a specified amount (typically 0.38% Δk/k) with the strongest control rod withdrawn. This demonstration will include any reactivity variations associated with actual control blade inventory.</p> <p>GEH has historically imposed a 1% SDM design criteria in its design and licensing process. This additional margin accommodates a number of factors that are not explicitly modeled, including the variation in control blade depletion within the allowable 10% criterion. This design margin provides assurance that sufficient SDM is present to account for the various operational and</p> | <p>Delete Limitation and Condition #4 and replace the last paragraph of Section 3.2.1 with the following:</p> <p>During this review, the NRC staff questioned the basis of the nuclear lifetime criterion (i.e., 10% reduction in ¼ segment cold worth) and to what extent the ¹⁰B depletion should be specifically accounted for in shutdown margin calculations and plant safety analyses. In response (Reference 9), GEH provided the historical basis of the nuclear lifetime criterion. Based on the information presented in Reference 9, the NRC staff finds the nuclear lifetime criterion acceptable.</p> |

| | | |
|--|--|--|
| | <p>methodology uncertainties, and that the SDM demonstration when performed at the plant will have a high degree of certainty of success. Section 2.3 of NEDC-33173P, Revision 1 (Applicability of GE Methods to Expanded Operating Domains) provides a broader discussion of this.</p> <p>The reactivity effects of control rod depletion on core performance during one plant operating cycle are small and are accounted for by the critical eigenvalue normalization process performed for each plant operating cycle. The cold critical eigenvalue used to calculate shutdown margin in core design and licensing analyses is determined from the most recent plant cold critical data. This plant data includes the small reactivity variations due to blade burnup for the specific control blade inventory in the reactor. Any blade replacements performed during the subsequent refueling outage will invariably increase the blade worth at those locations and provide a small decrease in cold reactivity. The blade worth restrictions - to match the OEM blade worth within 5% at beginning of life and to limit blade worth reduction to less than 10% of the OEM worth – ensures that the impact on cold reactivity and shutdown margin remains small compared to design margins.</p> | |
|--|--|--|

Table Of Contents

| | |
|---|------|
| Acronyms And Abbreviations | xi |
| Executive Summary | xii |
| 1. INTRODUCTION AND BACKGROUND..... | 1-1 |
| 2. DESIGN CHANGE DESCRIPTION | 2-1 |
| 2.1 Absorber Tube Geometry | 2-1 |
| 2.2 Capsule Geometry | 2-1 |
| 2.3 Capsule Length | 2-1 |
| 2.4 FabriCast Velocity Limiter | 2-2 |
| 2.5 Plain Handle..... | 2-2 |
| 2.6 Full Length Tie Rod..... | 2-2 |
| 3. SYSTEM DESIGN..... | 3-1 |
| 3.1 Analysis Method..... | 3-1 |
| 3.1.1 Combined Loading..... | 3-1 |
| 3.1.2 Unirradiated Versus Irradiated Material Properties | 3-2 |
| 3.2 Material Property Limits | 3-2 |
| 3.2.1 Stress Criteria | 3-2 |
| 3.2.2 Absorber Tube Material Isotropy | 3-3 |
| 3.2.3 Welded Connections..... | 3-3 |
| 3.2.4 Laser Welding Process | 3-3 |
| 3.2.5 Absorber Tube Axial Shrink Due to Welding..... | 3-4 |
| 3.3 SCRAM | 3-5 |
| 3.4 Seismic and fuel channel bow induced bending..... | 3-5 |
| 3.4.1 Wing Outer Edge Bending | 3-5 |
| 3.4.2 Absorber Tube to Tie Rod Weld | 3-6 |
| 3.4.3 Absorber Tube Lateral Load..... | 3-6 |
| 3.4.4 Marathon-5S Seismic Scram Tests..... | 3-6 |
| 3.5 Stuck Rod Compression | 3-7 |
| 3.6 Absorber Burn-Up Related Loads | 3-7 |
| 3.6.1 Irradiated Boron Carbide Swelling Design Basis..... | 3-8 |
| 3.6.2 Clearance Between Capsule and Absorber Tube | 3-8 |
| 3.6.3 Thermal Analysis..... | 3-9 |
| 3.6.4 Absorber Tube Pressurization Capability..... | 3-10 |
| 3.6.5 Irradiation Assisted Stress Corrosion Cracking Resistance | 3-13 |
| 3.7 Handling Loads..... | 3-14 |
| 3.8 Load Combinations and Fatigue..... | 3-14 |

NEDO-33284-A Revision 2
Non-Proprietary Information

| | |
|---|-----|
| 4. NUCLEAR EVALUATIONS..... | 4-1 |
| 4.1 Design criteria..... | 4-1 |
| 4.2 Methodology..... | 4-1 |
| 4.3 Control Rod Nuclear Lifetime..... | 4-2 |
| 4.4 Initial Control Rod Worth..... | 4-2 |
| 4.5 Heat Generation Rates..... | 4-3 |
| 4.6 Control Rod Mechanical Lifetime..... | 4-3 |
| 4.7 Control Rod Depletion Monitoring..... | 4-4 |
| 5. OPERATIONAL EVALUATIONS..... | 5-1 |
| 5.1 Dimensional Compatibility..... | 5-1 |
| 5.2 Scram Times..... | 5-1 |
| 5.3 'No Settle' Characteristics..... | 5-1 |
| 5.4 Drop Speeds..... | 5-2 |
| 5.5 Fuel Cell Thermal Hydraulics..... | 5-2 |
| 6. LICENSING CRITERIA..... | 6-1 |
| 6.1 Stress, Strain, and Fatigue..... | 6-1 |
| 6.1.1 Criteria..... | 6-1 |
| 6.1.2 Conformance..... | 6-1 |
| 6.2 Control Rod Insertion..... | 6-1 |
| 6.2.1 Criteria..... | 6-1 |
| 6.2.2 Conformance..... | 6-1 |
| 6.3 Control Rod Material..... | 6-2 |
| 6.3.1 Criteria..... | 6-2 |
| 6.3.2 Conformance..... | 6-2 |
| 6.4 Reactivity..... | 6-2 |
| 6.4.1 Criteria..... | 6-2 |
| 6.4.2 Conformance..... | 6-2 |
| 6.5 Surveillance..... | 6-3 |
| 6.5.1 Criteria..... | 6-3 |
| 6.5.2 Conformance..... | 6-3 |
| 7. EFFECT ON STANDARD PLANT TECHNICAL SPECIFICATIONS..... | 7-1 |
| 8. PLANT OPERATIONAL CHANGES..... | 8-1 |
| 9. EFFECTS ON SAFETY ANALYSES AND DESIGN BASIS ANALYSIS MODELS .. | 9-1 |
| 9.1 Anticipated Operational Occurrences and Other Malfunctions..... | 9-1 |
| 9.2 Accidents..... | 9-1 |
| 9.3 Special Events..... | 9-2 |
| 9.4 Fission Product Barrier Design Basis Limits..... | 9-2 |
| 9.5 Safety and Design Basis Analysis Models..... | 9-2 |

NEDO-33284-A Revision 2
Non-Proprietary Information

| | |
|---|------|
| 10. HAFNIUM NEUTRON ABSORBER OPTION | 10-1 |
| 11. SUMMARY AND CONCLUSIONS | 11-1 |
| 12. REFERENCES | 12-1 |
| APPENDIX A – PLAIN HANDLE EVALUATION..... | 1 |
| A-1 Plain Handle Description..... | A-1 |
| A-1.1 Fuel Channel and CRB Dimensions..... | A-1 |
| A-1.2 Handle Vertical Position | A-2 |
| A-1.3 Effect of Channel Bulge..... | A-2 |
| A-1.4 Friction and Wear..... | A-2 |
| A-1.5 Reactor Clearances..... | A-3 |
| A-1.6 Plain Handle CRB Experience | A-3 |
| A-1.7 Conformance to Design Requirements..... | A-4 |
| A-2 Plant Operational Changes | A-5 |
| A-3 Evaluation of Potential Areas of Concern..... | A-5 |
| A-4 Effect on Generic Plant Technical Specifications..... | A-6 |
| A-5 Effect on Licensing Basis..... | A-7 |
| A-6 Effects On Safety Analyses And Design Basis Analysis Models | A-8 |
| A-7 Summary and Conclusions | A-10 |
| APPENDIX B – FAILED BUFFER SCRAM STRESS EVALUATION..... | B-1 |
| B-1 Socket Minimum Cross-Sectional Area (Fig. 3-1)..... | B-1 |
| B-2 Socket to Transition Piece Weld (Fig. 3-1)..... | B-1 |
| B-3 Velocity Limiter Transition Piece to Fin Weld (Fig. 3-1)..... | B-1 |
| B-4 Velocity Limiter Fin Minimum Cross-Sectional Area (Fig. 3-1)..... | B-1 |
| B-5 Velocity Limiter to Absorber Section Weld (Fig. 3-2) | B-1 |
| B-6 Absorber Section (Fig. 3-2)..... | B-2 |
| B-7 Absorber Section to Handle Weld (Fig. 3-2)..... | B-2 |
| B-8 Handle Minimum Cross-Sectional Area (Fig. 3-2) | B-2 |
| APPENDIX C - GEH RESPONSE TO NRC RAI | C-1 |

List of Tables

Table 2-1 Comparison of Typical Parameters of Marathon and Marathon-5S CRBs

Table 3-1 Marathon-5S Material Properties

Table 3-2 Design Allowable Stresses for Primary Loads

Table 3-3 Weld Quality Factors

Table 3-4 Maximum Control Rod Failed Buffer Dynamic Loads

Table 3-5 D Lattice BWR/2-4 Failed Buffer Scram Stresses

Table 3-6 C Lattice BWR/4-5 Failed Buffer Scram Stresses

Table 3-7 S Lattice BWR/6 Failed Buffer Scram Stresses

Table 3-8 Outer Edge Bending Strain due to Seismic and Channel Bow Bending, Internal Absorber Tube Pressure and Failed Buffer Scram

Table 3-9 Absorber Tube to Tie Rod Weld Stress

Table 3-10 Stuck Rod Compression Buckling – Entire Control Rod (Mode A)

Table 3-11 Stuck Rod Compression Buckling – Control Rod Wing (Mode B)

Table 3-12 Boron Carbide Peak Temperatures

Table 3-13 Handle Lifting Load Stress

Table 3-14 Fatigue Usage due to Failed Buffer Scram

Table 3-15 Fatigue Usage at Absorber Section Outer Edge

Table 3-16 Fatigue Usage at Absorber Tube to Tie Rod Weld

Table 3-17 Irradiated Boron Carbide Diametral Swelling Data

Table 3-18 Irradiated Boron Carbide Axial Swelling Data

Table 3-19 Irradiated Boron Carbide Capsule Swelling Calculation

Table 3-20 Absorber Tube Pressurization Results: Minimum Material Condition with OD and ID Surface Defects

Table 3-21 Absorber Tube Pressurization Results: Principle Stress Results at Operating Temperature and Pressure and Maximum Allowable Pressure

Table 3-22 Control Rod Axial Elongation due to Absorber Tube Pressurization

Table 3-23 D/S Lattice Burst Pressure Results from FEA and Testing

Table 3-24 D/S Lattice Thermal Analysis Results

Table 3-25 C Lattice Thermal Analysis Results

Table 3-26 Type 304S Absorber Tube Mechanical Properties

Table 4-1 D Lattice Depletion Calculation Results

NEDO-33284-A Revision 2
Non-Proprietary Information

Table 4-2 C Lattice Depletion Calculation Results

Table 4-3 S Lattice Depletion Calculation Results

Table 4-4 Marathon-5S Control Rod Nuclear and Mechanical Depletion Limits

Table 4-5 Initial Reactivity Worth, D Lattice (BWR/2-4) Original Equipment and Marathon-5S CRBs

Table 4-6 Initial Reactivity Worth, C Lattice (BWR/4,5) Original Equipment and Marathon-5S CRBs

Table 4-7 Initial Reactivity Worth, S Lattice (BWR/6) Original Equipment and Marathon-5S CRBs

Table 4-8 Heat Generation Rates

Table 4-9 D Lattice Mechanical Lifetime Calculation

Table 4-10 C Lattice Mechanical Lifetime Calculation

Table 4-11 S Lattice Mechanical Lifetime Calculation

Table 4-12 Boron Carbide Ring Radii in MCNP Model

Table 4-13 D Lattice Original Equipment and Marathon-5S Dimensions

Table 4-14 C Lattice Original Equipment and Marathon-5S Dimensions

Table 4-15 S Lattice Original Equipment and Marathon-5S Dimensions

Table A-1 Plain Handle Control Rod Inspection Results

Table B-1. Socket Axial Stress Calculations

Table B-2. Socket to Transition Piece Weld Geometry

Table B-3. Socket to Transition Piece Weld Stress Calculations

Table B-4. Transition Piece to Fin Weld Stress Calculations

Table B-5. Minimum Fin Area Stress Calculations

Table B-6. Velocity Limiter to Absorber Section Weld Geometry

Table B-7. Velocity Limiter to Absorber Section Weld Stress Calculations

Table B-8. Absorber Section Geometry Calculation

Table B-9. Absorber Section Stress Calculation

Table B-10. Absorber Section to Handle Weld Area Calculation

Table B-11. Absorber Section to Handle Weld Stress Calculations

Table B-12. Handle Scram Stress Calculations

List of Figures

- Figure 2-1. Marathon-5S CRB Absorber Tube Geometry
- Figure 2-2. Marathon and Marathon-5S Absorber Tube Geometry
- Figure 2-3. Marathon-5S Absorber Wing Weld Locations
- Figure 2-4. Typical Absorber Material Configurations within Absorber Tubes
- Figure 2-5. Original Single Piece Cast and Replacement FabriCast Velocity Limiters
- Figure 2-6. BWR/2-4 D Lattice Marathon-5S Control Rod
- Figure 2-7. BWR/4,5 C Lattice Marathon-5S Control Rod
- Figure 2-8. BWR/6 S Lattice Marathon-5S Control Rod
- Figure 3-1. Velocity Limiter Welds and Cross-Sections Analyzed
- Figure 3-2. Control Rod Assembly Welds and Cross-Sections Analyzed
- Figure 3-3. Absorber Tube to Tie Rod Finite Element Model
- Figure 3-4. Control Rod Buckling Modes
- Figure 3-5. Absorber Tube Pressurization Finite Element Model
- Figure 3-6. Absorber Tube and Capsule Thermal Finite Element Model
- Figure 3-7. Handle Lifting Loads Finite Element Model
- Figure 3-8. Irradiated Test Capsule Configurations
- Figure 3-9. Irradiated Boron Carbide Diametral Swelling Data
- Figure 3-10. Neutron Radiograph of Irradiated Marathon Absorber Capsules
- Figure 3-11. D/S Lattice Thermal Analysis Results
- Figure 3-12. C Lattice Thermal Analysis Results
- Figure 3-13. Stress Intensity Distribution for Multiple Tube Pressurization Finite Element Model, All Tubes Pressurized
- Figure 3-14. Absorber Tube Burst Pressure Test Specimen – After Test
- Figure 3-15. Absorber Tube Burst Pressure Test Specimen Rupture
- Figure 3-16. Absorber Tube Material, 300X Magnification
- Figure 3-17. Absorber Tube Material, 300X Magnification
- Figure 3-18. Absorber Tube Material, 300X Magnification
- Figure 3-19. Absorber Section Tensile Test Specimen After Rupture
- Figure 3-20. Typical Autogenous Laser Weld of 304S Absorber Tubes
- Figure 3-21. Lateral Load Finite Element Model
- Figure 3-22. Lateral Load Finite Element Results (C Lattice)

NEDO-33284-A Revision 2
Non-Proprietary Information

Figure 4-1. D Lattice Fuel Bundle Rod Position and Enrichment

Figure 4-2. C Lattice Fuel Bundle Rod Position and Enrichment

Figure 4-3. S Lattice Fuel Bundle Rod Position and Enrichment

Figure 4-4. D Lattice Control Rod Cold Worth Reduction with Average Depletion

Figure 4-5. C Lattice Control Rod Cold Worth Reduction with Average Depletion

Figure 4-6. S Lattice Control Rod Cold Worth Reduction with Average Depletion

Figure 4-7. BWR/2-6 Original Equipment

Figure A-1. Plain and Roller Handle Marathon CRBs

Figure A-2. GEH 'C' Lattice (BWR/4,5) Fuel Channel Gap Dimensions

Figure A-3. GEH 'S' Lattice (BWR/6) Fuel Channel Gap Dimensions

Figure A-4. GEH 'C' Lattice (BWR/4,5) and 'S' Lattice (BWR/6) Channel Bulge

Figure A-5. Diagram of Lateral and Axial Friction Loads on the Control Rod

Revisions

| No. | Change |
|-----|--|
| 0 | NA |
| 1 | Revised report in entirety by incorporating GEH responses to the associated NRC requests for additional information regarding the Marathon-5S Control Rod Assembly. |
| 2 | <p>Duplicate Figure numbers 3-11 and 3-12 modified to Figure numbers 3-13 and 3-14</p> <p>Existing Figure numbers 3-13 to 3-20 modified to Figure numbers 3-15 to 3-22</p> <p>Section 3.2.2 – Figures 3-14 through 3-16 modified to Figures 3-16 through 3-18</p> <p>Section 3.2.2 – Figure 3-17 modified to Figure 3-19</p> <p>Section 3.2.2 – Figure 3-16 modified to Figure 3-18</p> <p>Section 3.4.3 – Figure 3-19 modified to Figure 3-21</p> <p>Section 3.4.3 – Figure 3-20 modified to Figure 3-22</p> <p>Section 3.6.4 – Figure 3-11 modified to Figure 3-13</p> <p>Section 3.6.4 – Figures 3-12 and 3-13 modified to Figures 3-14 and 3-15</p> <p>APPENDIX A – Section A-1.4: Modified (see Figure below) to (see Figure A-5)</p> |

ACRONYMS AND ABBREVIATIONS

| Acronym / Abbreviation | Description |
|-----------------------------------|--|
| AOO | Anticipated operational occurrence |
| ASME | American Society of Mechanical Engineers |
| ATWS | Anticipated Transient Without Scram |
| CFR | Code of Federal Regulations |
| CRB | Control rod blade |
| CRD | Control rod drive |
| CRDA | Control Rod Drop Accident |
| ECCS | Emergency core cooling system(s) |
| ECP | Engineering Computer Code |
| ESF | Engineered Safety Feature |
| FHA | Fuel Handling Accident |
| GEH | General Electric Hitachi Nuclear Energy |
| GNF | Global Nuclear Fuels |
| IASCC | Irradiation Assisted Stress Corrosion Cracking |
| LOCA | Loss of Coolant Accident |
| LTR | Licensing topical report |
| MCPR | Minimum Critical Power Ratio |
| MSLBA | Main Steamline Break Accident |
| NRC | U.S. Nuclear Regulatory Commission |
| OBE | Operating Basis Earthquake |
| QA | Quality assurance |
| RAI | Request for additional information |
| SRSS | Square root sum of squares |
| SSE | Safe Shutdown Earthquake |
| STS | Standard Technical Specifications |
| TS | Technical Specifications |

EXECUTIVE SUMMARY

The GEH Marathon-5S control rod is a derivative of the Marathon design approved by Reference 1. The primary difference between the Marathon-5S and the original Marathon design, in Reference 1, is a simpler absorber tube geometry. The new simplified absorber tubes use the same crack resistant, GEH proprietary, 304S “Rad Resist” stainless steel as the current Marathon design.

The Marathon-5S uses a B₄C capsule [[

]]

A nuclear evaluation of the Marathon-5S control rod shows that the initial cold and hot reactivity worths are within $\pm 5\%$ of the original equipment control rod (“matched worth criteria”). Therefore, the Marathon-5S is a direct nuclear replacement for previous control rod designs, and no special nuclear calculation or BWR plant change is required.

The structure of the Marathon-5S control rod has been evaluated during all normal and upset conditions, and has been found to be mechanically acceptable. The fatigue usage of the control rod has also been found to be well below lifetime limits.

[[

]] For all cases, the mechanical lifetime exceeds the nuclear lifetime. Therefore, the Marathon-5S control rod is nuclear lifetime limited.

The operational performance of the Marathon-5S is also evaluated. The scram time, no settle characteristics, and control rod drop speeds are all better than or equal to the original Marathon design. Installation of Marathon-5S control rods does not affect any item in the Standard Plant Technical Specifications, and no plant operational change is required. Further, there is no effect on plant safety analyses or on design basis analysis models.

The licensing acceptance criteria applied to the original Marathon design in Reference 1 are re-evaluated and are judged to be sufficient and complete. Therefore, the Marathon-5S is evaluated against the licensing acceptance criteria in Reference 1, and is found to be acceptable. GEH requests NRC approval for the use of Marathon-5S control rods in Boiling Water Reactors.

1. INTRODUCTION AND BACKGROUND

GEH currently manufactures the long life Marathon Control Rod Blade (CRB). The Nuclear Regulatory Commission (NRC) acceptance of the Marathon CRB is documented by a Licensing Topical Report (LTR), Reference 1. The Marathon CRB consists of 'square' absorber tubes, edge welded together to form the control rod wings, and welded to individual tie rod segments to form the cruciform assembly shape. The square absorber tubes are filled with a combination of boron carbide (B_4C) capsules, empty capsules, hafnium rods, and spacers. Previously, GEH manufactured original equipment and replacement Duralife Control Rod Blades, which consisted of a full-length tie rod, with boron carbide absorber rods and hafnium plates and/or strips enclosed within a sheath to form each wing. The most recent Duralife Licensing Topical Report is shown as Reference 2.

The Marathon-5S is a derivative version of the Marathon CRB in that the basic design is the same. For example, the outer absorber tubes are edge welded together to form the cruciform CRB shape, and they are filled with capsules containing boron carbide (B_4C) powder. However, several design changes are made to the Marathon CRB, resulting in a more producible, medium duty version of the Marathon CRB.

Potential effects of the proposed change are evaluated to ensure

- (i) the integrity of the reactor coolant pressure boundary;
- (ii) the capability to shut down the reactor and maintain it in a safe shutdown condition; and
- (iii) the capability to prevent or mitigate the consequences of accidents which could result in potential offsite exposures comparable to the applicable guideline exposures set forth in 10 CFR50.34(a)(1) and 10 CFR 100.11.

The following sections address the potential effect of the proposed changes on fission product barriers (e.g., fuel cladding) and other involved structures, systems and components, safety functions, design basis events, special events and Standard Technical Specifications (STS) to ensure continued compliance with design and regulatory acceptance criteria.

No design changes have been made to the Marathon-5S control rod since revision 0 of this report. This revision is made to incorporate responses to NRC Requests for Additional Information (RAI), per NRC request.

GEH requests NRC approval for the use of Marathon-5S control rods in Boiling Water Reactors.

2. DESIGN CHANGE DESCRIPTION

There are six design changes made to the long life Marathon CRB, as described in Reference 1, to produce the medium duty Marathon-5S CRB. These changes are described in the following subsections.

2.1 ABSORBER TUBE GEOMETRY

The geometry of the Marathon absorber tube is shown in Figure 2-3 of Reference 1. The geometry of the Marathon-5S absorber tube is shown in Figure 2-1 of this report. Table 2-1 provides a comparison of typical parameters for the Marathon and Marathon-5S CRBs. Figure 2-2 is a scale overlay of the original Marathon absorber tube (light blue) with the Marathon-5S absorber tube (dark blue). As shown in Figure 2-2 and Table 2-1, both the width [[]]. As demonstrated in Figure 2-2, due to the geometry difference, [[]].

This comparison shows that the use of the new absorber tube geometry has no effect on the thickness of the wing, nor on the material composition of the absorber tube, GEH proprietary type 304S. The advantage of the Marathon-5S is an absorber tube whose shape is simpler to manufacture than the Marathon absorber tube.

As in the Marathon control rod, the absorber tubes are edge welded together to form the wing of the control rod. A sketch of the control rod wing is shown in Figure 2-3.

2.2 CAPSULE GEOMETRY

The Marathon-5S CRB uses a capsule body tube geometry with [[]]. A comparison of the Marathon-5S and Marathon capsule dimensions is contained in Table 2-1. Due to irradiation induced B₄C powder swelling, a B₄C capsule expands as the absorber is depleted. [[]]

]].

2.3 CAPSULE LENGTH

The Marathon CRB LTR (Reference 1) identifies the nominal length of the B₄C capsules as 11.4 inches. Current Marathon CRB designs use 36" capsules [[]] and 24" [[]] B₄C capsules. [[]]

]]

The Marathon-5S CRB also uses 36" and 24" B₄C capsules. These capsule lengths are reflected in Table 2-1. Diagrams of absorber material columns are shown in Figure 2-4.

2.4 FABRICAST VELOCITY LIMITER

The velocity limiter currently used for Marathon CRBs is a cast/fabricated hybrid called the FabriCast. The FabriCast velocity limiter uses a casting for the "vane" of the velocity limiter (see Figure 2-5), which has identical geometry to the "vane" portion of the single piece cast velocity limiter (called "original" in Reference 1). Because the geometry is the same, the FabriCast velocity limiter has the same drop speed and scram insertion performance as the original single piece cast velocity limiter design. The Marathon-5S CRB may use a FabriCast velocity limiter or the previous cast velocity limiters used on Duralife and Marathon CRBs.

2.5 PLAIN HANDLE

The Marathon LTR (Reference 1) allows for the use of the traditional handle with rollers or handles with wear pads. To eliminate the possibility of stress corrosion cracking initiating within the handle pin-hole, Marathon-5S CRBs for C lattice (BWR/4,5) and S lattice (BWR/6) plants incorporate the use of plain, roller-less handles. These are handles with no handle pins and rollers, but also with no protruding wear pad. An evaluation of the use of plain, roller-less handles in C lattice (BWR/4,5) and S lattice (BWR/6) applications is provided in Appendix A.

Marathon-5S control rods for D lattice (BWR/2-4) applications will use spacer pads.

2.6 FULL LENGTH TIE ROD

The Marathon CRB uses multiple tie rod segments along the center of the cruciform shape. The Marathon-5S CRB utilizes a single tie rod that runs the entire length of the assembly similar to that used on Duralife control rods (see Reference 2). The cross-sectional geometry of this full-length tie rod is designed such that it does not alter the interface between the control rod and the adjacent fuel channels. This is achieved by ensuring that contact occurs between the wing of the control rod and the face of the fuel channel and not at the fuel channel corner and tie rod.

Sketches of Marathon-5S control rods are shown in Figures 2-6, 2-7 and 2-8 for D lattice BWR/2-4, C lattice BWR/4,5, and S lattice BWR/6 applications, respectively.

**Table 2-1
 Comparison of Typical Parameters of Marathon and Marathon-5S CRBs**

| Parameter | BWR/2-4 D Lattice | | BWR/4-5 C Lattice | | BWR/6 S Lattice | |
|---|------------------------------|-------------|------------------------------|-------------|------------------------------|-------------|
| | Marathon CRB ¹ | M-5S CRB | Marathon CRB ¹ | M-5S CRB | Marathon CRB ¹ | M-5S CRB |
| Control Rod Weight (lb) ² | [[| | | | | |
| Absorber Tubes per Wing | | | | | | |
| Nominal Wing Thickness (in) | | | | | | |
| Absorber Tube | | | | | | |
| Length (in) | | | | | | |
| Inside Diameter (in) | | | | | | |
| Nominal Thin Section Wall Thickness (in) | | | | | |]] |
| Material | 304S | 304S | 304S | 304S | 304S | 304S |
| Cross-sectional area (in ²) | [[| | | | |]] |
| B₄C Absorber Capsule | | | | | | |
| Length (in) | [[| | | | | |
| Inside Diameter (in) | | | | | | |
| Wall Thickness (in) | | | | | | |
| Material | | | | | | |
| B ₄ C Density (g/cc) | | | | | | |
| B ₄ C Density (% theoretical) | | | | | |]] |

1. Values from Table 2-1 of the Marathon LTR (Reference 1), except for absorber tube cross-sectional area from design calculations. Current Marathon absorber capsule lengths are also updated, see Section 2.3.
2. For ‘no settle’ considerations, the Marathon-5S CRB has been designed to have dry and wet weights not less than 5 lbs lighter than the current Marathon CRBs, which weigh less than the original equipment.
3. [[

]].

[[

]]

Figure 2-1. Marathon-5S CRB Absorber Tube Geometry

[[

]]

Figure 2-2. Marathon and Marathon-5S Absorber Tube Geometry

[[

]]

Figure 2-3. Marathon-5S Absorber Wing Weld Locations

[[

]]

Figure 2-4. Typical Absorber Material Configurations within Absorber Tubes

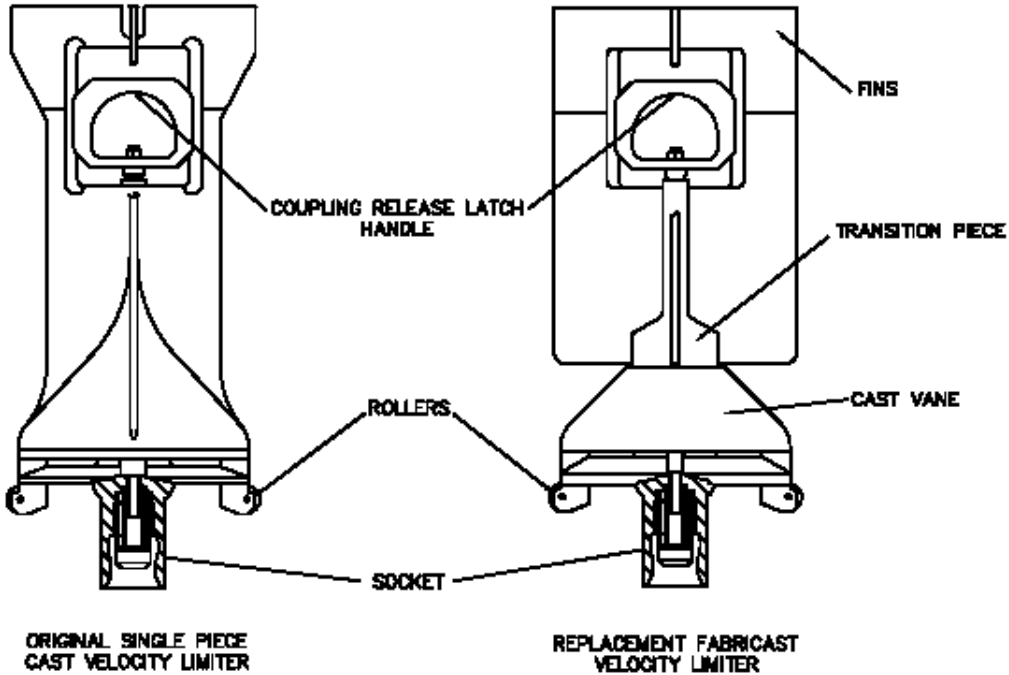


Figure 2-5. Original Single Piece Cast and Replacement FabriCast Velocity Limiters

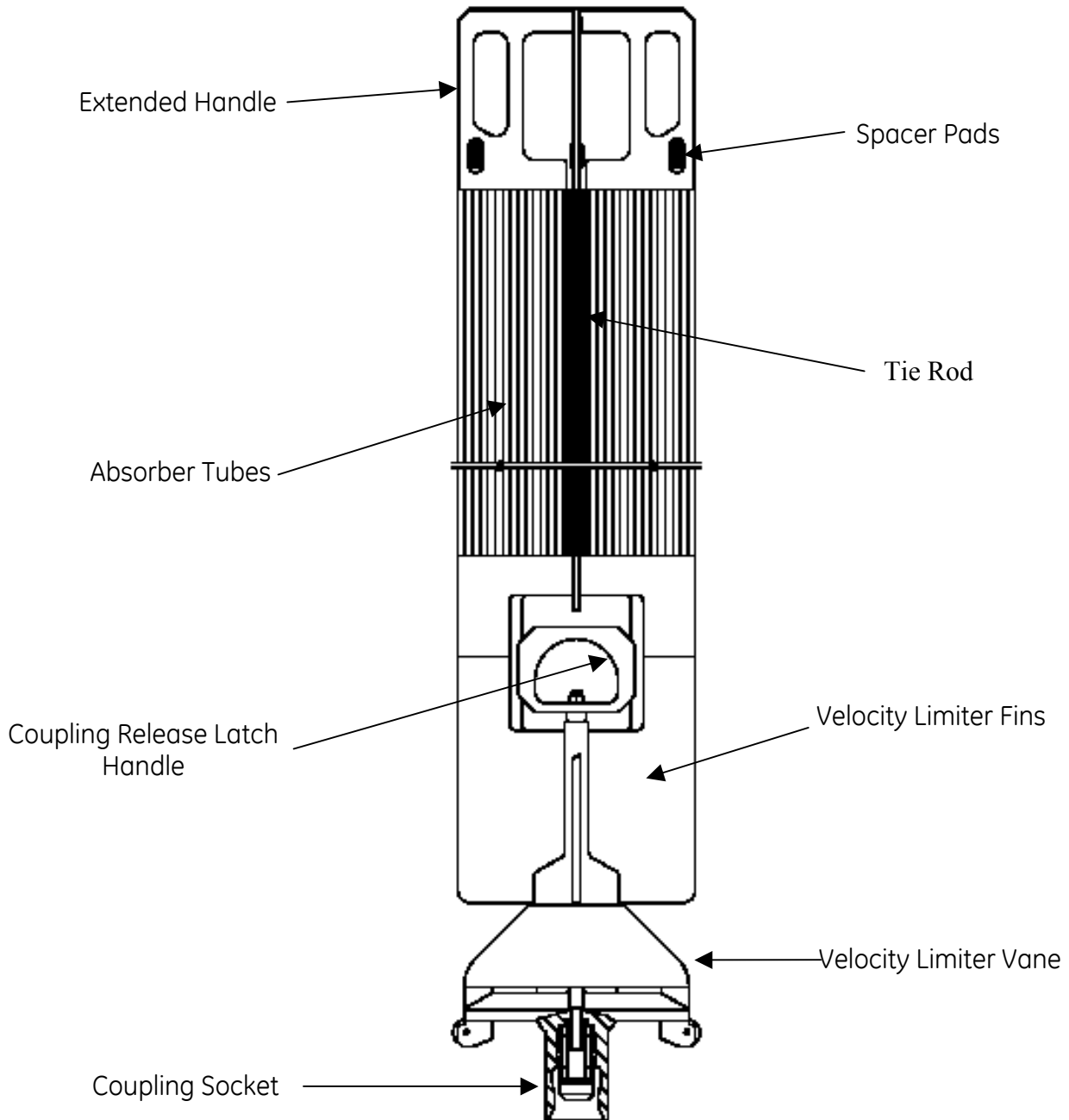


Figure 2-6. BWR/2-4 D Lattice Marathon-5S Control Rod
(Extended Handle Shown)

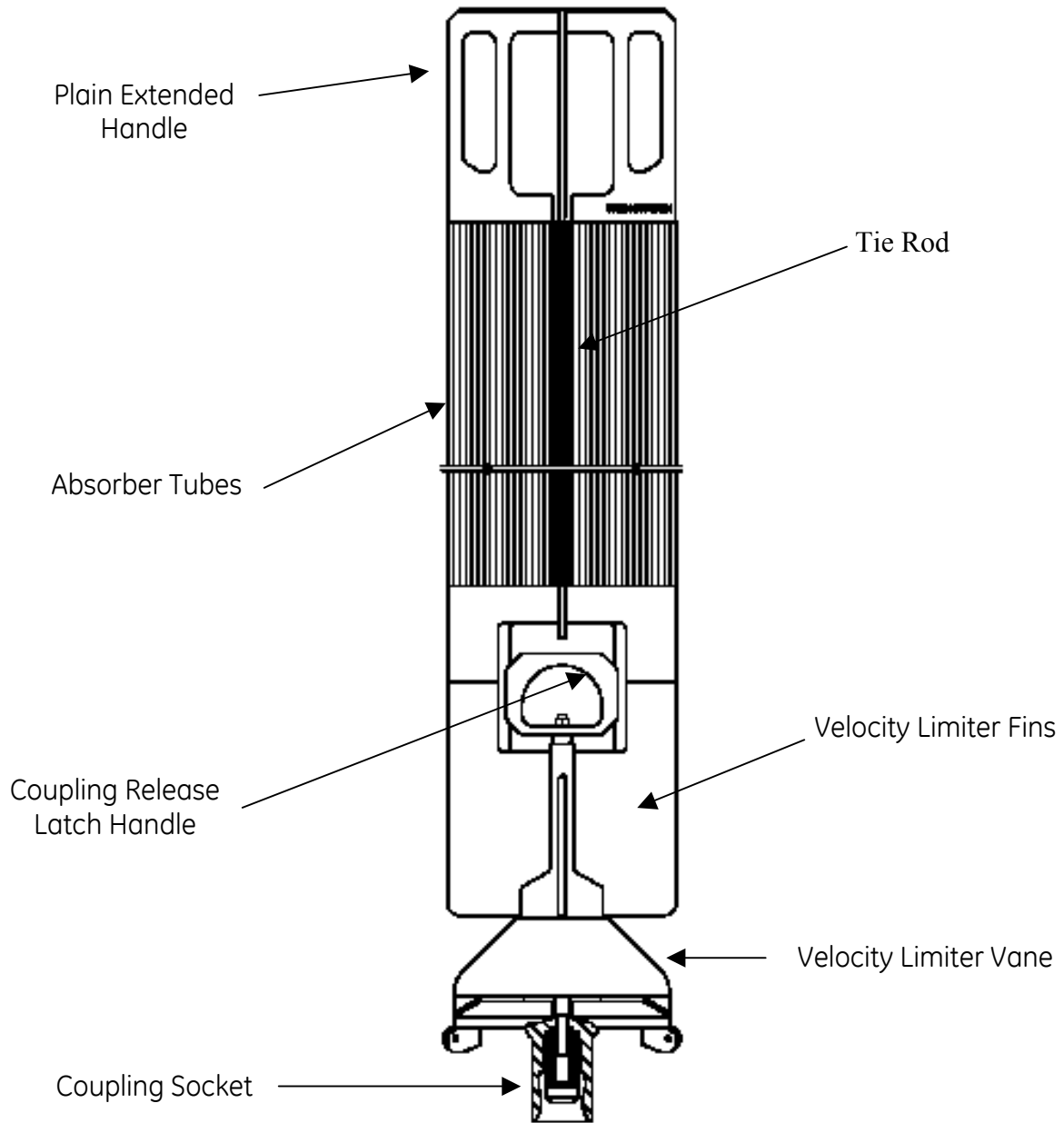


Figure 2-7. BWR/4,5 C Lattice Marathon-5S Control Rod
(Extended Handle Shown)

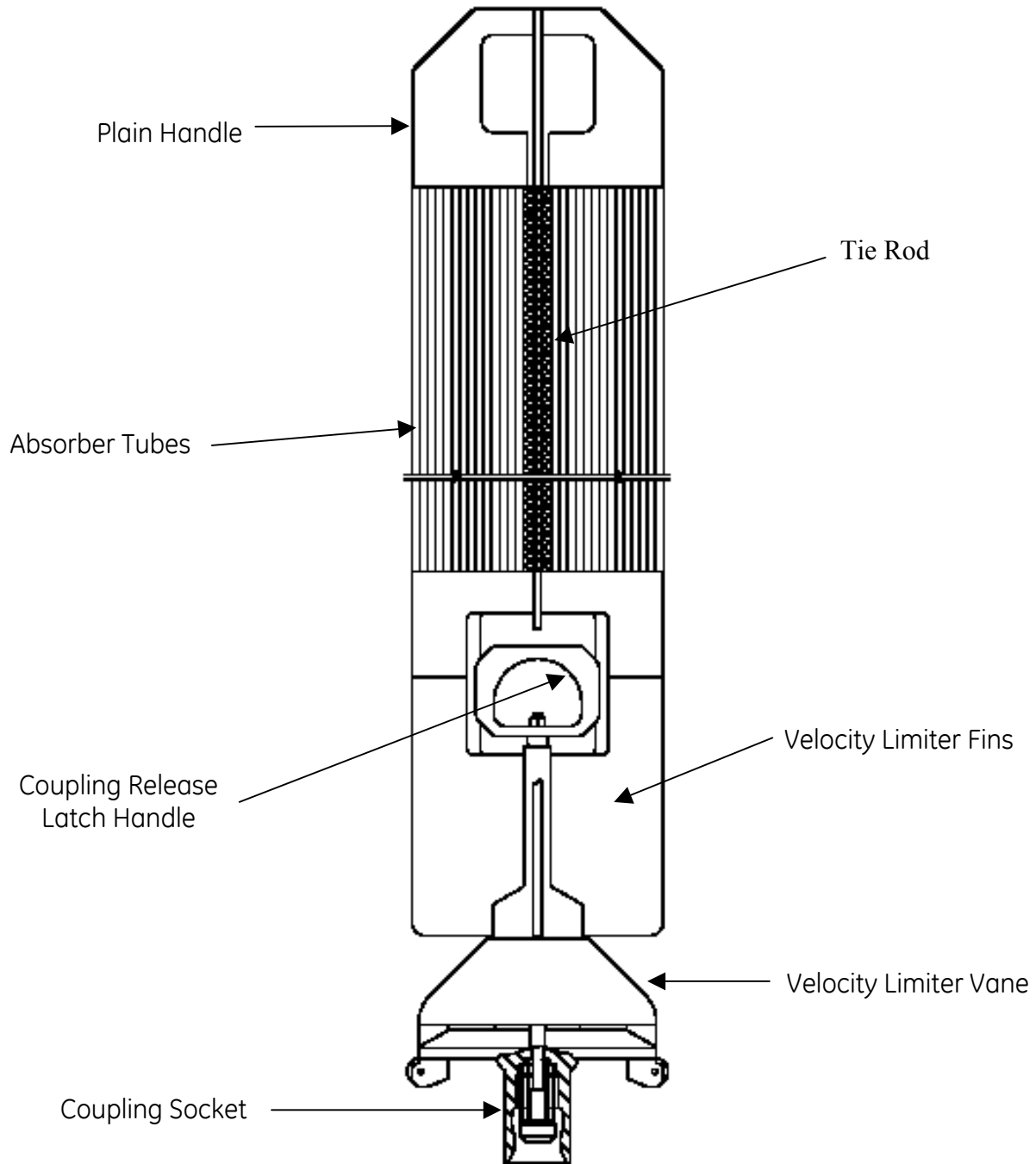


Figure 2-8. BWR/6 S Lattice Marathon-5S Control Rod

3. SYSTEM DESIGN

3.1 ANALYSIS METHOD

For each control rod load application, worst case or bounding loads are identified. Stresses are calculated using worst-case dimensions and limiting material properties. For analyses involving many tolerances, square root sum of squares (SRSS) or statistical tolerancing may be used. Corrosion, wear, and crud deposition are accounted for when appropriate.

3.1.1 Combined Loading

As in Reference 1, effective stresses and strains are determined using the distortion energy theory (Von Mises), and compared to allowable limits. Using the principal stresses: σ_1 , σ_2 , and σ_3 , the equivalent Von Mises stress is calculated as:

$$\sigma_{VM} = \sqrt{1/2[(\sigma_1 - \sigma_2)^2 + (\sigma_2 - \sigma_3)^2 + (\sigma_3 - \sigma_1)^2]}$$

Both the Von Mises and Tresca stress criteria are used to predict the conditions for yielding under both uniaxial and multiaxial stress states. The Tresca Criterion can be called the maximum shear criterion since it measures the maximum shear stress present. The Von Mises takes into account all principal stresses in the calculation of the conditions where yielding occurs. For thin walled tubes, under combined loads, the Von Mises Criterion appears to more accurately represent the condition under which yielding occurs (Reference 11). The use of the Von Mises criterion takes into consideration the hydrostatic component of stress and the corresponding strain value. It should be recognized that failure modes in thin walled structures such as control rod absorber tubes are initiated at the surface, a location where one of the three principal stresses is zero. The use of the von Mises criterion is therefore adequate to evaluate the potential for any of the important failure modes. First, ductile failure is associated with plastic flow. The criterion was developed to best assess that mode. Fatigue and crack growth processes would initiate on the surface. Again, plastic flow at the surface is necessary for these processes to start. As supported by the stress analyses results in Section 3.3 through 3.8, the stresses are below the un-irradiated stress limits. Therefore, the absorber tubes will only experience elastic deformation. This condition is also true in the irradiated condition where the stress ratio will decrease when compared to the actual irradiated yield strength value.

Given this, the effects of irradiation are well known. Specifically, the material will have a significant increase in yield strength and ultimate strength. Therefore, the design criteria used, one based on un-irradiated properties, will insure that as fluence is accumulated, the component continues to remain elastic and well below the actual yield strength. As stated in Reference 1, this approach has been previously accepted.

3.1.2 Unirradiated Versus Irradiated Material Properties

Each structural analysis is first evaluated to determine whether unirradiated or irradiated material properties are appropriate. In general, as stainless steel is irradiated, the yield and ultimate tensile strengths increase, while the ductility, or allowable strain decreases. In order to determine the correct technique, the analyses are broken into two categories:

1. Analyses with an applied load (ie, scram). For these analyses, a maximum stress is calculated, and compared to the limiting unirradiated stress limit.
2. Analyses with an applied displacement (ie, seismic bending). For these analyses, a maximum strain is calculated, and compared to the limiting irradiated strain limit.

Austenitic stainless steels do not display a ductile to brittle transition (DBTT). The material fracture toughness and ductility (in the unirradiated condition) does not vary significantly in the temperature range of interest (70 - 550°F). In turn, the effect of irradiation on austenitic stainless steel is to reduce the toughness and ductility somewhat; however, austenitic stainless steel still retains ductility after irradiation. There are existing data at high fluence that confirm the tensile ductility and fracture toughness. Specifically, ductility levels and fracture toughness data for irradiated components are documented in Reference 9. These data substantiate their ductile behavior at both room temperature as well as operating temperature.

3.2 MATERIAL PROPERTY LIMITS

The limiting unirradiated material strengths are first identified for the control rod structural materials, and shown in Table 3-1. For most materials, limiting values from the ASME Boiler and Pressure Vessel Code are used. In other cases, minimum material strengths are specified in GEH material specifications.

GEH requires that the mechanical properties of all material used in the fabrication of control rods be certified as meeting material specification limits. For example, the mechanical properties of finished, annealed, and un-irradiated type 304S absorber tubes are defined by a fabrication specification. These mechanical limits, along with the certification results of three recent absorber tube lots are shown in Table 3-26. As shown, all mechanical properties met the specification requirements. See section 3.2.4 for more information on GEH's stabilized type 304S stainless steel.

3.2.1 Stress Criteria

The licensing acceptance criteria of Reference 1 are used, in which the control rod stresses and strains and cumulative fatigue shall be evaluated to not exceed the ultimate stress or strain of the material.

The figure of merit employed for the stress-strain limit is the design ratio, where:

$$\text{Design ratio} = \text{effective stress/stress limit, or, effective strain/strain limit.}$$

The design ratio must be less than or equal to 1.0. Conservatism is included in the evaluation by limiting stresses for all primary loads to one-half of the ultimate tensile value.

Resulting allowable stresses for primary loads are shown in Table 3-2.

3.2.2 Absorber Tube Material Isotropy

The irradiation resistant special melt austenitic stainless steel (type 304S) used for the control rod absorber tubes is manufactured using standard industrial processes and solution annealing. There is no significant anisotropy produced in wrought product by these procedures. Photos of finished absorber tubes, at 300X magnification, in different orientations, are shown in Figures 3-16 through 3-18. The axial loading direction is the direction of design concern and is aligned with the direction of standard tensile tests on irradiated material. The necking observed in these irradiated tensile tests can be interpreted as supporting the adequacy of the strength and ductility of the material in the radial direction.

3.2.3 Welded Connections

For welded connections, a weld quality factor, q , is used to further reduce the allowable stress. Therefore, the allowable stress for a welded connection, S_m' , is:

$$S_m' = (q)S_m$$

Weld quality factors are determined based on the inspection type and frequency of the weld. Weld quality factors are shown in Table 3-3.

3.2.4 Laser Welding Process

Laser Beam Weld (LBW) processes are used extensively in the manufacture of Marathon and Marathon-5S control rods. Welding processes for control rods are developed and qualified against a set of acceptance standards which includes: (1) meeting minimum penetration requirements, (2) smooth blends between welded members, and (3) no cracks, holes, lack of fusion or porosity. During weld process development for the Marathon-5S control rod, it was found that good results for the absorber tube-to-tube laser welds were achieved using the same parameters as the Marathon control rod.

As a result of the complexity of the control rod geometry, GEH qualifies the welding process in a manner meeting the intent of the ASME Code. The qualification method selected is to confirm the mechanical properties of the weld by using a representative mockup of the laser weld. Mechanical tests confirm that the mechanical properties of the weld were higher than the minimum properties of the base metal.

The weld quality factor (q) provides a safety margin against manufacturing defects during processing. The critical to quality components of the weld are defined by ASME B&PV code weld procedure QW-264.1, Welding Procedure Specifications, Laser Beam Welding (LBW). GEH further refines its internal critical to quality requirements from the ASME B&PV code for its day-to-day operations. [[
]].

To evaluate the strength of the absorber section to handle/velocity limiter laser weld, test panels consisting of four edge-welded absorber tubes and end plates representing the handle/fin were fabricated. These test specimens used the same weld processes and parameters as production

welds in order to provide a real-world test of the weld strength. A tensile test was then performed.

The results of this test showed that the test specimens ruptured first in the absorber tube material, prior to the rupturing of the laser weld, as shown in the Figure 3-19.

GEH performs metallographic evaluation on sample laser welds on a weekly basis to confirm that the results of the welding process remain within parameters. These results are documented. Photomicrographs of a typical laser weld, taken as part of a recent qualification test, are shown in Figure 3-20. Comparing the grain structure at the edge of the weld to an area away from the weld shows that there is no effective heat affected zone for a laser weld. This combined lack of heat affected zone, Ta stabilization, and low carbon chemistry, accounts for the good carbide test results mentioned above.

Austenitic stainless steels have no inherent age hardening capability and lend themselves readily to the welding process. GEHs' proprietary Type 304 S composition is as follows:

[[

]]

A common concern in austenitic stainless steel welds is carbide precipitation. Carbide formation in a weld heat affected zone would encourage intergranular stress corrosion cracking in this location. The combination of low heat input welding practices, tantalum stabilization, and restrictive carbon limits, provides an effective barrier to such intergranular cracking.

3.2.5 Absorber Tube Axial Shrink Due to Welding

Due to the absorber tube-to-tube laser welding process, the absorber tubes shrink by varying amounts in the axial direction. Prior to welding, the length of the absorber tube is [[
]]. The lengths of the absorber tubes after welding were measured on a production Marathon control.

The biggest difference in relative length between the absorber tubes after welding is [[]].

The length of the finished absorber section is [[]]. Therefore, the maximum axial strain due to the differential weld shrinking of the absorber tubes is:

$$\text{Strain } (\epsilon) = \Delta L / L_{\text{initial}} = [[]].$$

A [[]] strain is metallurgically insignificant in terms of driving microstructural changes in the bulk tubing. This strain is an elastic driver towards overall distortion. Distortion is minimized through production controls. Please see section 3.2.4 for further discussion with regard to the mechanical properties of the laser welds.

3.3 SCRAM

The largest axial structural loads on a control rod blade are experienced during a control rod scram, due to the high terminal velocity. To be conservative, structural analyses of the control rod are performed assuming a 100% failed control rod drive buffer. A dynamic model of mass, spring and gap elements is used to simulate a detailed representation of the load bearing components of the assembly during a scram event. Simulations are run at atmospheric temperatures, pressures, speeds, and properties as well at operating temperatures, pressures, speeds, and properties. The resulting loads are shown in Table 3-4.

Structural stresses are determined from the scram loads shown in Table 3-4 using the limiting material properties, weld quality factors, and worst-case geometry for the area subject to the load. Figures 3-1 and 3-2 show the welds and cross-sections analyzed.

Resulting maximum stresses during a failed buffer scram are shown in Tables 3-5, 3-6 and 3-7 for D lattice BWR/2-4, C lattice BWR/4-5, and S lattice BWR/6 applications. These stresses are evaluated against the stress limits shown in Table 3-2. Specific details for each calculation are shown in Appendix B. As shown by the design ratios in Tables 3-5 through 3-7, sufficient margin exists against failure for all cross-sections and welds.

3.4 SEISMIC AND FUEL CHANNEL BOW INDUCED BENDING

Fuel channel deflections, which result from seismic events, impose lateral loads on the control rods. The Marathon-5S control rod is analyzed for Operating Basis Earthquake (OBE) events and Safe Shutdown Earthquake (SSE) events.

3.4.1 Wing Outer Edge Bending

The OBE analysis is performed by evaluating the strain in the Marathon-5S absorber section with maximum OBE deflection. In addition, maximum control rod deflections due to fuel channel bulge and bow are conservatively added to the calculated seismic bending deflections. [[]]

]]

The limiting location for strain due to bending of the control rod cross-section occurs at the outer edge of the control rod wing. At this location, a combined strain due to simultaneous application of the following loads is calculated: (1) control rod bending due to an OBE seismic event, (2) control rod bending due to worst case channel bulge and bow, (3) axial absorber tube stress due to maximum internal pressure, and (4) a failed buffer scram. The results of these strain calculations are shown in Table 3-8. As shown, even under these combined worst-case conditions, the maximum strain is well below the limiting maximum allowable strain at irradiated conditions.

3.4.2 Absorber Tube to Tie Rod Weld

The combined effect of control rod bending due to OBE and channel bulge and bow deflection combined with maximum absorber tube internal pressure is also evaluated at the full-length tie rod to absorber tube weld. A finite element model is used, as shown in Figure 3-3. Resulting worst-case stresses are shown in Table 3-9. As shown, the resulting stresses are acceptable against the design criteria.

3.4.3 Absorber Tube Lateral Load

Finally, the lateral load imposed on the control rod absorber tube due to an excessively bowed channel is evaluated. The finite element model is shown in Figure 3-21. As shown, the entire lateral load is applied to a single square absorber tube, along with reactor internal pressure. For conservatism, no internal pressure is applied to the tube, which would offset the external pressure and reduce the stresses in the tube.

The resulting stress intensity plot is shown in Figure 3-22. The maximum stress intensity is calculated as $[[\quad]]$, which is less than the absorber tube allowable load of $[[\quad]]$ from Table 3-2.

3.4.4 Marathon-5S Seismic Scram Tests

For the SSE analysis, the control rod must be capable of full insertion during fuel channel deflections. As discussed in Section 5.2, because the Marathon-5S control rod has a stiffness less than or equal to the Marathon assembly, and because the weight of the Marathon-5S control rod is less than previous designs, the Marathon-5S has seismic scram capability equal to or better than the Marathon control rod.

To confirm the seismic scram capability of the Marathon-5S control rod, seismic scram tests were performed. This test facility consists of a simulated pressure vessel and reactor internals, and a control rod drive. Prototype Marathon-5S control rods were installed, and the control rod drive was set to simulate D, C, and S lattice operation.

The Marathon-5S prototypes used for the test incorporated plain, roller-less handles. The acceptance criterion for the test was that scram time requirements were to be met up to fuel bundle oscillation consistent with an OBE (Operational Basis Earthquake) event. The results of the tests were very successful, in that scram time requirements were met through the much more severe SSE (Safe Shutdown Earthquake) event for both the C lattice and S lattice applications.

The D lattice application met scram time requirements with OBE fuel channel deflections. During the tests, the control rods received very little wear.

3.5 STUCK ROD COMPRESSION

Maximum compression loads from the control rod drive (CRD) are evaluated for a stuck control rod. Both buckling, and compressive yield are analyzed for the entire control rod cross-section (buckling mode A), and conservatively assuming that the entire compression load is applied to a single control rod wing (buckling mode B). Figure 3-4 shows the buckling modes. An additional axial load of 600 lb due to channel bulge and bow is also added to the compression load.

Results of the stuck rod compression loads are contained in Table 3-10 for the entire control rod cross-section (mode A), and in Table 3-11 for the single wing (mode B). As can be seen, neither compressive yielding nor buckling will occur for either buckling mode. Additionally, for both buckling modes, the compressive yield load is reached prior to the critical buckling load.

3.6 ABSORBER BURN-UP RELATED LOADS

The structure of a control rod must provide for positioning and containment of the neutron absorber material (Boron Carbide powder, Hafnium, etc) throughout its nuclear and mechanical life and prohibit migration of the absorber out of its containment during normal, abnormal, emergency and faulted conditions. The Marathon-5S CRB, like the Marathon CRB, contains boron carbide powder within capsules contained within absorber tubes (capsule within a tube design).

The boron neutron absorption reaction releases helium atoms. Some of this helium gas is retained within the compacted boron carbide powder matrix, causing the powder column to swell. This swelling causes the B₄C capsule to expand. The remainder of the helium is released as a gas. The capsule end caps for the Marathon and Marathon-5S designs are crimped to the capsule body tubes. This allows the helium gas to escape from the capsule and fill the absorber tube gap and any empty capsule plenum volume provided.

For the Marathon capsule design, [[

]].

For the Marathon-5S capsule design, [[

]].

Using the pressurization capability of the absorber tube, limits are determined for each absorber tube configuration (see Figure 2-4), in terms of B₄C column depletion.

These individual absorber tube depletion limits are then combined with radial depletion profiles and axial depletion profiles to determine the mechanical depletion limit for the control rod assembly. See Section 4.6.

3.6.1 Irradiated Boron Carbide Swelling Design Basis

Mechanical test data of the irradiated behavior of boron carbide was obtained by irradiating test capsules for a period of approximately ten years in a reactor. Test capsules were placed in neutron monitor tubes and irradiated in a reactor. The configurations of two types of test capsules used are shown in Figure 3-8.

The dimensions of the test capsules were measured prior to irradiation, and post-irradiation in a hot cell using standard laboratory practice. For test capsules with a mandrel, the diametral strains were mathematically corrected to compensate for the mandrel, resulting in an increase of reported strain value.

Diametral swelling results are shown in the Table 3-17 and Figure 3-9. The Marathon-5S swelling analysis conservatively uses the $+3\sigma$ upper bound value of [[]].

Axial swelling data is shown in Table 3-18. As shown, the axial swelling is [[]].

]].

3.6.2 Clearance Between Capsule and Absorber Tube

As a result of the welding process forming the control rod wings, the inside diameter of the absorber tubes shrink. Therefore, a minimum inside diameter is established, and is 100% inspected following the welding, before the absorber section is loaded with capsules.

The worst-case capsule dimensions are used, which result in the maximum outside diameter at 100% local depletion. These consist of the original maximum outside diameter, and minimum wall thickness, resulting in the maximum beginning boron carbide diameter

The strain at the ID of the capsule is equal to the diametral strain of the boron carbide powder. The $+3\sigma$ upper limit of [[]] from Table 3-17 is used. Then, assuming constant volume deformation of the capsule, the strain on the outside diameter of the capsule is:

$$[[]]$$

Then, the capsule outside diameter at 100% local depletion is:

$$OD_{100\%} = OD_0(1 + \epsilon_{OD}).$$

A summary of this calculation is shown in Table 3-19 for both the D/S lattice and C lattice absorber tube and capsule combinations. [[]]

]].

3.6.3 Thermal Analysis

Pressure in the absorber tube due to helium release is calculated accounting for worst-case capsule and absorber tube dimensions and B₄C helium release fraction. Because the amount of helium released from the B₄C powder increases with temperature, a finite element thermal analysis is performed to determine the peak B₄C temperature (see Figure 3-6). This thermal analysis is performed using worst-case dimensions, maximum end-of-life crud buildup, combined with maximum beginning-of-life heat generation.

For the thermal model, corrosion is modeled as the build-up of an insulating layer of crud. This crud may be corrosion products from the control rod absorber tube, or deposited from other reactor internals. For all thermal analyses, a crud layer corresponding to a 32-year residence time is used ([[]]).

A temperature distribution is shown in Figure 3-6 for the D/S lattice case. The model used assumes that the tube is interior to the wing, in that there is another absorber tube to the left and right. The boundary on the left and right is conservatively assumed to be insulated (zero heat flux).

Results for both D/S lattice and C lattice are shown in Tables 3-24 and 3-25, and in Figures 3-11 and 3-12. The following conservatisms are applied to the thermal model:

- Peak beginning-of-life heat generation rates are used, these are combined with:
- End-of-life combined corrosion and crud build-up of [[]], twice that used in previous analyses.
- Peak heat generation rates are used from the highest heat generation tube, which is actually the outermost edge tube. In reality, this tube will have coolant on one side, rather than be insulated. Further some heat transfer will occur from the peak heat generation tube to the adjacent tube, rather than be perfectly insulated.
- Maximum wall thickness dimensions are used.

Peak B₄C temperatures are shown in Table 3-12. The temperatures shown in this table are based on peak beginning-of-life boron carbide heat generation rates (see section 4.5), and are from the peak heat generation absorber tube at the peak axial location. They are radially averaged only across the cross-section of an individual boron carbide capsule.

Helium release fractions are based on models developed using data from multiple sources. The data shows a significant dependence of helium release fraction on the irradiation temperature. The helium release fractions used for each lattice type are shown in Table 3-12. The helium release model is based on data from 500 °F to 1000 °F, which envelopes the temperatures shown in Table 3-12.

3.6.4 Absorber Tube Pressurization Capability

[[

]]. Finite element analyses are performed to determine the pressurization capability of the absorber tube. These analyses incorporate the use of worst-case dimensions, maximum expected wear, and the largest allowable surface defects (see Figure 3-5).

Absorber Tube Defects

The limiting case used for establishment of the absorber tube allowable pressure simultaneously combines worst-case absorber tube dimensions (thinnest wall per drawings), surface defects at the center of the flat portion of the tube, on the round portion of the tube, and a crack-like defect on the thinnest portion of the inside diameter of the tube.

The largest sized allowable surface defects are based on the manufacturing capability of the absorber tube. A collaborative effort was undertaken with the supplier of the absorber tubes to determine a maximum surface defect size that would maintain reasonable yield rates, but would not reduce the pressurization capability of the tube below acceptable values. A surface defect depth limit of [[]] in depth was determined, applied to the absorber tubing specification, and factored into the pressurization analysis.

At receipt inspection, the acceptance criteria for surface defects is based primarily on the depth of the defect. Additionally, matching sets of visual standards are used by both the supplier and by GEH to identify acceptable and unacceptable surface features.

The finite element analysis shows that smaller diameter defects result in larger stress concentrations around the defect. A survey was performed of surface defects, and the smallest area defect was found to be [[]] in diameter. Therefore, a diameter of [[]] was used for the finite element model surface defects.

After factoring in maximum allowable surface defects and worst-case (thinnest wall) absorber tube geometry, the finite element analysis is performed. An example stress distribution is shown in Figure 3-5. The surface defect geometry is also shown.

The burst pressure is defined as the internal pressure at which any point in the tube reaches a stress intensity equal to the true ultimate strength of the material. Then, to calculate an allowable pressure, a safety factor of 2.0 is applied to the differential pressure across the absorber tube wall such that:

$$P_{allow} = \frac{(P_{burst} - P_{external})}{2} + P_{external}$$

The calculated burst and allowable pressures are shown in Table 3-20. The results at operating temperature are limiting, and are used as the design basis allowable pressure of the tubes.

Absorber Tube Wear and Corrosion

Corrosion and wear are significant to the pressurization capability analysis of the absorber tube. In the pressurization analysis, the peak stress concentrations occur on the 'flat' portion of the tube. Combined corrosion and wear on this surface are modeled as a removal of material.

The analysis shows that combined corrosion and wear, modeled as a removal of material for the pressurization analysis, can exceed [[]] without affecting the design basis allowable pressure of the outer absorber tube shown in Table 3-20. For the D/S lattice absorber tube, the upper limit for combined corrosion and wear that occurs after control rod installation is [[]]. For the C lattice absorber tube, the upper limit is [[]]. This amount of wear is considered sufficiently conservative.

Maximum Stress Components

Stress components at the point of maximum stress intensity were analyzed for the absorber tube with the maximum allowable internal pressure. The point of maximum stress intensity is found to be on the outer edge of the absorber tube, at the middle of the flat portion. Principle stress components are shown in Table 3-21. All stress values shown in Table 3-21 are within the allowable stress value for 304S tubing of [[]] shown in Table 3-2.

Effect of the Welded Connection Between Absorber Tubes

The effect of the welded connection between adjacent absorber tubes on the stresses in the tube due to internal pressure was evaluated using a multiple tube finite element model. In this model, three adjacent absorber tubes were pressurized. A stress intensity distribution is shown in Figure 3-13. As shown, the maximum stress is at the flat portion of the tube exposed to the coolant. The effect of the adjacent pressurized tubes is to produce compressive rather than tensile stresses in the flat portions of the tube that are welded together. In this way, the opposing pressures from opposite sides of this welded ligament is actually beneficial in terms of the pressurization capability of the tubes.

A comparison of this multiple tube model to the single tube model showed that the single tube model predicts lower burst pressures. Therefore, the single tube model is used to determine design basis allowable pressures, and there is no degrading effect due to the lack of gaps between the absorber tubes in the Marathon-5S design.

The Marathon and Marathon-5S Control Rod Blades (CRB) are manufactured using very low heat input laser weld processes. The resulting regions of microstructural change including the associated heat affected zones (HAZ) are very small (see section 3.2). Based on general understanding, the fine HAZ microstructure will have mechanical properties that are equivalent to, or exceed, those of the wrought base material. Therefore, the HAZ will have mechanical properties that exceed the required minimum properties of the associated wrought material.

Two potential issues arise from welding of the absorber section: (1) sensitization and (2) residual stress. These issues are addressed below:

Sensitization: The low heat input laser welding processes have minimal impact on the wrought tube material, in that they typically do not result in sensitized material. To confirm this

conclusion, the processes are continually evaluated metallographically to confirm the acceptability of the weld region (i.e., lack of sensitization). In addition, [[

]]. Note also from section 3.6.2 that these contact hoop stresses (and associated strains) have been eliminated for the Marathon-5S control rod.

Residual stress: One major effect of the welding process is that it will introduce tensile residual stresses in the narrow weld/HAZ region. These stresses are not a significant concern for two reasons: (1) The field cracking has not been associated with the weld HAZ and (2) the irradiation experienced by the CRB over the initial time of operation can significantly reduce these stresses by 60% or more through radiation creep processes (Reference 12). At this level of reduced stress, there is little concern for any effect on stress corrosion cracking (SCC) initiation or their applied stresses and strains. In that the major concern are strains from swelling, this level of stress is well below those levels required to even produce yielding. See also section 3.2.

Absorber Tube Expansion

As the outer absorber tube is pressurized, a small amount of radial expansion is experienced. The radial expansion is evaluated using the two-dimensional finite element pressurization model. For this evaluation, the maximum allowable internal pressure is applied. The model showed that the maximum expansion of the width of the tube is [[]] for D/S lattice and [[]] for C lattice. This amount of expansion is very small, and will have no adverse effect on the fit, form or function of the control rod.

The pressurization of the absorber tubes will also cause an axial expansion of the tubes. This is due to the internal pressure pushing against the end plugs that seal the ends of the absorber tubes. Using the maximum allowable internal pressure, the area of the end plugs, and the number of pressurized tubes in the absorber section, the maximum axial load is calculated and shown in Table 3-22.

Assuming stresses remain in the elastic range, the axial strain on the absorber tubes is calculated as $\epsilon = \sigma/E = P/AE$, with the elongation being $\Delta L = \epsilon L$. For an absorber section that is nominally [[]] long, the total elongation is also shown in Table 3-22. These maximum elongations are relatively small, and will not affect the fit, form or function of the control rod.

The analyses presented in part b above independently evaluate the diametral and axial expansion of the absorber tubes due to the internal pressure in the tubes. In reality, expansion in the diametral direction will generally reduce expansion in the axial direction, and vice versa. Therefore, the strains and displacements shown in Table 3-22 are conservative.

Effect of Irradiated Material

The pressurization finite element model uses unirradiated material properties. To test the assertion that the use of unirradiated properties in the pressurization finite element model is conservative, a test case is performed. The D lattice, 550 °F case is chosen for the test, with worst-case dimensions and maximum allowable surface defects. An internal pressure of [[

]] is applied, which is the burst pressure found using unirradiated materials, as shown in Table 3-20. At this internal pressure, the maximum stress intensity using irradiated materials is [[]], which is less than the true ultimate strength of the irradiated material, [[]]. Therefore, since the test case using irradiated material properties does not reach the ultimate strength of the irradiated material, the burst pressure analysis using unirradiated material properties is conservative. Further, the maximum strain intensity in the tube for the irradiated property test is low, at [[]].

Burst Pressure Tests

As discussed above, the allowable pressure for the absorber tube for the Marathon-5S is based on a finite element model incorporating worst-case dimensions, along with maximum specification permitted surface defects and expected wear. The finite element analysis shows that the worst-case burst pressure, on which the allowable pressure of the Marathon-5S tube is based, is [[]] lower than the burst pressure using nominal dimensions and no surface defects. See Table 3-22.

To confirm the finite element results, burst pressure tests were performed on two test specimens consisting of a short panel of welded absorber tubes, in which all tubes are pressurized, see Figures 3-14 and 3-15. The resulting tested burst pressures are compared to the finite element calculated burst pressures in Table 3-23.

As shown, the test results exceed the nominal predicted burst pressure by approximately [[]], and exceed the worst-case burst pressure (worst-case dimensions and surface defects) by a wide margin (~[[]]). Since the design basis allowable pressure for the absorber tube is based on the worst-case burst pressure combined with a safety factor of 2.0, the design is conservative.

Conclusions

The analysis is conservative because it considers the combined effects of: (1) worst case tube dimensions (thinnest wall), (2) maximum allowable surface defects, (3) a large amount of combined corrosion and wear, and (4) unirradiated material properties. The true ultimate strength of the material will increase with irradiation. Burst pressure tests further validate the design basis allowable pressures.

3.6.5 Irradiation Assisted Stress Corrosion Cracking Resistance

In order for the stress corrosion cracking mechanism to activate it requires a material that is susceptible, a conducive environment and a sustained tensile stress. If one of these three mechanisms is not present to a sufficient degree, the likelihood of a stress corrosion crack to form is significantly reduced.

The Marathon absorber tube is made from a GEH proprietary stainless steel, “Rad Resist 304S”, which is optimized to be resistant to Irradiation Assisted Stress Corrosion Cracking (IASCC). The Marathon-5S absorber tubes are also fabricated from this material, and thus, are expected to have the same crack resistant properties. The chemistry of this material is shown in section 3.2.4.

In addition to using IASCC resistant material, the Marathon-5S is designed such that [[

]]. See section 3.6.2. This significantly reduces the amount of stress/strain present in the absorber tubes at the end of life, and significantly reduces the likelihood of stress-corrosion cracking.

3.7 HANDLING LOADS

The Marathon-5S control rod is designed to accommodate twice the weight of the control rod during handling, to account for dynamic loads. The handle is analyzed using a finite element model, using worst-case geometry (see Figure 3-7). Table 3-13 shows the results of the handle loads analysis.

3.8 LOAD COMBINATIONS AND FATIGUE

The Marathon-5S control rod is designed to withstand load combinations including anticipated operational occurrences (AOOs) and fatigue loads associated with those combinations. The fatigue analysis is based on the following assumed lifetime, which is consistent with previous analyses,

[[

]]

For scram, each cycle represents a single scram insertion. Scram simulations show that the oscillations in the control rod structure damp out quickly. Further, it is extremely conservative to assume [[]] scrams with a 100% inoperative control rod drive buffer, as the loads experienced by the control rod in a normal buffered scram are much less severe.

For the Operational Basis Earthquake (OBE), a total of [[]] seismic events, in which each event consists of [[]] cycles of control rod lateral bending. The assumption of [[]] lifetime OBE events is also considered very conservative.

Based on the reactor cycles, the combined loads are then evaluated for the cumulative effect of maximum cyclic loadings. The fatigue usage is evaluated against a limit of 1.0. The maximum cyclic stress is determined using a conservative stress concentration factor of 3.0. Table 3-14 shows the fatigue usage due to control rod SCRAM at three limiting weld locations. In this analysis, it is assumed that each scram occurs with a 100% failed CRD buffer.

Table 3-15 shows the fatigue usage at the control rod outer edge due to bending from OBE seismic events and severe channel bow, control rod scram, and maximum absorber tube internal pressure. As can be seen, the combined fatigue usage is much less than 1.0.

Table 3-16 shows the fatigue usage at the tie rod to first absorber tube weld. The combined loading due to failed buffer scram, maximum absorber tube internal pressure, OBE seismic events and severe channel bow is considered. As shown, the combined fatigue usage is much less than 1.0.

NEDO-33284-A Revision 2
Non-Proprietary Information

It is well known that the cycles for fatigue initiation are dependent on the stress or strain range. The number of loading cycles that the control rod blade experience are limited to 100 for all of the different designs. The stress amplitudes are all in the elastic range. As shown in Tables 3-14 through 3-16, based upon the ASME Section III fatigue design curve for un-irradiated austenitic material (ref. 6), the low number of cycles represents only a small amount of cumulative damage, well below the design limit. The $\frac{1}{2}$ ultimate tensile stress value represents the ASME design limit for $\sim 30,000$ cycles. It has been established that an increase in the strength level, consistent with the effect of irradiation, would only increase the margin. This is supported by data on high strength materials, which confirm that the endurance limit is close to $\frac{1}{2}$ ultimate tensile stress (Reference 7).

The last consideration with regard to fatigue is an evaluation of whether there is any flow-induced vibration that could in turn provide the potential for fatigue initiation. An assessment was performed to evaluate the loads induced by transverse loading. The evaluation that treated the control blade as a cantilever beam, found that the loads were very small and would not be sufficient to even close the gap between the blade and the fuel assembly. This load is considered so small as to be negligible, and would not lead to any risk of fatigue.

**Table 3-1
 Marathon-5S Material Properties**

| Material Type | Control Rod Components | Ultimate Tensile Strength, S _U (ksi) | | Yield Strength, S _Y (ksi) | | Modulus of Elasticity, E (x 10 ⁶ psi) | | Poisson's Ratio, ν | |
|----------------------|--|---|--------|--------------------------------------|--------|--|--------|--------------------|--------|
| | | 70 °F | 550 °F | 70 °F | 550 °F | 70 °F | 550 °F | 70 °F | 550 °F |
| 316 Plate | Handles and pads; VL fins, VL Hardware | [[| | | | | | | |
| 316 Bar | Handle pads; VL hardware | | | | | | | | |
| XM-19 Bar | VL socket | | | | | | | | |
| CF3 Casting | VL vane casting, latch handle casting | | | | | | | | |
| ER 308L | Capsule end caps, absorber tube end plugs, weld filler metal | | | | | | | | |
| 304S Bar | Tie rods | | | | | | | | |
| 304S Tubing | Absorber Tubes | | | | | | | | |
| Hardened 304L Tubing | Capsule body tubes | | | | | | | |]] |

NEDO-33284-A Revision 2
Non-Proprietary Information

**Table 3-2
Design Allowable Stresses for Primary Loads**

| Material Type | CR Components | $\frac{1}{2}$ Ultimate Tensile Stress S_m (ksi) | |
|-------------------------|---|--|--------|
| | | 70 °F | 550 °F |
| 316 Plate | Handles and pads; VL fins, VL Hardware |]] | |
| 316 Bar | Handle pads; VL hardware | | |
| XM-19 Bar | VL socket | | |
| CF3 Casting | VL vane casting, latch handle casting | | |
| ER 308L | Capsule end caps, absorber tube end plugs, weld filler metal | | |
| 304S Bar | Tie rods | | |
| 304S Tubing | Absorber Tubes | | |
| Hardened 304L Tubing | Capsule body tubes | |]] |

**Table 3-3
 Weld Quality Factors**

| Weld | Weld Inspection | Weld Quality Factor, q |
|----------------------------|------------------------|-----------------------------------|
| Socket to Transition Piece | [[| |
| Transition Piece to Fin | | |
| Fin to Absorber Section | | |
| Handle to Absorber Section | | |
| End Plug to Absorber Tube | | |
| Vane to Transition Piece | |]] |

**Table 3-4
 Maximum Control Rod Failed Buffer Dynamic Loads**

| Components | Maximum Equivalent Loads in Kips (10³ lbs) (Tension Listed as Negative) | | | | | |
|-----------------------------------|--|---------------|------------------|---------------|------------------|---------------|
| | D Lattice | | C Lattice | | S Lattice | |
| | 70 °F | 550 °F | 70 °F | 550 °F | 70 °F | 550 °F |
| Coupling | [[| | | | | |
| Velocity Limiter (VL) | | | | | | |
| VL/Absorber Section Interface | | | | | | |
| Absorber Section | | | | | | |
| Handle/Absorber Section Interface | | | | | | |
| Handle | | | | | | |
| Capsules (Per Capsule) | | | | | |]] |

Table 3-5
D Lattice BWR/2-4 Failed Buffer Scram Stresses

| Location | Room Temperature (70 °F) | | | Operating Temperature (550 °F) | | |
|---|--------------------------|-----------------|--------------|--------------------------------|-----------------|--------------|
| | Maximum Stress | Allowable Limit | Design Ratio | Maximum Stress | Allowable Limit | Design Ratio |
| Socket Minimum Cross-Sectional Area | [[| | | | | |
| Socket to Transition Piece Weld | | | | | | |
| VL Transition Piece to Fin Weld | | | | | | |
| VL Fin Minimum Cross-Sectional Area | | | | | | |
| Velocity Limiter to Absorber Section Weld | | | | | | |
| Absorber Section | | | | | | |
| Handle to Absorber Section Weld | | | | | | |
| Handle Minimum Cross-Sectional Area | | | | | |]] |

Table 3-6
C Lattice BWR/4-5 Failed Buffer Scram Stresses

| Location | Room Temperature (70 °F) | | | Operating Temperature (550 °F) | | |
|---|--------------------------|-----------------|--------------|--------------------------------|-----------------|--------------|
| | Maximum Stress | Allowable Limit | Design Ratio | Maximum Stress | Allowable Limit | Design Ratio |
| Socket Minimum Cross-Sectional Area | [[| | | | | |
| Socket to Transition Piece Weld | | | | | | |
| VL Transition Piece to Fin Weld | | | | | | |
| VL Fin Minimum Cross-Sectional Area | | | | | | |
| Velocity Limiter to Absorber Section Weld | | | | | | |
| Absorber Section | | | | | | |
| Handle to Absorber Section Weld | | | | | | |
| Handle Minimum Cross-Sectional Area | | | | | |]] |

Table 3-7
S Lattice BWR/6 Failed Buffer Scram Stresses

| Location | Room Temperature (70 °F) | | | Operating Temperature (550 °F) | | |
|---|--------------------------|-----------------|--------------|--------------------------------|-----------------|--------------|
| | Maximum Stress | Allowable Limit | Design Ratio | Maximum Stress | Allowable Limit | Design Ratio |
| Socket Minimum Cross-Sectional Area | [[| | | | | |
| Socket to Transition Piece Weld | | | | | | |
| VL Transition Piece to Fin Weld | | | | | | |
| VL Fin Minimum Cross-Sectional Area | | | | | | |
| Velocity Limiter to Absorber Section Weld | | | | | | |
| Absorber Section | | | | | | |
| Handle to Absorber Section Weld | | | | | | |
| Handle Minimum Cross-Sectional Area | | | | | |]] |

Table 3-8
Outer Edge Bending Strain due to Seismic and Channel Bow Bending, Internal Absorber Tube Pressure and Failed Buffer Scram

| Description | D Lattice | C Lattice | S Lattice |
|--|-----------|-----------|-----------|
| | 550 °F | 550 °F | 550 °F |
| Outer Edge Bending Strain, Seismic (%) | [[| | |
| Outer Edge Bending Strain, Seismic + Channel Bow (%) | | | |
| Max Internal Pressure Axial Stress (ksi) | | | |
| Max Failed Buffer Scram Stress (ksi) | | | |
| Total Outer Edge Strain, Seismic + Failed Buffer Scram + Absorber Tube Internal Pressure (%) | | | |
| Total Outer Edge Strain, Seismic + Channel Bow + Failed Buffer Scram + Absorber Tube Internal Pressure (%) | | | |
| Allowable Strain (%) ½ Ultimate, Irradiated | | | |
| Design Ratio | | |]] |

Table 3-9
Absorber Tube to Tie Rod Weld Stress

| Description | D Lattice 550 °F | C Lattice 550 °F | S Lattice 550 °F |
|--|---------------------|---------------------|---------------------|
| Seismic + Internal Pressure, Max S_{INT} (ksi) | [[| | |
| Seismic + Channel Bow + Internal Pressure, Max S_{INT} (ksi) | | | |
| Ultimate Tensile Stress (ksi) | | | |
| Design Ratio | | |]] |

Table 3-10
Stuck Rod Compression Buckling – Entire Control Rod (Mode A)

| Description | D Lattice | | C Lattice | | S Lattice | |
|--|-----------|--------|-----------|--------|-----------|--------|
| | 70 °F | 550 °F | 70 °F | 550 °F | 70 °F | 550 °F |
| Critical Buckling Load, P_{cr} (lb) | [[| | | | | |
| Compressive Yield Load (lb) | | | | | | |
| Maximum Stuck Rod Compression Load (lb) | | | | | | |
| Added Compression Load due to Channel Bow (lb) | | | | | | |
| Total Compressive Load (lb) | | | | | | |
| Design Ratio, Buckling | | | | | | |
| Design Ratio, Compressive Yield | | | | | |]] |

Table 3-11
Stuck Rod Compression Buckling – Control Rod Wing (Mode B)

| Description | D Lattice | | C Lattice | | S Lattice | |
|---------------------------------------|-----------|--------|-----------|--------|-----------|--------|
| | 70 °F | 550 °F | 70 °F | 550 °F | 70 °F | 550 °F |
| Critical Buckling Load, P_{cr} (lb) | [[| | | | | |
| Compressive Yield Load (lb) | | | | | | |
| Total Compressive Load (lb) | | | | | | |
| Design Ratio, Buckling | | | | | | |
| Design Ratio, Compressive Yield | | | | | |]] |

Table 3-12
Boron Carbide Peak Temperatures

| Parameter | Nominal Dimensions | | Worst Case Dimensions | |
|--|--------------------|-----------|-----------------------|-----------|
| | D/S Lattice | C Lattice | D/S Lattice | C Lattice |
| B ₄ C Centerline Temperature (°F) | [[| | | |
| Average B ₄ C Temperature (°F) | | | | |
| Helium Release Fraction (%) | | | |]] |

Table 3-13
Handle Lifting Load Stress

| Lattice Type | Handle Type | Maximum Stress Intensity (ksi) | Design Ratio, 1/2 Ultimate Stress |
|----------------------|-----------------------|--------------------------------|-----------------------------------|
| D Lattice BWR/2-4 | BWR/4 Extended Handle | [[| |
| | BWR/3 Extended Handle | | |
| | Standard Handle | | |
| C Lattice BWR/4-5 | Extended Handle | | |
| | Standard Handle | | |
| S Lattice BWR/6 | Standard Handle | |]] |

Table 3-14
Fatigue Usage due to Failed Buffer Scram

| Location | D Lattice | | | | C Lattice | | | | S Lattice | | | |
|---------------------------------|-------------------|------------------|---------------|-------|-------------------|------------------|---------------|-------|-------------------|------------------|---------------|-------|
| | Stress Amp. (ksi) | Allow Cycles (N) | Actual Cycles | Usage | Stress Amp. (ksi) | Allow Cycles (N) | Actual Cycles | Usage | Stress Amp. (ksi) | Allow Cycles (N) | Actual Cycles | Usage |
| Socket to Transition Piece Weld | [[| | | | | | | | | | | |
| Transition Piece to Fin Weld | | | | | | | | | | | | |
| VL Fin to Absorber Section Weld | | | | | | | | | | | |]] |

Table 3-15
Fatigue Usage at Absorber Section Outer Edge

| Stress Type | D Lattice | | | | C Lattice | | | | S Lattice | | | |
|---|-------------------|------------------|---------------|-------|-------------------|------------------|---------------|-------|-------------------|------------------|---------------|-------|
| | Stress Amp. (ksi) | Allow Cycles (N) | Actual Cycles | Usage | Stress Amp. (ksi) | Allow Cycles (N) | Actual Cycles | Usage | Stress Amp. (ksi) | Allow Cycles (N) | Actual Cycles | Usage |
| Absorber Section Outer Edge - Scram + Internal Pressure | [[| | | | | | | | | | | |
| Absorber Section Outer Edge – Seismic + Channel Bow | | | | | | | | | | | |]] |
| | Total Usage = | [[|]] | | Total Usage = | [[|]] | | Total Usage = | [[|]] | |

Table 3-16
Fatigue Usage at Absorber Tube to Tie Rod Weld

| Stress Type | D Lattice | | | | C Lattice | | | | S Lattice | | | |
|---|-------------------|------------------|---------------|-------|-------------------|------------------|---------------|-------|-------------------|------------------|---------------|-------|
| | Stress Amp. (ksi) | Allow Cycles (N) | Actual Cycles | Usage | Stress Amp. (ksi) | Allow Cycles (N) | Actual Cycles | Usage | Stress Amp. (ksi) | Allow Cycles (N) | Actual Cycles | Usage |
| Absorber Tube to Tie Rod Weld - Scram | [[| | | | | | | | | | | |
| Absorber Tube to Tie Rod Weld – Seismic + Channel Bow + Internal Pressure | | | | | | | | | | | |]] |
| | Total Usage = | | [[|]] | Total Usage = | | [[|]] | Total Usage = | | [[|]] |

Table 3-19
Irradiated Boron Carbide Capsule Swelling Calculation

| Parameter | D/S Lattice | C Lattice |
|--|-------------|-----------|
| Absorber Tube ID Before Welding (in) | [[| |
| Minimum Absorber Tube ID After Welding (in) | | |
| Capsule OD (in) | | |
| Capsule Wall Thickness (in) | | |
| Maximum Capsule OD ₀ (in) | | |
| Maximum Capsule ID ₀ (in) | | |
| Capsule ID strain (in/in) | | |
| Capsule OD strain (in/in) | | |
| Capsule OD at 100% local depletion | |]] |

Table 3-20
Absorber Tube Pressurization Results: Minimum Material Condition with OD and ID Surface Defects

| Lattice | Temp (°F) | External Pressure (psi) | FEA Burst Pressure (psi) | Allowable Pressure (psi) |
|---------|-----------|-------------------------|--------------------------|--------------------------|
| C | 70 | 14.7 | [[| |
| C | 550 | 1050 | | |
| D | 70 | 14.7 | | |
| D | 550 | 1050 | |]] |

Table 3-21
Absorber Tube Pressurization Results: Principle Stress Results at Operating Temperature and Pressure and Maximum Allowable Pressure

| Stress Component | D/S Lattice | C Lattice |
|-------------------------|--------------------|------------------|
| S1 (Hoop) | [[| |
| S2 (Axial) | | |
| S3 (Radial) | | |
| Stress Intensity | | |
| Equivalent Stress | |]] |

Table 3-22
Control Rod Axial Elongation due to Absorber Tube Pressurization

| Parameter | D Lattice | C Lattice | S Lattice |
|--|------------------|------------------|------------------|
| Axial Load due to Pressurization (kips) | [[| | |
| Absorber Section Cross-Sectional Area (in ²) | | | |
| Modulus of Elasticity, E (ksi) | | | |
| Strain (in/in) | | | |
| Elongation, ΔL (inch) | | |]] |

Table 3-23
D/S Lattice Burst Pressure Results from FEA and Testing

| Parameter (D/S Lattice) | Burst Pressure (psia) |
|--|------------------------------|
| Nominal Dimensions (FEA) | [[|
| Worst-Case Dimensions and Maximum Surface Defects (Design Basis) (FEA) | |
| Specimen 1 Tested Burst Pressure | |
| Specimen 2 Tested Burst Pressure |]] |

Table 3-24
D/S Lattice Thermal Analysis Results

| Location | Nominal Dimensions | | Worst Case Dimensions | |
|--------------|--------------------|-----------------|-----------------------|-----------------|
| | Radius (in) | Nodal Temp (°F) | Radius (in) | Nodal Temp (°F) |
| Centerline | [[| | | |
| Ring1 OD | | | | |
| Ring2 OD | | | | |
| Ring3 OD | | | | |
| Ring4 OD | | | | |
| Ring5 OD | | | | |
| Ring6 OD | | | | |
| Ring7 OD | | | | |
| Ring8 OD | | | | |
| Capsule ID | | | | |
| Capsule OD | | | | |
| Abs Tube ID | | | | |
| Abs Tube OD | | | | |
| Crud Surface | | | | |
| Avg B4C | | | | |
| Avg He Void | | | |]] |

Table 3-25
C Lattice Thermal Analysis Results

| Location | Nominal Dimensions | | Worst Case Dimensions | |
|--------------|--------------------|-----------------|-----------------------|-----------------|
| | Radius (in) | Nodal Temp (°F) | Radius (in) | Nodal Temp (°F) |
| Centerline | [[| | | |
| Ring1 OD | | | | |
| Ring2 OD | | | | |
| Ring3 OD | | | | |
| Ring4 OD | | | | |
| Ring5 OD | | | | |
| Ring6 OD | | | | |
| Ring7 OD | | | | |
| Ring8 OD | | | | |
| Capsule ID | | | | |
| Capsule OD | | | | |
| Abs Tube ID | | | | |
| Abs Tube OD | | | | |
| Crud Surface | | | | |
| Avg B4C | | | | |
| Avg He Void | | | |]] |

Table 3-26
Type 304S Absorber Tube Mechanical Properties

| Property | Room Temperature Yield Stress (ksi) | 550 °F Yield Stress (ksi) | Room Temperature Ultimate Tensile Stress (ksi) | 550 °F Ultimate Tensile Stress (ksi) | Room Temperature Elongation (% in 2 inches) |
|----------------------------|-------------------------------------|---------------------------|--|--------------------------------------|---|
| Specification Requirement* | [[| | | | |
| Example Lot 1 | | | | | |
| Example Lot 2 | | | | | |
| Example Lot 3 | | | | |]] |

* These material requirements are specified in the fabrication specification for the absorber tubes. The tubing supplier certifies each lot of absorber tubes as meeting these requirements.

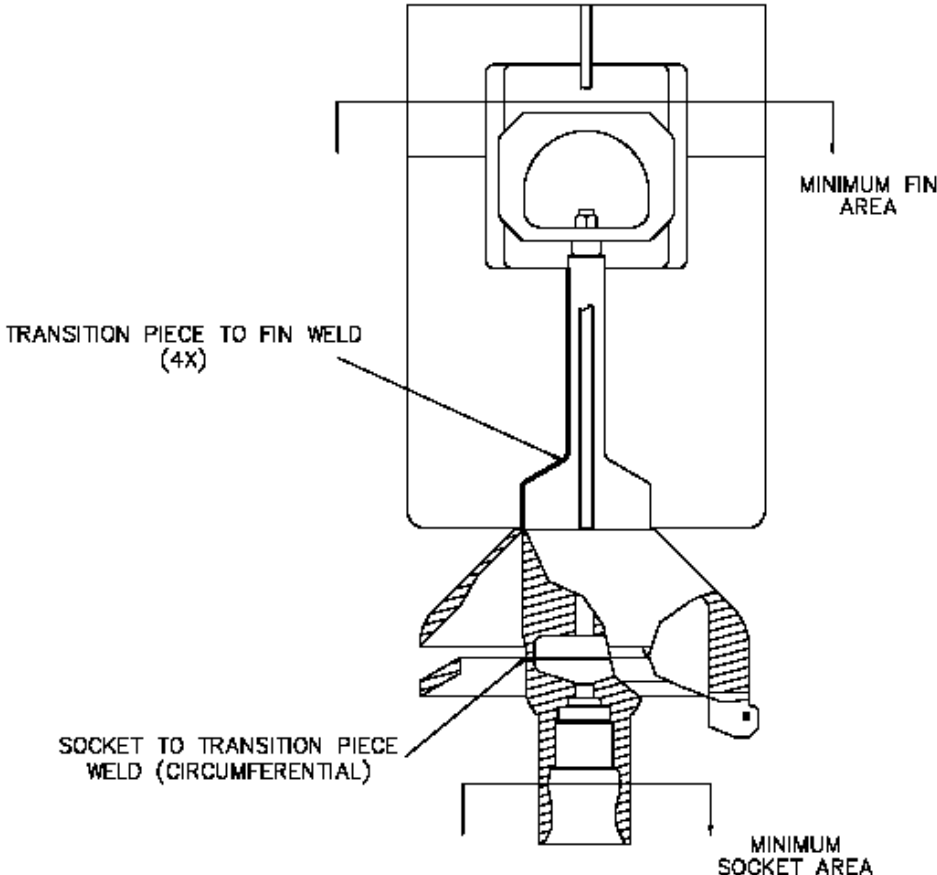


Figure 3-1. Velocity Limiter Welds and Cross-Sections Analyzed

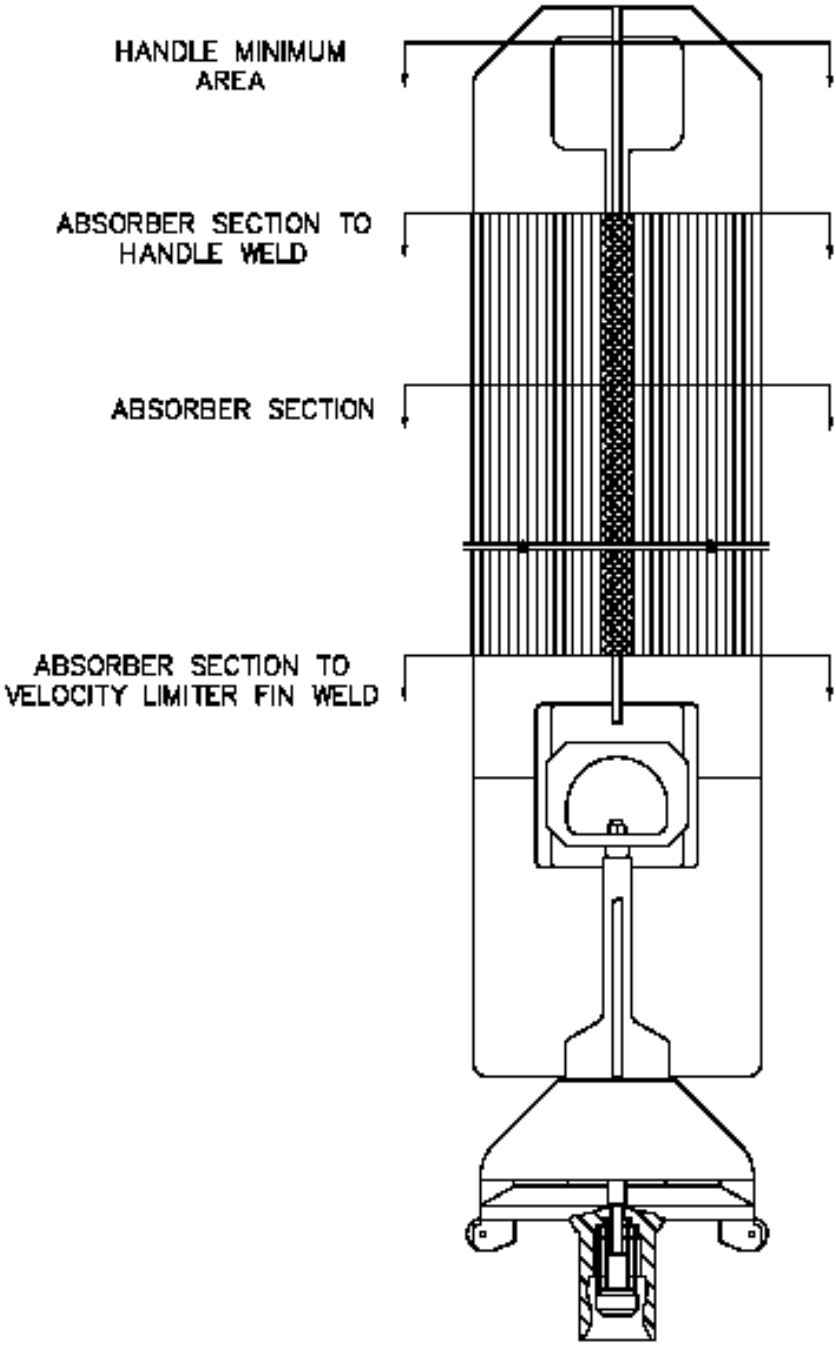


Figure 3-2. Control Rod Assembly Welds and Cross-Sections Analyzed

[[

]]

Figure 3-3. Absorber Tube to Tie Rod Finite Element Model

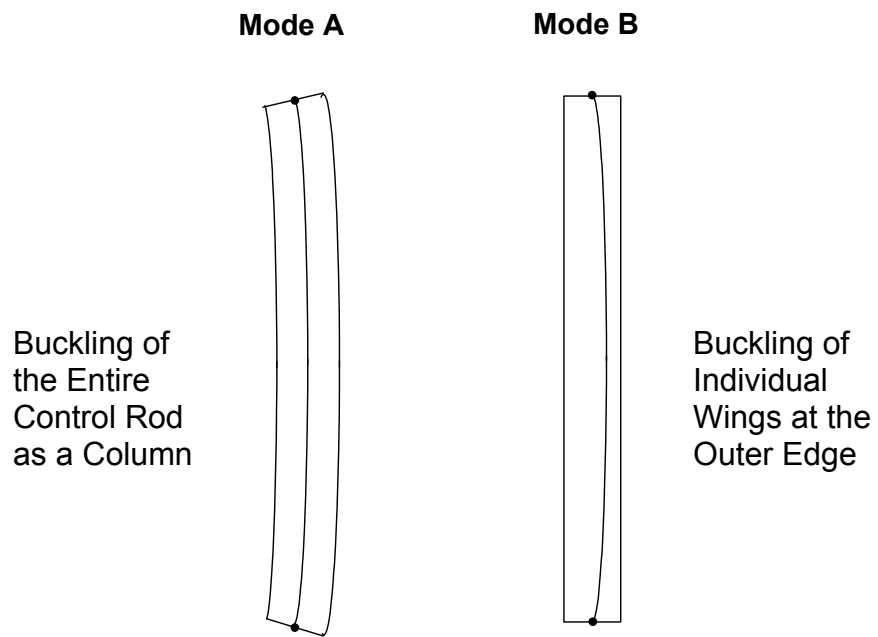


Figure 3-4. Control Rod Buckling Modes

[[

]]

Figure 3-5. Absorber Tube Pressurization Finite Element Model

[[

]]

Figure 3-6. Absorber Tube and Capsule Thermal Finite Element Model

[[

]]

Figure 3-7. Handle Lifting Loads Finite Element Model

[[

]]

Figure 3-8. Irradiated Test Capsule Configurations

[[

]]

Figure 3-9. Irradiated Boron Carbide Diametral Swelling Data

[[

]]

Figure 3-10. Neutron Radiograph of Irradiated Marathon Absorber Capsules

[[

]]

Figure 3-11. D/S Lattice Thermal Analysis Results

[[

]]

Figure 3-12. C Lattice Thermal Analysis Results

[[

]]

Figure 3-13. Stress Intensity Distribution for Multiple Tube Pressurization Finite Element Model, All Tubes Pressurized

[[



]]

Figure 3-14. Absorber Tube Burst Pressure Test Specimen – After Test

[[

Figure 3-15. Absorber Tube Burst Pressure Test Specimen Rupture

]]

[[

Figure 3-16. Absorber Tube Material, 300X Magnification

]]

[[

Figure 3-17. Absorber Tube Material, 300X Magnification

[[

]]

|

Figure 3-18. Absorber Tube Material, 300X Magnification

]]

|

[[

Figure 3-19. Absorber Section Tensile Test Specimen After Rupture

[[

]]

|

Figure 3-20. Typical Autogenous Laser Weld of 304S Absorber Tubes

]]

|

[[

]]

Figure 3-21. Lateral Load Finite Element Model

[[

]]

Figure 3-22. Lateral Load Finite Element Results (C Lattice)

4. NUCLEAR EVALUATIONS

4.1 DESIGN CRITERIA

A control rod's nuclear worth characteristics shall be compatible with reactor operation requirements. As approved in Reference 1, a replacement control rod can meet these requirements by demonstrating that the initial hot and cold CRB reactivity worths are within $\pm 5\%$ $\Delta k/k$ (where $\Delta k/k$ is $1-k_{con}/k_{unc}$) of the original equipment control rod blade design worth. Replacement rods with reactivity worth outside this tolerance require, as a minimum, evaluations on cold shutdown margin, AOO CPR, control rod drop accident, fuel cycle economics, nuclear methods, and control rod lifetime.

For GEH original equipment control rods, the nuclear lifetime is defined as the quarter-segment depletion at which the control rod cold worth ($\Delta k/k$) is 10% less than its zero-depletion cold worth. The original equipment (DuraLife 100) control rods consist of thin sheaths enclosing boron carbide filled tubes. The sheaths are welded to a central tie rod to form the cruciform shape of the control rods. The original equipment control rods are shown in Figure 4-7.

As discussed above, a retrofit design may have an initial cold worth that differs from the original equipment control rod that it is replacing, within $\pm 5\%$ of the initial worth of that control rod (the "matched worth" criterion). The nuclear lifetime for such a retrofit control rod is defined as the quarter-segment depletion at which the cold worth is the same as the end-of-nuclear-life cold worth of the original equipment control rod that it is replacing.

4.2 METHODOLOGY

The nuclear lifetime for a particular control blade design is determined with a two-dimensional step-wise depletion of the control blade poisons. This is done by computing the eigenvalue for hot, voided conditions with a Monte Carlo neutron transport code. The poison reaction rates from the analysis are then assumed to be constant for a fixed period of time (Δt) to obtain the number of absorptions for each discrete area of the blade. The poison number densities are then updated in the Monte Carlo code input and another eigenvalue calculation is performed. This process continues until the reduction in cold worth – as computed by companion cold Monte Carlo eigenvalue calculations – reaches the end-of-nuclear-life criterion.

For locations within the blade that use boron carbide as a poison, the change in the number of absorber atoms is computed as:

$$\frac{dN_{B-10}}{dt} = -(N \cdot \sigma)_{B-10}$$

Here, σ is the reaction rate for B-10 from the Monte Carlo code.

The number of absorptions from each of the regions is summed to obtain the total number of absorptions (A) for the time interval. This total number of absorptions is normalized by the total number of B-10 atoms if the design would have incorporated only boron carbide as an absorber. The resulting value is the B-10 equivalent depletion:

$$\%_{\text{depletion}} = \frac{A}{N_{\text{B-10}}}$$

Reactivity worth calculations for the Marathon-5S are performed using a GEH controlled version of MCNP4A developed by the Los Alamos National Laboratory (Reference 3). MCNP is a Monte Carlo code for solving the neutral-particle transport equation as a fixed source or an eigenvalue problem in three dimensions. Continuous energy cross section data is used in the calculation, thus making creation of multi-group cross sections unnecessary. The use of MCNP is the only process change from the original Marathon nuclear analysis which used MERIT. Otherwise, depletion calculations remain unchanged.

Two additional utility codes are used in conjunction with MCNP. The GEH utility code "MODL" is used to set up the MCNP input deck, based on lattice design data and control rod design data. The GEH utility code "HO" is coupled to MCNP for the depletion calculation. It reads the MCNP tallies (cell fluxes and absorber cross sections) and then performs the control blade depletion calculation. The depleted absorber atom densities are then used to update the MCNP inputs for the next time step. MCNP input data for cold case are also generated with "HO" by modifying the input data from the hot inputs.

For the depletion calculations that are performed for each fuel lattice, the time step used is 100 days. In order to reach the 10% cold worth reduction for the nuclear lifetime evaluation, a total of 21 time steps are used for the re-calculation of DuraLife 100 (original equipment), and a total of 30 time steps are used for the calculation of Marathon-5S lifetime. Tables 4-13 through 4-15 contain input parameters used to model the original equipment and Marathon-5S control rods.

B-10 drift, defined as the faster depletion of B-10 on the outer edge of B₄C column than the average pin due to spatial self-shielding of B-10 is accounted for in the MCNP calculations. The calculations use a ring model that divides each B₄C column into four concentric rings of equal cross-sectional area. The radii of the boron carbide rings used in the updated analysis are shown in Table 4-12.

4.3 CONTROL ROD NUCLEAR LIFETIME

A description of the fuel bundles used for the D, C, and S lattice control rod nuclear lifetime calculations are shown in Figures 4-1 through 4-3. Both the hot and cold calculation results for the peak ¼ segment are shown in Tables 4-1 through 4-3. The cold calculation results, on which the nuclear lifetime is based, are shown graphically in Figures 4-4 through 4-6. The nuclear lifetimes, based on a cold worth equal to a cold worth reduction of 10% for an original equipment control rod are summarized in Table 4-4.

4.4 INITIAL CONTROL ROD WORTH

As discussed above, a control rod with an initial (non-depleted) reactivity worth within ±5% of the original equipment control rod is considered "matched worth" and therefore, does not require any special treatment in plant core analyses. The initial cold and hot worths (0% depletion) of the Marathon-5S control rod designs are found in Tables 4-1 through 4-3. These values of Δk/k

are then compared to the worths of the original equipment control rods in Tables 4-5 through 4-7. Although the Marathon-5S control rod has a lower initial worth than the previous Marathon control rod (Reference 1), all cold and hot initial control rod worths are within $\pm 5\%$ of the original equipment, and can be considered to be direct nuclear replacements of the original equipment.

4.5 HEAT GENERATION RATES

The capture of neutrons by boron-10 atoms results in the release of energy, or heat generation. As discussed in Section 3.6, a thermal model of the absorber tube and capsule is used to calculate boron carbide temperatures within the capsules, which affects the rate of helium release. The heat generation rates for the Marathon-5S designs are calculated assuming 2.79 MeV per neutron capture in boron-10. Then, a radial peaking factor is employed to determine the heat generation rate in the highest fluence absorber tube, which is the outermost tube.

Both average and peak heat generation rates are shown in Table 4-8. The peak heat generation rates are used in the thermal model discussed in Section 3.6 to determine the capsule boron carbide temperatures shown in Table 3-12.

4.6 CONTROL ROD MECHANICAL LIFETIME

As discussed in Section 3.6, the lifetime limiting mechanism for the Marathon-5S control rod is the pressurization of the absorber tubes due to the helium release from the irradiated boron carbide. An absorber tube mechanical limit as a function of average B-10 per cent depletion is calculated based on peak heat generation, temperatures and helium release fractions, combined with worst-case component geometries. As discussed in Section 3.6, the method for evaluating the swelling phenomenon of irradiated boron carbide is very conservative, using worst-case capsule and absorber tube dimensions, along with a $+3\sigma$ upper limit swelling rate assumption. Using these conservatisms, the Marathon-5S capsule is designed [[

]].

The calculation of the control rod mechanical lifetime limit, in terms of a four-segment average B-10 depletion, is shown in Tables 4-9, 4-10 and 4-11 for D, C, and S lattice applications. Along the top of the table is the absorber tube number, where tube 1 is the first absorber tube, welded to the cruciform tie rod. Also shown are the span-wise radial peaking factors, which show the relative absorption rate of each absorber tube. A limiting axial depletion profile is used to calculate the B-10 depletion for each absorber tube and axial node. At the bottom of the table, the average depletion for each tube is shown, along with the depletion limit for that tube, which varies depending on the number of empty capsule plenums employed at the bottom of the absorber column. Through an iterative process, the peak $\frac{1}{4}$ segment depletion is raised until the limiting absorber tube reaches its mechanical limit. The 4-segment mechanical lifetime of the control rod is then the average of the four $\frac{1}{4}$ segments.

The 4 segment mechanical lifetime limits are summarized in Table 4-4, along with the peak $\frac{1}{4}$ segment nuclear lifetime limits. [[

]]. Therefore, the nuclear lifetime of the

Marathon-5S control rod is limiting, in that the mechanical lifetime exceeds the nuclear lifetime for all cases.

4.7 CONTROL ROD DEPLETION MONITORING

The nuclear depletion calculation summarized above is performed to establish limits on the lifetime of the control rod, expressed as a maximum $\frac{1}{4}$ -segment depletion. The nodal and $\frac{1}{4}$ -segment depletions for each control rod are tracked by the core monitoring computer. For those plants that use GNF's 3D Monicore for core monitoring, control rod depletions are updated hourly.

"Quarter-segment depletion" is defined as the average depletion of nodal depletion values in a given axial $\frac{1}{4}$ segment (6 nodes) of the control rod, averaged over four wings. So for any depletion time step, there are 4 quarter-segment depletion values for a given axial depletion profile. In GEH control rod design, the nuclear lifetime is defined as the depletion value of any quarter segment at which the control rod cold worth is 10% less than the zero-depletion cold worth of the Original Equipment. "Local depletion" is normally defined as the depletion value for each absorber rod in a one-inch segment.

As part of a destructive examination of a DuraLife type control rod, the nodal depletions taken from the monitoring computer were compared to measured values from the control rod being examined. The two sets of depletions were found to be in good agreement.

Table 4-1
D Lattice Depletion Calculation Results

| Irradiation Time (days) | Equivalent B-10 Depletion (%) | Hot, Voided Eigenvalue | Hot Worth ($\Delta k/k$) | Hot Change in Worth (%) | Cold Eigenvalue | Cold Worth ($\Delta k/k$) | Cold Change in Worth (%) |
|-------------------------|-------------------------------|------------------------|----------------------------|-------------------------|-----------------|-----------------------------|--------------------------|
| [] | | | | | | | [] |

Table 4-2
C Lattice Depletion Calculation Results

| Irradiation Time (days) | Equivalent B-10 Depletion (%) | Hot, Voided Eigenvalue | Hot Worth ($\Delta k/k$) | Hot Change in Worth (%) | Cold Eigenvalue | Cold Worth ($\Delta k/k$) | Cold Change in Worth (%) |
|-------------------------|-------------------------------|------------------------|----------------------------|-------------------------|-----------------|-----------------------------|--------------------------|
| [] | | | | | | | [] |

Table 4-3
S Lattice Depletion Calculation Results

| Irradiation Time (days) | Equivalent B-10 Depletion (%) | Hot, Voided Eigenvalue | Hot Worth ($\Delta k/k$) | Hot Change in Worth (%) | Cold Eigenvalue | Cold Worth ($\Delta k/k$) | Cold Change in Worth (%) |
|-------------------------|-------------------------------|------------------------|----------------------------|-------------------------|-----------------|-----------------------------|--------------------------|
| [] | | | | | | | [] |

**Table 4-4
 Marathon-5S Control Rod Nuclear and Mechanical Depletion Limits**

| Application | End of Life B-10 Equivalent Depletion (%) | |
|--------------------|--|--|
| | Nuclear Peak Quarter Segment | Mechanical Four Segment Average |
| D Lattice, BWR/2-4 | [[| |
| C Lattice, BWR/4,5 | | |
| S Lattice, BWR/6 | |]] |

Table 4-5
Initial Reactivity Worth, D Lattice (BWR/2-4) Original Equipment and Marathon-5S CRBs

| Condition | Original Equipment $\Delta k/k$ | Marathon-5S $\Delta k/k$ | Marathon-5S Change from Original Equipment |
|------------------|---|--|---|
| Cold | [[| | |
| Hot (40% Void) | | |]] |

Table 4-6
Initial Reactivity Worth, C Lattice (BWR/4,5) Original Equipment and Marathon-5S CRBs

| Condition | Original Equipment $\Delta k/k$ | Marathon-5S $\Delta k/k$ | Marathon-5S Change from Original Equipment |
|------------------|---|--|---|
| Cold | [[| | |
| Hot (40% Void) | | |]] |

Table 4-7
Initial Reactivity Worth, S Lattice (BWR/6) Original Equipment and Marathon-5S CRBs

| Condition | Original Equipment $\Delta k/k$ | Marathon-5S $\Delta k/k$ | Marathon-5S Change from Original Equipment |
|------------------|---|--|---|
| Cold | [[| | |
| Hot (40% Void) | | |]] |

Table 4-8
Heat Generation Rates

| Application | Average Heat Generation Rate (Watts/gram B₄C) | Radial Peaking Factor | Peak Tube Heat Generation Rate (Watts/gram B₄C) |
|--------------------|---|------------------------------|---|
| D Lattice, BWR/2-4 | [[| | |
| C Lattice, BWR/4,5 | | | |
| S Lattice, BWR/6 | | |]] |

Table 4-9
D Lattice Mechanical Lifetime Calculation

[[

]]

Table 4-10
C Lattice Mechanical Lifetime Calculation

[[

]]

Table 4-11
S Lattice Mechanical Lifetime Calculation

[[

]]

Table 4-12
Boron Carbide Ring Radii in MCNP Model

| Ring Number | Ring Radial Thickness (cm) | |
|-------------|---------------------------------|---------------------------|
| | Marathon-5S, D and S Lattice | Marathon-5S, C Lattice |
| 1 (inner) | [[| |
| 2 | | |
| 3 | | |
| 4 (outer) | |]] |

Table 4-13
D Lattice Original Equipment and Marathon-5S Dimensions

| Description | | DuraLife 100 D | | Marathon-5S D | |
|---|-------------|----------------|------|---------------|------|
| | | (inches) | (cm) | (inches) | (cm) |
| Span | | [[| | | |
| Half Span | SBL | | | | |
| Wing Thickness (Square Tube Width) | | | | | |
| Half Wing Thickness | TBL | | | | |
| Tie Rod Half Thickness | TTR | | | | |
| Radius of Central Support Filet | RBLF | | | | |
| Radius of Blade Tip | RBLT | | | | |
| Span of Central Support (Tie Rod) | | | | | |
| Half Span of Central Support | SCS | | | | |
| Thickness of Sheath | TSH | | | | |
| Inner Diameter of Tube (Capsule) | TID | | | | |
| Outer Diameter of Tube | TOD | | | | |
| Wall Thickness of Tube | | | | | |
| Type | IBLADE | | | | |
| Number of B4C Tubes (Capsules) | NOPT | | | | |
| Number of Hafnium Rods | NOHFT | | | | |
| Number of Empty Tubes | NOBT | | | |]] |

Table 4-14
C Lattice Original Equipment and Marathon-5S Dimensions

| Description | | DuraLife 100 C | | Marathon-5S C | |
|---|-------------|----------------|------|---------------|------|
| | | (inches) | (cm) | (inches) | (cm) |
| Span | | [[| | | |
| Half Span | SBL | | | | |
| Blade Thickness (Square Tube Width) | | | | | |
| Half Blade Thickness | TBL | | | | |
| Tie Rod Half Thickness | TTR | | | | |
| Radius of Central Support Filet | RBLF | | | | |
| Radius of Blade Tip | RBLT | | | | |
| Span of Central Support (Tie Rod) | | | | | |
| Half Span of Central Support | SCS | | | | |
| Thickness of Sheath | TSH | | | | |
| Inner Diameter of Tube (Capsule) | TID | | | | |
| Outer Diameter of Tube (Hafnium Rod) | TOD | | | | |
| Wall Thickness of Tube | | | | | |
| Type | IBLADE | | | | |
| Number of B4C Tubes (Capsules) | NOPT | | | | |
| Number of Hafnium Rods | NOHFT | | | | |
| Number of Empty Tubes | NOBT | | | |]] |

Table 4-15
S Lattice Original Equipment and Marathon-5S Dimensions

| Description | | DuraLife 100 S | | Marathon-5S S | |
|---|-------------|----------------|------|---------------|------|
| | | (inches) | (cm) | (inches) | (cm) |
| Span | | [[| | | |
| Half Span | SBL | | | | |
| Wing Thickness (Square Tube Width) | | | | | |
| Half Wing Thickness | TBL | | | | |
| Tie Rod Half Thickness | TTR | | | | |
| Radius of Central Support Filet | RBLF | | | | |
| Radius of Blade Tip | RBLT | | | | |
| Span of Central Support (Tie Rod) | | | | | |
| Half Span of Central Support | SCS | | | | |
| Thickness of Sheath | TSH | | | | |
| Inner Diameter of Tube (Capsule) | TID | | | | |
| Outer Diameter of Tube | TOD | | | | |
| Wall Thickness of Tube | | | | | |
| Type | IBLADE | | | | |
| Number of B4C Tubes (Capsules) | NOPT | | | | |
| Number of Hafnium Rods | NOHFT | | | | |
| Number of Empty Tubes | NOBT | | | |]] |

[[

]]

Figure 4-1. D Lattice Fuel Bundle Rod Position and Enrichment

[[

]]

Figure 4-2. C Lattice Fuel Bundle Rod Position and Enrichment

[[

]]

Figure 4-3. S Lattice Fuel Bundle Rod Position and Enrichment

[[

]]

Figure 4-4. D Lattice Control Rod Cold Worth Reduction with Average Depletion

[[

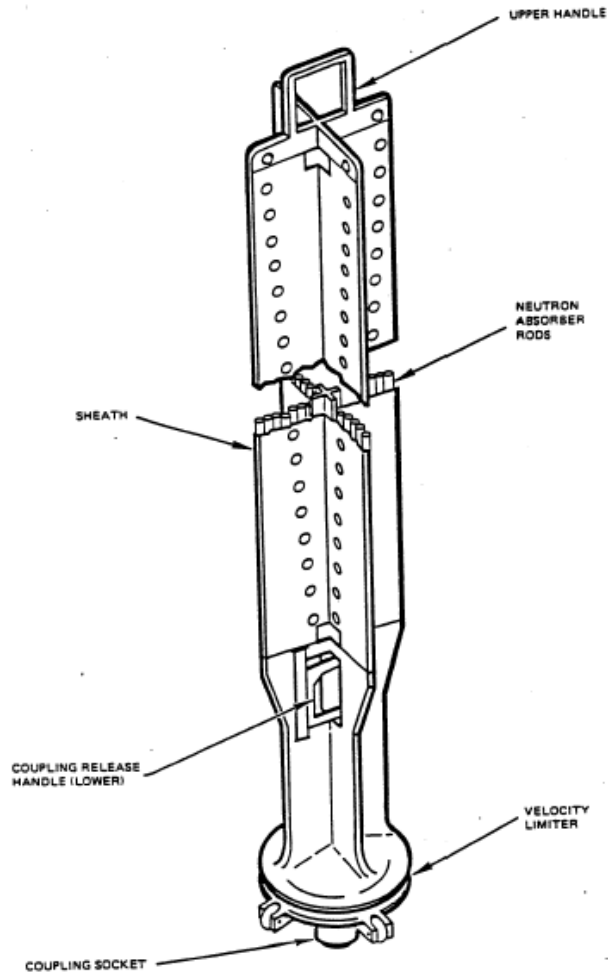
]]

Figure 4-5. C Lattice Control Rod Cold Worth Reduction with Average Depletion

[[

]]

Figure 4-6. S Lattice Control Rod Cold Worth Reduction with Average Depletion



ORIGINAL EQUIPMENT CONTROL ROD DESIGN

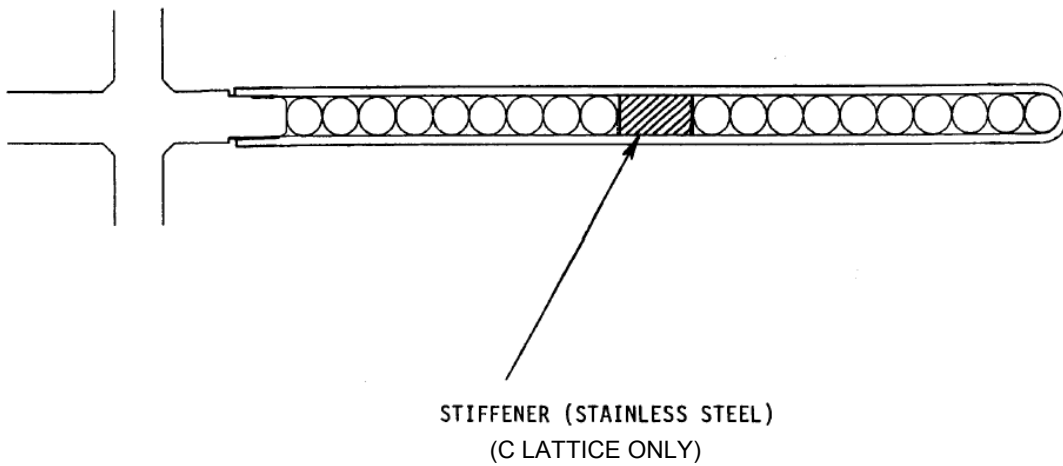


Figure 4-7. BWR/2-6 Original Equipment

5. OPERATIONAL EVALUATIONS

5.1 DIMENSIONAL COMPATIBILITY

The width of the absorber tube and the width of the control rod wing of the Marathon-5S CRB are identical to the Marathon CRB (see Table 2-1). Plus, all other envelope dimensions, including tie rod, handle, and velocity limiter are identical. Therefore, the fit and clearance of the Marathon-5S CRB in the fuel cell is identical to the Marathon CRB.

Reference 10 provides a summary of the inspection history of the Marathon control rod. For all of these inspections, no issues have been identified with respect to the lack of dimensional stability of the Marathon control rod assembly. The inspections have not shown signs of excessive wear on the control rod due to any distortion of the control rod assembly.

Therefore, the inspection history of the Marathon control rod demonstrates that the Marathon design is dimensionally stable, even with significant amounts of irradiation and residence time.

5.2 SCRAM TIMES

An OBE or SSE earthquake condition could cause the fuel channels to temporarily bow or bend. In addition, as fuel channels age, they tend to both bulge and bow, which can negatively affect the insertion capability of the control rod blade.

Previous Marathon prototype scram testing shows that the insertion capability of the CRB is affected by the stiffness of the assembly. The stiffer (less flexible) the control rod assembly, the longer the scram times. The stiffness of the Marathon-5S CRB has been evaluated to be equal to or less stiff than the Marathon CRB, in terms of the assembly cross-sectional area moment of inertia. Therefore, the Marathon-5S CRB will have a scram insertion capability equal to or better than the Marathon CRB, in the event of temporary or permanent channel deformation.

The overall assembly weight of the Marathon-5S CRB is not greater than the maximum weights of Marathon CRB designs produced. This, combined with the bending stiffness characteristics, ensure that the Marathon-5S CRB design will not have an adverse effect on scram times.

The results of seismic scram tests are discussed in section 3.4.4. As discussed, for all lattice types, the control rods successfully inserted within scram time requirements under OBE fuel channel deflection conditions, and successfully inserted under SSE fuel channel deflection conditions.

5.3 'NO SETTLE' CHARACTERISTICS

A 'no settle' condition may occur in the event of excessive friction between the control rod and the fuel channels. If this additional friction does not allow the weight of the CRB to settle the assembly into a control rod drive (CRD) positional notch, a 'no settle' condition occurs. As previously discussed, the envelope dimensions for the Marathon-5S CRB are identical to the Marathon CRB. Further, the wet (buoyant) weight of the Marathon-5S assembly is within five pounds of the lightest Marathon CRB design. Therefore, the ability of the Marathon-5S assembly to settle into a CRD notch is equal to that of the Marathon CRB.

5.4 DROP SPEEDS

The parameters that affect the drop speed of the control rod in the event of a rod drop accident are the weight of the control rod assembly, and the geometry of the “bell” of the velocity limiter. The Marathon-5S CRB uses the same cast or FabriCast (hybrid cast/fabricated) velocity limiters as those on the Duralife and Marathon CRBs. Alternately, the Marathon-5S control rod may also use a cast velocity limiter, similar to the original equipment. Because, with either velocity limiter, the weight of the Marathon-5S CRB is less than the weight of the Duralife CRBs used for the original drop tests, the Marathon-5S CRB will have drop speeds less than the [[]] required. Therefore, the Marathon-5S CRB will limit the reactivity insertion rate during a CRDA within the existing safety analysis parameters.

5.5 FUEL CELL THERMAL HYDRAULICS

The surface geometry of the Marathon-5S is different than the Marathon control rod due to the different outer absorber tube geometry. In order to evaluate the effect on the thermal hydraulics of the fuel cell, the total displaced volume of the Marathon-5S control rod is compared to the Marathon control rod, approved in Reference 1. The S lattice, BWR/6 version of these control rods are chosen for this comparison.

The total displaced volume for the Marathon control rod is [[]]. The total displaced volume of the Marathon-5S control rod is [[]], for a difference of [[]] from the Marathon control rod. This small difference is judged to be negligible in its effect on the thermal hydraulics of the fuel cell.

The topographic differences between the Marathon-5S and the Marathon control rods is less significant than the differences between the Marathon control rods and DuraLife type control rods and control rods from other vendors. These small topographic changes will have no significant effect on the thermal hydraulics of the fuel cell.

6. LICENSING CRITERIA

The NRC Safety Evaluation Report for the Marathon Control Rod Blade (within Reference 1) identifies five criteria for the licensing and evaluation of the Marathon CRB. These same five criteria are used for the Marathon-5S control rod, with the fifth criteria modified to require a surveillance program.

6.1 STRESS, STRAIN, AND FATIGUE

6.1.1 Criteria

The control rod stresses, strains, and cumulative fatigue shall be evaluated to not exceed the ultimate stress or strain of the material.

6.1.2 Conformance

As discussed in Section 3, the design changes for the Marathon-5S CRB have been evaluated using the same or more conservative design bases and methodology than the Marathon CRB. All components of the Marathon-5S control rod are found to be acceptable when analyzed for stresses due to normal, abnormal, emergency, and faulted loads. The design ratio, which is the effective stress divided by the stress limit or the effective strain divided by the strain limit, is found to be less than or equal to 1.0 for all components. Conservatism is included in the evaluation by limiting stresses for all primary loads to one-half of the ultimate strength (i.e., a safety factor of two is employed).

The fatigue usage of the Marathon-5S CRB is calculated using the same methodology as the Marathon CRB. The fatigue analysis assumes [[]]. It is found that the calculated fatigue usage is less than the material fatigue capability (the fatigue usage factor is much less than 1.0).

6.2 CONTROL ROD INSERTION

6.2.1 Criteria

The control rod shall be evaluated to be capable of insertion into the core during all modes of plant operation within the limits assumed in the plant analyses.

6.2.2 Conformance

The thickness of the wing of the Marathon-5S CRB, [[]], is identical to the Marathon CRB. Other envelope dimensions, including those for control rods with plain handles or with spacer pads, are also identical. Therefore, the fit and clearance of the Marathon-5S CRB in the fuel cell is identical to the Marathon CRB.

An OBE or SSE earthquake condition potentially could cause the fuel channels to temporarily bow or bend. In addition, as fuel channels age, they tend to both bulge and bow, which can negatively affect the insertion capability of the control rod blade.

Previous Duralife and Marathon prototype seismic scram testing has shown that the insertion capability of the CRB is affected by the stiffness of the assembly and by the assembly weight. If the control rod assembly is stiffer (less flexible), then the scram times are longer. The stiffness of the Marathon-5S CRB has been evaluated to be equal to or less stiff than the Marathon CRB, in terms of the assembly cross-sectional area moment of inertia. This, combined with the fact that the Marathon-5S assembly is lighter than previous control rod designs shows that the Marathon-5S CRB has a scram insertion capability equal to or better than the Marathon CRB in the event of temporary or permanent channel deformation.

The results of seismic scram tests are discussed in section 3.4.4. As discussed, for all lattice types, the control rods successfully inserted within scram time requirements under OBE fuel channel deflection conditions, and successfully inserted under SSE fuel channel deflection conditions.

6.3 CONTROL ROD MATERIAL

6.3.1 Criteria

The material of the control rod shall be shown to be compatible with the reactor environment.

6.3.2 Conformance

The Marathon-5S CRB uses the same materials as the Marathon CRB (see Section 3.6). No new material has been introduced. The new design absorber tubes are made from the same high purity stabilized type 304 stainless steel (Radiation Resist 304S) as the Marathon absorber tubes. Material testing and the service history of the Marathon control rod blades confirm the resistance to IASCC.

6.4 REACTIVITY

6.4.1 Criteria

The reactivity worth of the control rod shall be included in the plant core analyses.

6.4.2 Conformance

The compatibility of the Marathon-5S CRB is evaluated using the matched worth criterion approved in the Marathon CRB LTR (Reference 1); that is, replacement control rods whose initial reactivity worth is $\pm 5\% \Delta k/k$ with respect to the original equipment do not need special treatment in plant core analyses. The nuclear design of the Marathon-5S CRB meets this criterion as discussed in Section 4. Therefore, Marathon-5S CRBs can be used without change to current GEH lattice physics codes and design procedures.

6.5 SURVEILLANCE

6.5.1 Criteria

As the new design absorber tube is judged a sufficiently significant design change, a surveillance program is required.

6.5.2 Conformance

With the assistance of the BWR plant sites, GEH will monitor the depletions of installed Marathon-5S control rods and will make arrangements to visually inspect the two highest depletion Marathon-5S control rods during each refueling outage until the control rods have reached as close to end of life as practical and are removed from the high depletion locations.

Should evidence of a problem with material integrity arise; (1) arrangements will be made to inspect additional Marathon-5S control rods to the extent necessary to identify the root cause and (2) if appropriate, GEH will recommend a revised lifetime limit to the NRC based on the inspections and other applicable information.

GEH will report to NRC the status of the Marathon-5S surveillance program, including the results of all visual inspections, at least annually.

7. EFFECT ON STANDARD PLANT TECHNICAL SPECIFICATIONS

The purpose and function of control rods are discussed in the Bases sections of the standard BWR/4 and BWR/6 Standard Technical Specifications (STS), References 4 and 5. Section B3.1.3, of both states:

“...the CRD System provides the means for the reliable control of reactivity changes to ensure under conditions of normal operation, including anticipated operational occurrences, that specified fuel design limits are not exceeded. In addition, the control rods provide the capability to hold the reactor core subcritical under all conditions and to limit the potential amount and rate of reactivity increase caused by a malfunction in the CRD System.”

The nuclear worth characteristics of the Marathon-5S CRB are compatible with the core cold shutdown requirements and hot operational requirements of the original equipment control rods. This is achieved by meeting the matched worth criteria, described in the Marathon LTR (Reference 1), as a reactivity worth within $\pm 5\%$ $\Delta k/k$ of the reactivity worth of the original equipment CRB. Therefore, the Marathon-5S CRB provides the means for the reliable control of reactivity changes to ensure that under conditions of normal operation, including AOOs, specified fuel design limits are not exceeded. Furthermore, the Marathon-5S CRB provides the capability to hold the reactor core subcritical under all conditions, while meeting current Technical Specification shutdown margin requirements. The overall Marathon-5S assembly weight and velocity limiter design will limit the amount and rate of reactivity increase caused by a malfunction of the CRD system, i.e.) a Control Rod Drop Accident (CRDA).

Therefore, there is no effect on the STS from introduction of the Marathon-5S control rod blade.

8. PLANT OPERATIONAL CHANGES

The fit, form and function of the Marathon-5S CRB are equivalent to the existing Duralife and Marathon CRB designs. The Marathon-5S CRB meets all scram insertion criteria, reactivity control criteria, and CRDA.

No changes to the STS or their Bases (References 3 and 4) are needed. Therefore, it is expected that no plant-specific Technical Specifications (TS) or their Bases will require a change to implement the Marathon-5S control rod. Thus, no plant operating procedure change is expected, except for CRB replacement schedules. Therefore, the introduction of the Marathon-5S CRB has no effect on plant operations.

9. EFFECTS ON SAFETY ANALYSES AND DESIGN BASIS ANALYSIS MODELS

9.1 ANTICIPATED OPERATIONAL OCCURRENCES AND OTHER MALFUNCTIONS

As previously discussed, the reactivity worth of the Marathon-5S CRB is an equivalent replacement for previous control rod designs. Furthermore, the Marathon-5S CRB meets all scram time criteria. Therefore, use of the Marathon-5S CRB does not adversely affect the mitigating response function (i.e., scram) for AOOs.

Introduction of the Marathon-5S CRB is unrelated to the initiating events of the analyzed AOOs, and thus, the probabilities of the different AOOs occurring are unaffected.

Because the Marathon-5S CRB meets the existing design and licensing requirements for Marathon CRBs, the probability of any CRB-related malfunction or of causing a malfunction is not increased, and no new malfunction scenario is created.

The introduction of the Marathon-5S CRB does not (1) introduce a new failure mode or sequence of events that could result in the MCPR safety limit being challenged, (2) cause a 10 CFR 50.2 design bases criterion or limit to be changed or exceeded (such that a safety-related function is adversely affected), (3) create a possibility of a new safety-related component interaction. Therefore, the change does not create a possibility for a malfunction of equipment important to safety different than previously evaluated.

In the safety analyses, the equipment modeled or assumed to function for mitigating the radiological consequences of all design basis abnormal events is not affected by the use of Marathon-5S CRBs. Therefore, the analyzed consequences of the malfunctions in plant Safety Analysis Reports are not affected.

9.2 ACCIDENTS

The ECCS-LOCA performance, LOCA radiological, containment performance, and Main Steamline Break Accident (MSLBA) analyses all assume reactor scram within Technical Specifications requirements, and these are met by Marathon-5S CRBs. The Engineered Safety Feature (ESF) functions, which are modeled/assumed in the accident radiological consequence analyses, are also not affected by the use of Marathon-5S CRBs. Therefore, these analyses' models, scenarios, and the final radiological consequences are not affected.

The failures assumed in the initiating events for the LOCA and MSLBA are not related to the CRBs, and thus, the probabilities of these accidents occurring are not affected.

Other than the event evaluation assumption that the CRBs maintain structural integrity, the Fuel Handling Accident (FHA) initiating event and its related mitigation functions do not involve the CRBs. Therefore, the probability and consequences of a FHA are unaffected.

There is no additional friction between the Marathon-5S CRB relative to the Marathon CRB, and the CRD coupling mechanism is unchanged. Therefore, the probability of a stuck and decoupled

control rod occurring does not change, and thus, the probability of a CRDA cannot significantly increase.

The reactivity insertion rate during a CRDA is controlled by the weight of the control rod and by the shape of the velocity limiter. The Marathon-5S CRB remains within all rod drop parameters assumed or modeled in the safety analysis. Therefore, the analysis and consequences of a CRDA are unchanged.

The change to Marathon-5S CRBs does not create a new fission product release path, result in a new fission product barrier failure mode, or create a new sequence of events that results in significant fuel cladding failures. Therefore, the use of Marathon-5S CRBs cannot create an accident of a different type.

9.3 SPECIAL EVENTS

The ATWS event assumes a failure to scram (without a specific cause) and that the Standby Liquid Control System is used for reactor shutdown. Therefore, the ATWS analysis scenario and results are independent of control rod blade design, and thus, the ATWS analysis is unaffected.

The station blackout, shutdown from outside control room, and safe shutdown fire analyses all assume reactor scram within TS requirements, which are not affected by the use of Marathon-5S CRBs. The other safe shutdown functions, which are modeled/assumed in the analyses, are also not related to or affected by the use of Marathon-5S CRBs. Therefore, these analyses' models, scenarios, and the final results are not affected.

9.4 FISSION PRODUCT BARRIER DESIGN BASIS LIMITS

During all design basis events, Marathon-5S CRB performance is equal to or better than existing CRBs. The margins to the thermal limits on fuel cladding, Minimum Critical Power Ration (MCPR) Safety Limit, Reactor Coolant Pressure Boundary stress limits (e.g., temperature and pressure), and containment structural stress limits are unaffected by the use of Marathon-5S CRBs. Therefore, the fission product barrier design basis limits are not affected.

9.5 SAFETY AND DESIGN BASIS ANALYSIS MODELS

Marathon-5S CRB implementation does not change any safety analysis input, model, or result. No design analysis methodology change is used or needed in the design of the Marathon-5S CRB. Therefore, this change does not involve a departure from a method of evaluation used in establishing a design basis or in a safety analysis

10. HAFNIUM NEUTRON ABSORBER OPTION

In the future, hafnium may be offered as an optional neutron absorber material in high absorption rate absorber tubes. As was approved for the original Marathon control rod in Reference 1, the hafnium will be in the form of a rod, sealed inside the absorber tube. However, before the hafnium option is offered, a related technical safety evaluation shall demonstrate that the hafnium containing control rods meet all the safety, design and operational acceptance criteria presented within the report.

11. SUMMARY AND CONCLUSIONS

The Marathon Marathon-5S control rod blade is designed as an acceptable direct replacement control rod for BWR/2-6. Conservative mechanical evaluations show acceptability of the control rod structure. Conservative nuclear analyses show that the Marathon-5S is a 'matched worth' control rod and is interchangeable with the original equipment.

Operational evaluations show no adverse effect on plant operations, including control rod scram, 'no settle' characteristics, and control rod drop.

The Marathon-5S control rod, which is a derivative of the Marathon design, meets all licensing acceptance criteria of the Marathon design (Reference 1).

The introduction of the Marathon-5S CRB does not affect the Standard Technical Specifications (References 3 and 4) or their Bases, any plant safety analysis, or any plant design basis. In addition, no adverse effect is found when examining safety analyses and design basis analysis models. The Marathon-5S CRB meets all applicable design and regulatory requirements. Therefore, the use of the Marathon-5S CRB is judged to be acceptable.

12. REFERENCES

1. GE Nuclear Energy, "GE Marathon Control Rod Assembly," NEDE-31758P-A, GE Proprietary, October 1991.
2. GE Nuclear Energy, "Safety Evaluation of the General Electric Duralife 230 Control Rod Assembly," NEDE-22290-P-A Supplement 3, GE Proprietary, May 1988.
3. MNCP4A – A General Monte Carlo N-Particle Radiation Transport Code, Version 4A, LA-12625, March 1994.
4. USNRC, "Standard Technical Specifications General Electric Plants, BWR/4," NUREG-1433 Vol. 1 & 2, Revision 3.0, June 2004.
5. USNRC, "Standard Technical Specifications General Electric Plants, BWR/6," NUREG-1434 Vol. 1 & 2, Revision 3.0, June 2004.
6. 1989 ASME Section III, Division 1, Appendix I, Figure I-9.2.1.
7. JA Bannantine, JJ Comer and JL Handrock, 'Fundamentals of Metal Fatigue Analysis', Prentice Hall, 1990.
8. BWR Vessel and Internals Project: Fracture Toughness and Tensile Properties of Irradiated Austenitic Stainless Steel Components Removed from Service (BWRVIP-35)," EPRI TR-108279, June 1997.
9. BWR Vessel and Internals Project: Review of Test Data for Irradiated Stainless Steel Components (BWRVBIP-66)," EPRI TR-112611, March 1999.
10. MFN 07-138, "Marathon Control Rod Assembly Surveillance Program Status", February 26, 2007.
11. *Mechanical Behavior of Materials*, F. A. McClintock and A. S. Argon, pages 277-278, Addison-Wesley Publishing Company, Inc., 1966.
12. "Boiling Water Reactor Vessel and Internal Project: Crack Growth Rates in Irradiated Stainless Steels in BWR Internal Components (BWRVIP-99)", EPRI TR 1003018 Final Report, December 2001.

APPENDIX A – PLAIN HANDLE EVALUATION

GEH currently recommends the use of plain, roller-less handles for our ‘C’ Lattice (BWR/4,5) and ‘S’ Lattice (BWR/6) Marathon Control Rod Blades (CRBs). While the majority of our operational history with the pin-and-roller design, which dates to at least the 1970’s, has been very positive, on a few occasions, GEH has had reported cracking at the handle pin-hole. The pin to pin-hole interface represents a crevice condition, which is a potential corrosion concern. Extensive investigation of the handle cracking has led to several improvements in the manufacturing process, but the pin and roller design inherently transfers cracking prevention to control of processes. Therefore, the potential for cracking cannot be unconditionally eliminated with the current pin and roller design. It is, however, eliminated with the plain handle design.

A-1 PLAIN HANDLE DESCRIPTION

With the plain handle control rod blade design, the handle pins and rollers and associated holes are eliminated, leaving the flat plate material of the handle intact, as shown in Figure A-1.

A-1.1 Fuel Channel and CRB Dimensions

In-service CRBs travel in the gap between fuel bundle channels. The dimensions of this gap vary with the type of fuel channel employed. Three cases for ‘C’ Lattice applications are shown in Figure A-2. Two cases for ‘S’ Lattice applications are shown in Figure A-3.

As shown in Figure A-2 for ‘C’ Lattice BWR/4,5 control rods, the protrusion of the handle roller from the face of the handle is nominally [[]]. Therefore, for uniform thick channels, a plain handle control rod is able to lean up to [[]] closer to one set of fuel channels than the same control rod with handle rollers. For thick/thin channels (120/75 and 100/65/50), removal of the roller has no effect nominally, because the roller protrusion is less than the depth of the channel ‘groove’ (see Figure A-2) so the CRB is supported by the thicker ‘corner’ of the fuel channel.

As shown in Figure A-3 for ‘S’ Lattice BWR/6 control rods, the protrusion of the handle roller from the face of the handle is nominally [[]]. Therefore, for uniform thick channels, a plain handle control rod is able to lean up to [[]] closer to one set of fuel channels than the same control rod with handle rollers. For 120/75 thick/thin channels, removal of the roller has no effect nominally, because the roller protrusion is less than the depth of the channel ‘groove’ (see Figure A-3) so the CRB is supported by the thicker ‘corner’ of the fuel channel.

GEH evaluated the nuclear effect of eliminating the handle pins and rollers for both C and S lattice applications. The review considered two possible effects: (1) the effect of the control rod leaning closer to one set of fuel bundles, (2) the effect of additional stainless steel due to not having drilled roller holes in the handle.

The conclusion for the effect of the small amount of lean of the control rod was that the effect of leaning slightly closer to one set of fuel bundles would be offset by leaning slightly further away from the opposite set of fuel bundles. The conclusion is that the net effect would not be observable in any neutron transport calculation performed.

The evaluation of the additional stainless steel in the handle plate concluded that the effect would be offset by the removal of the handle rollers. The evaluation concluded that even if the entire core of control rods were replaced with plain handles, no net change in reactivity would be expected.

A-1.2 Handle Vertical Position

In order to determine if removal of the handle rollers creates the opportunity for the CRB to ‘snag’ or ‘hang-up’ during insertion or withdrawal, the position of the handle relative to the fuel channel is examined.

For ‘C’ Lattice, BWR/4,5 applications, when fully withdrawn, the top of the absorber section (absorber section to handle weld) is a minimum [[]] above the bottom of the fuel channel. When fully inserted, the top of the extended handle is a minimum [[]] below the top of the fuel channel.

For ‘S’ Lattice, BWR/6 applications, when fully withdrawn, the top of the absorber section (absorber section to handle weld) is a minimum [[]] above the bottom of the fuel channel. When fully inserted, the top of the handle is a minimum [[]] below the top of the fuel channel.

Therefore, for both ‘C’ and ‘S’ Lattice applications, the handle remains within the axial (vertical) bounds of the fuel channel throughout its insertion or withdrawal stroke. Because the fuel channels have only smooth transitions in the axial direction, there are no opportunities for the control rod to ‘snag’ or ‘hang-up’ during insertion or withdrawal.

A-1.3 Effect of Channel Bulge

As fuel channels age, they can bulge outward at the fuel channel centerline. As can be seen in Figure A-4, the position of the roller is offset [[]] from the centerline of the fuel channel for both ‘C’ Lattice and ‘S’ Lattice applications. The offset and roller diameter were designed so that in the case of excessive bulge, the fuel channels would bind inboard of the roller rather than on the roller itself. This has been confirmed by inspections done on control rods from fuel cells with highly bulged channels which have shown contact occurring inboard of the roller. Also note that, if the roller were to be impinged by the channels on both sides, the roller would not rotate but ‘skid’ or slide. Because of this, there is no negative effect from the removal of the handle rollers on the performance of the CRB in fuel cells with highly bulged channels.

A-1.4 Friction and Wear

Lateral loads on the handle rollers were determined during testing of alternate roller materials. The tests showed that the lateral loads on the rollers were small, typically between [[]], with a maximum of [[]]. To determine the axial friction load at this contact, the lateral load is multiplied by a friction coefficient between stainless steel and zircaloy (fuel channels) of [[]] (see Figure A-5). This results in a maximum axial friction load of [[]]. For conservatism, this load is rounded up to [[]], which is much less than control rod drive normal insertion and scram forces. Therefore, removal of the handle rollers has no significant effect on normal insertion, or on scram speeds and times.

GEH has completed seismic scram testing for the Marathon-5S control rod. This test uses a simulated reactor pressure vessel, including fuel bundles and other reactor internals. In the test, the core plate is oscillated to produce fuel bundle oscillation that would be experienced during a seismic event.

The Marathon-5S prototypes used for the test incorporated plain, roller-less handles. The acceptance criterion for the test was that scram time requirements were to be met up to fuel bundle oscillation consistent with an OBE (Operational Basis Earthquake) event. The results of the tests were very successful, in that scram time requirements were met through the much more severe SSE (Safe Shutdown Earthquake) event for both the C lattice and S lattice applications. This is further evidence that the implementation of the plain, roller-less handle will not degrade the ability of the control rod to scram.

Fuel cells with highly bulged and/or bowed channels can experience a 'no settle' condition in which the CRB does not settle into a control rod drive notch due to increased friction. [[

]]. Therefore, removal of the handle rollers does not exacerbate a 'no settle' condition.

[[

]]. Therefore, wear between the fuel channel and the control rod is not a concern.

A-1.5 Reactor Clearances

As noted above, for uniform thickness channels, removal of the handle rollers allows the CRB to lean closer to one set of fuel channels. All clearances potentially impacted by this increased lean have been examined for 'C' and 'S' Lattice applications. Sufficient clearances are demonstrated for all reactor components, including the top guide and the orificed fuel support.

A-1.6 Plain Handle CRB Experience

As of July 2007, GEH Nuclear Energy has delivered over 248 plain handle CRBs to BWRs world-wide since 1990. Operational experience from these BWRs has shown no excessive friction, wear or functional concerns.

Table A-1 contains a list of 16 visual inspections of plain handle Marathon control rods at an international BWR. As shown, the inspections have not identified any issues with the plain handle design. There has been no reported cracking, neutronics problems, corrosion, excessive crud formation, nor any other unanticipated or anticipated problems or degradation at any location. Because this reactor has similar internal dimensions to domestic 'C' Lattice GEH BWRs, this experience shows that plain handle CRBs will perform their functions without issue in domestic 'C' Lattice reactors.

A-1.7 Conformance to Design Requirements

The effect of the plain handle design on the following design requirements is evaluated for 'C' Lattice and 'S' Lattice Marathon CRBs.

A-1.7.1 Dimensional Compatibility with Fuel Assemblies

Because the handle roller is the widest component of the absorber wing, removal of the handle pins and rollers will not cause the control rod to exceed maximum allowable control rod wing thicknesses.

A-1.7.2 Dimensional Compatibility with Orificed Fuel Support

The clearance between the control rod and the orificed fuel support has been evaluated throughout the control rod stroke. The small amount of additional lean that the control rod may experience is unlikely to cause contact between the control rod and the fuel support. The likelihood for contact between the plain handle 'C' Lattice CRB and the orificed fuel support is less than 0.3 % when inserted adjacent to 80 mil thick uniform channels. For other 'C' Lattice channels and all 'S' Lattice applications, this likelihood is significantly less.

A-1.7.3 Insertion Capability

Elimination of the handle pins and rollers does not adversely affect the ability of the control rod to be inserted during normal or upset conditions. The amount of axial friction added by introduction of the plain handle [[]] does not prevent control rod insertion. Section A-1.4 discusses the results of seismic scram tests for plain handle Marathon-5S control rods, which show that the introduction of plain, roller-less handles will not degrade the insertion capability of the control rod.

A-1.7.4 Scram Time Performance

Introduction of the plain handle control rod does not adversely affect scram speeds or times as the amount of added friction and mass is not significant when compared to control rod drive scram forces.

A-1.7.5 Flow Induced Vibrations (FIV)

The effect of removal of the handle rollers on the likelihood of experiencing flow-induced vibration of inserted control rods has been evaluated analytically. The conclusion is [[

]]. Therefore, the removal of the handle rollers results in no adverse change in control rod FIV.

A-1.7.6 Normal Operation and Transient Loading

The maximum additional axial load due to removal of the handle rollers does not cause the control rod to exceed its design criteria.

A-2 PLANT OPERATIONAL CHANGES

As discussed above, the function of the 'C' Lattice and 'S' Lattice Marathon CRB is unaffected by the removal of the handle rollers. There is no significant effect on scram speeds and times, and no significant effect on normal insertion or withdrawal. All clearances potentially affected by removal of the handle rollers have been evaluated and no interference with any plant components occurs.

No Technical Specification or Bases change is needed, and thus, no plant operating procedure change is expected. Therefore, the removal of the handle pins and rollers has no effect on plant operations.

A-3 EVALUATION OF POTENTIAL AREAS OF CONCERN

Safety Functions

The safety functions of the control rods are to:

- shut down the reactor and maintain the reactor in a shutdown condition with adequate shutdown margin, per the plant TS limits, during and following normal operation, Anticipated Operational Occurrences (AOOs) and accidents;
- allow for rapid insertion (i.e., scram function) of all control rods within TS scram time limits, during all design basis events (i.e., normal operation, AOOs and accidents); and
- limit the reactivity insertion rate during a Control Rod Drop Accident (CRDA).

The nuclear control rod worth is determined by the neutron absorbing material (e.g., B₄C, Hafnium) content and distribution (e.g., control rod capsule distribution), which are unaffected by the use of plain handles. The use of plain handles does not affect the structural integrity of the control rods. Therefore, the use of plain handle CRBs does not affect ability of the control rods to shutdown the reactor and maintain the reactor in a shutdown condition, per the plant TS limits.

As discussed previously, the plain handle CRB has no significant effect on scram speeds or times, and compliance with TS scram time limits is not adversely affected. Therefore, the use of plain handle CRBs does not affect the control rod scram function, during all design basis events.

The reactivity insertion rate during a CRDA is controlled by the weight of the control rod and by the shape of the velocity limiter, which are not changed. Therefore, the use of plain handle control rods does not affect the reactivity insertion rate during a CRDA.

Design Requirements and Limits

As discussed in Section A-1.7, the only design requirements and limits potentially affected by the use of plain handles are: dimensional compatibility with fuel assemblies and the fuel support, insertion capability, scram time performance, flow induced vibrations, and normal and transient loadings. None of these design requirements and limits are violated by the plain handle design. Therefore, the structural integrity and qualification of the Marathon CRB are not affected.

Acceptance Criteria

As discussed in Section A-5, below, the plain handle control rod meets all acceptance criteria from the Marathon CRB Safety Evaluation Report (Reference 1).

Control Rod Drive Reliability

The effect on the control rod drive reliability is minimal, because the added axial loads are very small [[]] when compared to the axial loads experienced by the control rod drive.

Materials Compatibility

No new material is introduced by changing to plain handles. GEH inspection experience shows that the rubbing contact, which normally occurs between stainless steel control rods and Zircaloy fuel channels, results in minimal material wear.

Clearance Requirements

All control rod clearances with reactor internals have been thoroughly investigated. No clearance or fit issue is created as a result of the introduction of plain handle CRBs.

Response Time Requirements

As previously discussed, removal of the handle pins and rollers has no significant effect on scram speeds or times, nor on normal control rod insertions and withdrawals.

Flow Induced Vibrational Effects

The potential for flow induced vibrational effects from the use of CRBs has been investigated, and there is no adverse change in control blade vibration. Therefore, there is no adverse vibrational effect related to the removal of the handle rollers.

Potential for Increased Erosion, Corrosion or IGSCC

Elimination of the handle pins and rollers has no negative effect on the potential for increased erosion, corrosion, or Intergranular Stress Corrosion Cracking (IGSCC) of the Marathon square tubes. It does, however, eliminate the potential for IGSCC of the handle at the pin-hole locations.

A-4 EFFECT ON GENERIC PLANT TECHNICAL SPECIFICATIONS

The purpose and function of control rods are discussed in the Bases sections of the standard BWR/4 and BWR/6 Technical Specifications (References 3 and 4). In section B 3.1.3, it states:

“...the CRD System provides the means for the reliable control of reactivity changes to ensure under conditions of normal operation, including anticipated operational occurrences, that specified fuel design limits are not exceeded. In addition, the control rods provide the capability to hold the reactor core subcritical under all conditions and to limit the potential amount and rate of reactivity increase caused by a malfunction in the CRD System.”

The removal of the handle pins and rollers adds a small amount of friction [[]] to the insertion or withdrawal of the CRBs. This amount of friction does not impede the normal insertion or withdrawal of the control rods, nor does it affect the operation of the control rod drive. Therefore, transitioning to the plain handle control rod has no negative effect on the ability of the CRD system to control reactivity changes under any condition. Further, this added friction has no significant effect on scram speeds or times or on the ability to insert the control rod. Because there also is no significant change to the nuclear worth of the blade, the ability of the control rods to maintain the reactor subcritical is unaffected.

A-5 EFFECT ON LICENSING BASIS

The Safety Evaluation Report for the Marathon Control Rod Blade (within Reference 1) identifies five criteria for the licensing and evaluation of the Marathon CRB. The impact of incorporating plain handle on each of the five criteria is evaluated below.

The control rod stresses, strains, and cumulative fatigue shall be evaluated to not exceed the ultimate stress or strain of the material.

The effect of handle roller removal on control rod stresses, strains and cumulative fatigue have been thoroughly evaluated, and have been found to not exceed the ultimate stress or strain of the materials. The plain handle control rod would not fail because of loads due to shipping, handling, and normal, abnormal, emergency and faulted operating modes. Removal of the handle pins and rollers has no significant effect on axial loads, as the amount of added friction is small. Removal of the handle pins and rollers has no effect on the stress and strain experienced by the square tubes due to B₄C depletion, which is the limiting factor on the mechanical lifetime of the Marathon CRB.

The control rod shall be evaluated to be capable of insertion into the core during all modes of plant operation within the limits assumed in the plant analyses.

The original purpose of the handle rollers was to help guide the control rod between the fuel channels. An evaluation of reactor internal geometries has concluded that there is no interference or fit issue related to the plain handle control rod.

Because of the small amount that the control rod can lean in the channel gap, the lateral loads, and therefore the axial friction loads are small [[]]. This small amount of added friction has no significant effect on scram speeds and times. Neither does this small additional axial load impede normal insertion or withdrawal, nor does it result in a 'no settle' condition in which the control rod drive is unable to settle into the appropriate notch.

In the case of excessively bulged or bowed channels, [[

]]. Therefore, removal of the handle pins and rollers has no adverse effect on the amount of friction experienced in fuel cells with excessively bulged or bowed channels.

An Operational Basis Earthquake (OBE) or Safe Shutdown Earthquake (SSE) condition could cause the fuel channels to temporarily bow or bend. The impact on the control rod – channel interaction is similar to the bulged and bowed channel condition previously discussed. [[

]]. In the event of impingement on the rollers, the rollers would not roll, but slide or skid resulting in friction similar to the plain handle control rod. Therefore, there is no adverse effect on response to an OBE or SSE event from the removal of the control rod handle rollers.

The material of the control rod shall be shown to be compatible with the reactor environment.

Because no new materials are introduced to the control rod by deleting the handle pins and rollers, all CRB materials remain compatible with the reactor environment.

Elimination of the handle rollers results in a small amount of additional rubbing contact between the stainless steel of the control rod, and the Zircaloy fuel channels. GEH's inspection experience from highly bulged and bowed channels has shown that this rubbing results in very little wear on the control rod or on the fuel channel.

The reactivity worth of the control rod shall be included in the plant core analyses.

Elimination of the handle pins and rollers has no effect on vertical position of the neutron absorbing materials. Removal of the rollers may allow the control rod to experience slightly more lean within the fuel cell. A nuclear analysis has concluded that any additional lean of the control rod would have an insignificant effect on the nuclear worth of the CRB.

Prior to the use of new design features on a production basis, lead surveillance control rods may be used.

In the Marathon CRB Safety Evaluation Report (Reference 1), GEH commits to using lead surveillance control rods if a design change impacts the form or function of the control rod assembly, or if new absorber or other materials are used which have not been previously used in reactor cores. As discussed above, removal of the handle pins and rollers has no effect on the form or function of the control rod assembly, and no new materials have been introduced. Therefore, the use of lead surveillance control rods is not required. However, as discussed in Section A-1.4, GEH has supplied over 100 roller-less handle control rod blades to European BWRs, with no reported issues.

A-6 EFFECTS ON SAFETY ANALYSES AND DESIGN BASIS ANALYSIS MODELS

Anticipated Operational Occurrences and Other Malfunctions

Because the use of plain handled CRBs, does not adversely affect the control rod reactivity worth or its scram time, the mitigating response function (i.e., scram) to AOOs is not affected. Therefore, plant AOO (i.e., transient) analyses are unaffected.

The change to plain handled CRBs is unrelated to the initiating events of the analyzed AOOs, and thus, the probabilities of the different AOOs occurring are unaffected.

Because plain handled CRBs meet the existing design and licensing requirements for Marathon CRBs, the probability of any CRB related malfunction or of causing a malfunction is not increased, and no new malfunction scenario is created.

The change to plain handles does not (1) introduce a new failure mode or sequence of events that could result in the MCPR safety limit being challenged, (2) cause a 10 CFR 50.2 design bases criterion to be exceeded (such that a safety-related function is adversely affected), or (3) create possibility of a new safety-related component interaction. Therefore, the change does not create a possibility for a malfunction of equipment important to safety different than previously evaluated.

Accidents

The ECCS-LOCA performance, LOCA radiological, Containment performance and Main Steamline Break Accident (MSLBA) analyses all assume reactor scram within TS requirements, which is not affected by the use of plain handled CRBs. The Engineered Safety Features (ESF) functions, which are modeled/assumed in the accident radiological consequence analyses, are also not related to or affected by the use of plain handled CRBs. Therefore, these analyses' models, scenarios and the final radiological consequences are not affected.

The failures assumed in the initiating events for the LOCA and MSLBA are not related to the CRBs, and thus, the probabilities of these accidents occurring are not affected.

Other than assuming that the CRBs maintain structural integrity, the fuel handling accident (FHA) initiating event and its related mitigation functions do not involve the CRBs. Therefore, the probability and consequences of a FHA are unaffected.

The change in the normal friction force due to the use of the plain handles is judged to be insignificant. The change in handle design is not related to the capability for a control rod to remain coupled to its control rod drive. Therefore, the probability of a stuck and decoupled control rod occurring does not significantly change, and thus, the probability of a CRDA cannot significantly increase.

The reactivity insertion rate during a control rod drop accident (CRDA) is controlled by the weight of the control rod and by the shape of the velocity limiter, which are not affected by the use of a plain handle. The safety-related functions that mitigate the radiological consequences of a CRDA are not related to any CRB handle design. Therefore, the analysis and consequences of a CRDA are unchanged.

The change to CRBs does not allow for a new fission product release path, result in a new fission product barrier failure mode, or create a new sequence of events that results in significant fuel cladding failures. Therefore, the use of plain handles cannot create an accident of a different type.

Special Events

The ATWS event assumes a failure to scram (without a specific cause) and that the Standby Liquid Control System is used for reactor shutdown. Therefore, the ATWS analysis scenario and results are independent of control rod blade handle design, and thus, the ATWS analysis is unaffected.

The station blackout, shutdown from outside control room and safe shutdown fire analyses all assume reactor scram within TS requirements, which is not affected by the use of plain handled CRBs. The other safe shutdown functions, which are modeled/assumed in the analyses, are also not related to or affected by the use of plain handled CRBs. Therefore, these analyses' models, scenarios and the final results are not affected.

Safety and Design Basis Analysis Models

No new analysis methodology is used or needed in the design change to plain handles. Therefore, this change does not involve a departure from a method of evaluation used in establishing a design basis or in a safety analysis.

A-7 SUMMARY AND CONCLUSIONS

The introduction of plain, roller-less handle, 'C' Lattice and 'S' Lattice Marathon control rod blades does not affect the standard plant Technical Specifications or their Bases, any plant safety analysis or any plant design basis. In addition, no adverse effect is found when examining potential areas of concern. Plain handle Marathon CRBs continue to meet all applicable and existing design and regulatory requirements. Therefore, the use of plain handle Marathon CRBs is found to be acceptable.

NEDO-33284-A Revision 2
Non-Proprietary Information

**Table A-1
Plain Handle Control Rod Inspection Results**

| Manufacture Year | Inspection Date | ¼ Segment % Depletion | ¼ Segment % Depletion Limit | % of Nuclear Life | Inspection Results |
|-------------------------|------------------------|------------------------------|------------------------------------|--------------------------|---------------------------|
| 1990 | 7/92 | [[| | ~0 | No issues identified |
| 1990 | 9/93 | | | ~0 | No issues identified |
| 1993 | 9/95 | | | 19% | No issues identified |
| 1993 | 9/96 | | | 33% | No issues identified |
| 1993 | 9/97 | | | 49% | No issues identified |
| 1993 | 7/98 | | | 65% | No issues identified |
| 1996 | 2/99 | | | Unknown | No issues identified |
| 1993 | 3/00 | | | 65% | No issues identified |
| 1993 | 4/01 | | | 65% | No issues identified |
| 1996 | 9/03 | | | 56% | No issues identified |
| 2000 | 9/03 | | | 13% | No issues identified |
| 2000 | 9/03 | | | 25% | No issues identified |
| 2000 | 9/03 | | | 16% | No issues identified |
| 1996 | 9/04 | | | 58% | No issues identified |
| 2000 | 9/04 | | | 47% | No issues identified |
| 2000 | 9/04 | |]] | 47% | No issues identified |

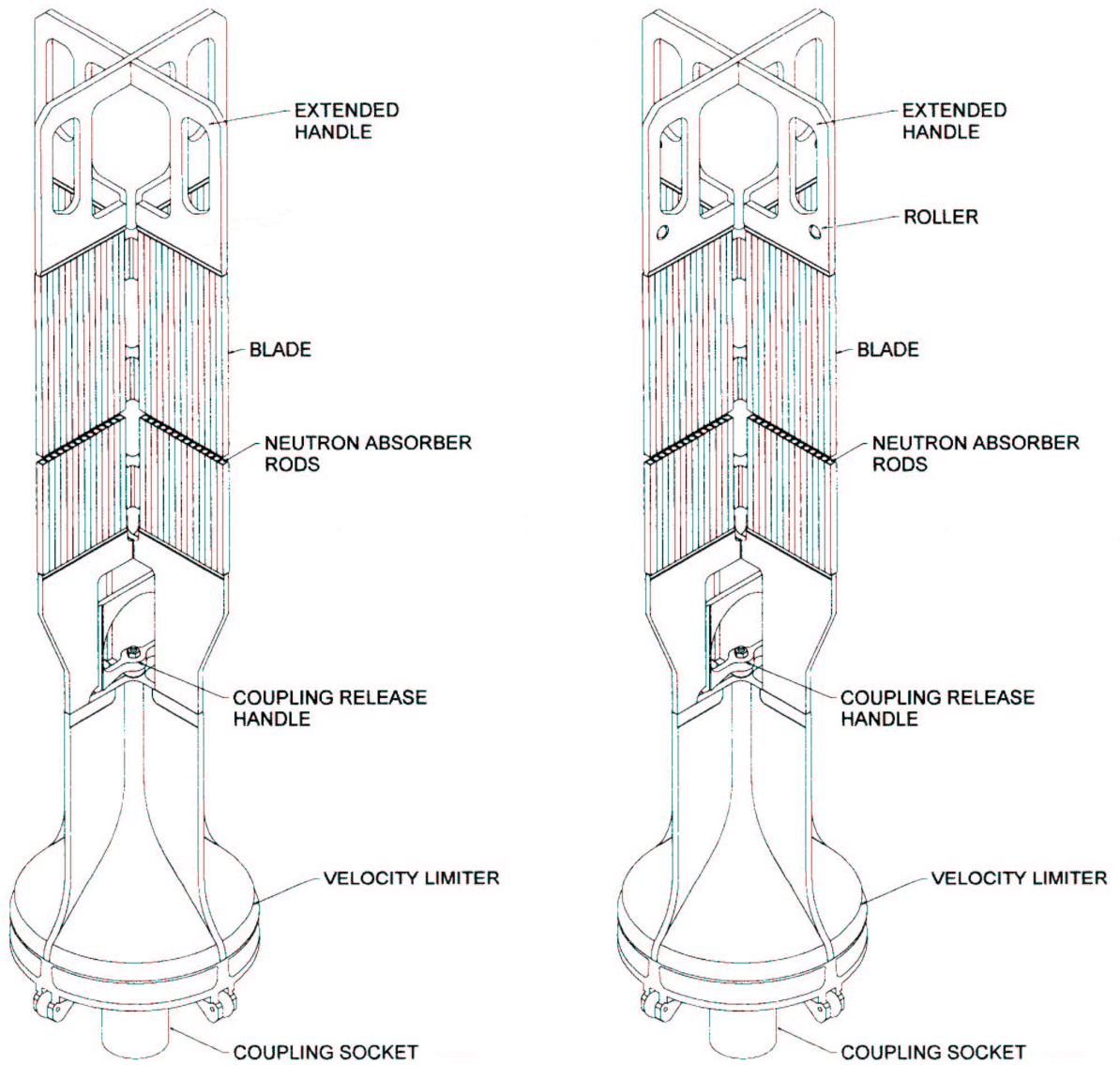


Figure A-1. Plain and Roller Handle Marathon CRBs
(‘C’ Lattice Extended Handle Shown)

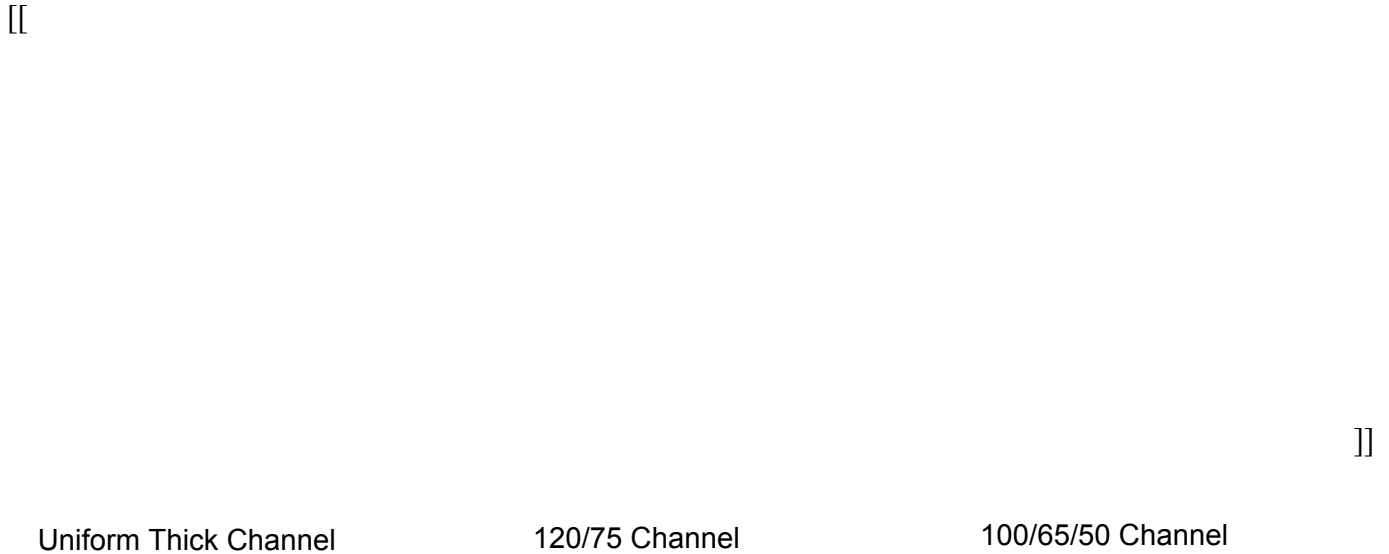


Figure A-2. GEH 'C' Lattice (BWR/4,5) Fuel Channel Gap Dimensions
(Not to Scale)



Figure A-3. GEH 'S' Lattice (BWR/6) Fuel Channel Gap Dimensions
(Not to Scale)

[[

]]

Figure A-4. GEH 'C' Lattice (BWR/4,5) and 'S' Lattice (BWR/6) Channel Bulge
(Not to Scale)

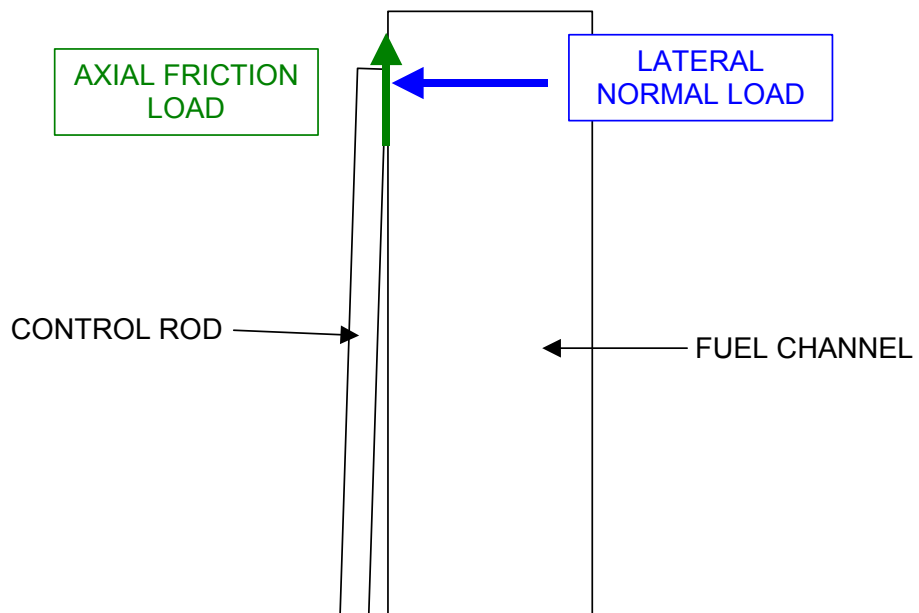


Figure A-5. Diagram of Lateral and Axial Friction Loads on the Control Rod
(Control Rod Lean Exaggerated)

APPENDIX B – FAILED BUFFER SCRAM STRESS EVALUATION

Failed buffer scram stress calculations for all cross-sections shown in Figures 3-1 and 3-2 are shown in Table 3-5 through 3-7. During a control rod scram, large axial loads are imparted on the control rod. These axial loads are determined using a dynamic spring and mass model, the results of which are presented in Table 3-4. For this analysis, the scram loads are determined assuming a 100% inoperative control rod drive buffer. The following cross-sections are analyzed.

B-1 SOCKET MINIMUM CROSS-SECTIONAL AREA (FIG. 3-1)

The minimum cross-sectional area of the socket is calculated from the drawing to be [[]]. Actual and allowable stress calculations are shown in Table B-1. As shown, all design ratios are less than 1.0. Therefore, the structure is acceptable.

B-2 SOCKET TO TRANSITION PIECE WELD (FIG. 3-1)

The socket to transition piece weld is a full penetration groove weld. It joins the XM-19 socket to the type 316 transition piece, with ER 308L filler metal required. The minimum cross-sectional area is shown in Table B-2. Table B-3 calculates the actual and allowable stresses for this weld. As shown, all design ratios are less than 1.0. Therefore, the weld is acceptable.

B-3 VELOCITY LIMITER TRANSITION PIECE TO FIN WELD (FIG. 3-1)

The transition piece to fin welds are double fillet welds, joining the type 316 transition piece and fins, with ER 308L filler metal required.

For the calculation of the area of these welds, only the vertical portions of the welds are considered. The angled portions of the welds are conservatively neglected (Figure 3-1). Also, since the welds are in shear, the resulting area is multiplied by $(1/\sqrt{3})$ to calculate an equivalent normal area. The minimum equivalent normal weld area is calculated to be [[]].

Table B-4 shows the actual and allowable stresses for this weld. As shown, all design ratios are less than 1.0. Therefore, the weld is acceptable.

B-4 VELOCITY LIMITER FIN MINIMUM CROSS-SECTIONAL AREA (FIG. 3-1)

The minimum cross-sectional area of the fins is calculated from the drawing to be [[]]. Actual and allowable stress calculations are shown in Table B-5. As shown, all design ratios are less than 1.0. Therefore, the structure is acceptable.

B-5 VELOCITY LIMITER TO ABSORBER SECTION WELD (FIG. 3-2)

The weld connecting the absorber section to the velocity limiter is analyzed using the combined loading of the scram loads and axial loads due to the maximum allowable internal pressure of the absorber tubes.

Since both the scram loads and the load due to the internal pressure of the absorber tubes is considered, a combined weld area of the absorber section to handle weld, and the end plug to

absorber tube weld is calculated. Since the end plug weld is in shear for this loading, the weld area is multiplied by $(1/\sqrt{3})$ to calculate an effective normal weld area. This is added to the minimum absorber section to velocity limiter weld area, which is determined using CAD software:

$$A_{\text{normal}} = (\# \text{ of tubes}) \{ (1/\sqrt{3})(\pi)OD_{\text{plug,min}}(\text{weld penetration}) + (\text{absorber section to handle/VL area per tube}) \}.$$

The weld area per tube is then multiplied by the number of tubes. The weld area calculation is summarized in Table B-6.

Once the effective normal weld area is known, the combined maximum stresses due to scram and internal pressure are calculated as described in Table B-7. As shown, all design ratios are less than 1.0. Therefore, the weld is acceptable.

B-6 ABSORBER SECTION (FIG. 3-2)

The minimum cross-sectional area of the absorber section is calculated in Table B-8. Actual and allowable stresses are shown in Table B-9. As shown, all design ratios are less than 1.0. Therefore, the structure is acceptable.

B-7 ABSORBER SECTION TO HANDLE WELD (FIG. 3-2)

The weld connecting the absorber section to the handle is analyzed using the combined loading of the scram loads and axial loads due to the maximum allowable internal pressure of the absorber tubes.

Since both the scram loads and the load due to the internal pressure of the absorber tubes is considered, a combined weld area of the absorber section to handle weld, and the end plug to absorber tube weld is calculated. Since the end plug weld is in shear for this loading, the weld area is multiplied by $(1/\sqrt{3})$ to calculate an effective normal weld area. This is added to the minimum absorber section to handle weld area, which is determined using CAD software:

$$A_{\text{normal}} = (\# \text{ of tubes}) \{ (1/\sqrt{3})(\pi)OD_{\text{plug,min}}(\text{weld penetration}) + (\text{absorber section to handle/VL area per tube}) \}.$$

The weld area per tube is then multiplied by the number of tubes. The weld area calculation is summarized in Table B-10. Once the effective normal weld area is known, the combined maximum stresses due to scram and internal pressure are calculated as described in Table B-11. As shown, all design ratios are less than 1.0. Therefore, the structure is acceptable.

B-8 HANDLE MINIMUM CROSS-SECTIONAL AREA (FIG. 3-2)

The minimum cross-sectional areas of the handle, and actual and allowable stresses, are shown in the Table B-12. As shown, all design ratios are less than 1.0. Therefore, the structure is acceptable.

Table B-1. Socket Axial Stress Calculations

| Description | Source | D Lattice | | C Lattice | | S Lattice | |
|--------------------------------------|-------------------|-----------|--------|-----------|--------|-----------|--------|
| | | 70 °F | 550 °F | 70 °F | 550 °F | 70 °F | 550 °F |
| Max Failed Buffer Scram Load (kips) | Table 3-4 | [[| | | | | |
| Max Failed Buffer Scram Stress (ksi) | [[]] | | | | | | |
| Allowable Stress (ksi) | Table 3-2 (XM-19) | | | | | | |
| Design Ratio | =stress/allow | | | | | |]] |

Table B-2. Socket to Transition Piece Weld Geometry

| Description | Source | All Lattice Types |
|---|--|-------------------|
| Minimum Socket/Transition Piece OD (in) | Drawings | [[|
| Maximum Socket/Transition Piece ID (in) | Drawings | |
| Min Cross-sectional Area (in ²) | =PI/4(OD ² -ID ²) |]] |

Table B-3. Socket to Transition Piece Weld Stress Calculations

| Description | Source | D Lattice | | C Lattice | | S Lattice | |
|--------------------------------------|---------------------|-----------|--------|-----------|--------|-----------|--------|
| | | 70 °F | 550 °F | 70 °F | 550 °F | 70 °F | 550 °F |
| Max Failed Buffer Scram Load (kips) | Table 3-4 | [[| | | | | |
| Max Failed Buffer Scram Stress (ksi) | =P/A | | | | | | |
| Allowable Stress (ksi) | Table 3-2 (ER 308L) | | | | | | |
| Weld Quality Factor | Table 3-3 | | | | | | |
| Allowable Weld Stress (ksi) | =S _m *q | | | | | | |
| Design Ratio | =stress/allow | | | | | |]] |

Table B-4. Transition Piece to Fin Weld Stress Calculations

| Description | Source | D Lattice | | C Lattice | | S Lattice | |
|--------------------------------------|---------------------|-----------|--------|-----------|--------|-----------|--------|
| | | 70 °F | 550 °F | 70 °F | 550 °F | 70 °F | 550 °F |
| Max Failed Buffer Scram Load (kips) | Table 3-4 | [[| | | | | |
| Max Failed Buffer Scram Stress (ksi) | =P/A | | | | | | |
| Allowable Stress (ksi) | Table 3-2 (ER 308L) | | | | | | |
| Weld Quality Factor | Table 3-3 | | | | | | |
| Allowable Weld Stress (ksi) | =S _m *q | | | | | | |
| Design Ratio | =stress/Allow | | | | | |]] |

Table B-5. Minimum Fin Area Stress Calculations

| Description | Source | D Lattice | | C Lattice | | S Lattice | |
|--------------------------------------|-----------------------|-----------|--------|-----------|--------|-----------|--------|
| | | 70 °F | 550 °F | 70 °F | 550 °F | 70 °F | 550 °F |
| Max Failed Buffer Scram Load (kips) | Table 3-4 | [[| | | | | |
| Max Failed Buffer Scram Stress (ksi) | =P/A | | | | | | |
| Allowable Stress (ksi) | Table 3-2 (316 plate) | | | | | | |
| Design Ratio | =stress/allow | | | | | |]] |

Table B-6. Velocity Limiter to Absorber Section Weld Geometry

| Description | Reference | D Lattice | C Lattice | S Lattice |
|--|-------------------------|-----------|-----------|-----------|
| Absorber Tube to VL Weld Area (in ²) | CAD analysis | [[| | |
| Min End Plug OD (in) | Drawing | | | |
| Max End Plug OD (in) | Drawing | | | |
| Min End Plug Weld Penetration (in) | Assembly Drawing | | | |
| Total Normal Weld Area Per Tube | Equation in Section B-5 | | | |
| Number of Absorber Tubes per Assembly | Assembly Drawing | | | |
| Total Weld Area (in ²) | =(# tubes)(area) | | |]] |

[[

]]

Table B-7. Velocity Limiter to Absorber Section Weld Stress Calculations

| Description | Source | D Lattice | | C Lattice | | S Lattice | |
|--|---------------------------------------|-----------|--------|-----------|--------|-----------|--------|
| | | 70 °F | 550 °F | 70 °F | 550 °F | 70 °F | 550 °F |
| Max Failed Buffer Scram Load (kips) | Table 3-4 | [[| | | | | |
| Maximum Allowable Internal Pressure (ksi) | Finite Element Analysis | | | | | | |
| End Plug Pressure Area (in ²) | = $\pi/4 \cdot (OD_{plug})^2$ | | | | | | |
| Number of Pressurized Tubes | Assembly Drawing | | | | | | |
| Total Axial Load (kips) | =Scram Load + (press)(area) (# tubes) | | | | | | |
| Total Weld Area (in ²) | Table B-6 | | | | | | |
| Max Failed Buffer Scram + Internal Pressure Stress (ksi) | = P_{tot}/A | | | | | | |
| Allowable Stress (ksi) | Table 3-2 (304S Tubes) | | | | | | |
| Weld Quality Factor | Table 3-3 | | | | | | |
| Allowable Weld Stress (ksi) | = $S_m \cdot q$ | | | | | | |
| Design Ratio | =Stress/Allow | | | | | |]] |

Table B-8. Absorber Section Geometry Calculation

| Description | Source | D Lattice | C Lattice | S Lattice |
|--|--------------------------------------|-----------|-----------|-----------|
| Min Absorber Tube Area (in ²) | CAD Analysis | [[| | |
| Min Tie Rod Area (in ²) | CAD Analysis | | | |
| Number of Absorber Tubes | Assembly Drawing | | | |
| Total Minimum Absorber Section Cross-sectional Area (in ²) | =(# tubes)(tube area) + tie rod area | | |]] |

Table B-9. Absorber Section Stress Calculation

| Description | Source | D Lattice | | C Lattice | | S Lattice | |
|--------------------------------------|------------------------|-----------|--------|-----------|--------|-----------|--------|
| | | 70 °F | 550 °F | 70 °F | 550 °F | 70 °F | 550 °F |
| Max Failed Buffer Scram Load (kips) | Table 3-4 | [[| | | | | |
| Max Failed Buffer Scram Stress (ksi) | =P/A | | | | | | |
| Allowable Stress (ksi) | Table 3-2 (304S Tubes) | | | | | | |
| Design Ratio | =stress/allow | | | | | |]] |

Table B-10. Absorber Section to Handle Weld Area Calculation

| Description | Source | D Lattice | C Lattice | S Lattice |
|--|-----------------------|-----------|-----------|-----------|
| Absorber Tube to Handle Weld Area (in ²) | From CAD analysis | [[| | |
| Min End Plug OD (in) | From drawing | | | |
| Max End Plug OD (in) | From drawing | | | |
| Min End Plug Weld Penetration (in) | From assembly drawing | | | |
| Total Normal Weld Area Per Tube (in ²) | Equation above | | | |
| Number of Absorber Tubes per Assembly | From assembly drawing | | | |
| Total Weld Area (in ²) | =(# tubes)(area) | | |]] |

[[

]]

Table B-11. Absorber Section to Handle Weld Stress Calculations

| Description | Source | D Lattice | | C Lattice | | S Lattice | |
|--|---------------------------------------|-----------|--------|-----------|--------|-----------|--------|
| | | 70 °F | 550 °F | 70 °F | 550 °F | 70 °F | 550 °F |
| Max Failed Buffer Scram Load (kips) | Table 3-4 | [[| | | | | |
| Maximum Allowable Internal Pressure (ksi) | Finite Element Analysis | | | | | | |
| End Plug Pressure Area (in ²) | = $\pi/4*(OD_{plug})^2$ | | | | | | |
| Number of Pressurized Tubes | From assembly drawing | | | | | | |
| Total Axial Load (kips) | =Scram Load + (press)(area) (# tubes) | | | | | | |
| Total Weld Area (in ²) | Table B-10 | | | | | | |
| Max Failed Buffer Scram + Internal Pressure Stress (ksi) | = P_{tot}/A | | | | | | |
| Allowable Stress (ksi) | Table 3-2 (304S Tubes) | | | | | | |
| Weld Quality Factor | Table 3-3 | | | | | | |
| Allowable Weld Stress (ksi) | = $S_m * q$ | | | | | | |
| Design Ratio | =Stress/Allow | | | | | |]] |

Table B-12. Handle Scram Stress Calculations

| Description | Reference | D Lattice | | C Lattice | | S Lattice | |
|--|--------------------------|-----------|--------|-----------|--------|-----------|--------|
| | | 70 °F | 550 °F | 70 °F | 550 °F | 70 °F | 550 °F |
| Max Failed Buffer Scram Load (kips) | Table 3-4 | [[| | | | | |
| Handle Minimum Cross-Sectional Area (in ²) | Calculated from Drawings | | | | | | |
| Max Failed Buffer Scram Stress (ksi) | = P/A | | | | | | |
| Allowable Stress (ksi) | Table 3-2 (316 plate) | | | | | | |
| Design Ratio | =stress/allow | | | | | |]] |

Appendix C – GEH Response to NRC RAI
MFN 09-156

NRC Request

Provide a detailed description of this model and its supporting empirical database. Relate this model and predicted release fractions to the 3-sigma approach used in the previous Marathon LTR.

GEH Response

For the original Marathon design, GE used a constant, [[]] helium release fraction, which bounded all of the helium release data GE had gathered (Reference 1, Response 1a(iv)). This same statement is reflected in paragraph 3.4 of the Marathon SE (NEDE-31758P-A), when discussing high temperature data. Current design work uses [[

]]

For current design work, GEH uses a model for helium release fraction [[

]] As shown in Figure 1, and discussed in Section 3.6.3 of the LTR (NEDE-33284P Rev. 1), helium release data shows that the helium release fraction has a [[

]]

[[

]]

Figure 1: Helium Release Fraction Design Basis and Test Results

Figure 1 shows the design basis model for helium release fraction, for a compacted boron carbide powder at [[]] of theoretical density. In addition, the helium release fractions that are used for the Marathon and Marathon-5S designs, versus boron carbide temperatures, are shown on the graph and in Table 1. The Marathon-5S temperatures and helium release fractions are the same as those shown in Table 3-12 of the LTR.

| Application | Average B ₄ C Temperature at Peak Location (°F) | Helium Release Fraction (%) |
|----------------------------|--|-----------------------------|
| Marathon D/S | [[| |
| Marathon C | | |
| Marathon-5S D/S Nominal | | |
| Marathon-5S D/S Worst Case | | |
| Marathon-5S C Nominal | | |
| Marathon-5S C Worst Case | |]] |

Table 1: GEH Marathon Control Rod Design Basis Helium Release Fractions

NEDO-33284-A Revision 2
Non-Proprietary Information

GEH has conducted two tests to evaluate helium release fractions in BWR control rods. The coolant temperature and measured helium release fractions for these tests are shown in Table 2, and plotted against the design basis model in Figure 1. Note that the use of coolant temperature is conservative, as the temperature of the boron carbide will be higher than the coolant temperature due to the heat generation of the neutron capture.

In the first test, three test capsules were irradiated in a commercial BWR with a coolant temperature of 550 °F. In the second test, two test capsules were inserted in the instrument tubes of two fuel assemblies, and irradiated in a commercial BWR.

As shown in Table 2 and Figure 1, the measured helium released fractions are much smaller than the design basis model predicts. This indicates that there is significant conservatism in the design basis helium release fraction model.

| Test | Coolant Temperature (°F) | Measured Helium Release Fraction (%) |
|--------|--------------------------|--------------------------------------|
| Test 1 | 550 | [[|
| | 550 | |
| | 550 | |
| Test 2 | 750 | |
| | 750 |]] |

Table 2: GEH Helium Release Fraction Test Results

Ultimately, the purpose for defining helium release fractions is to predict the pressurization of the Marathon absorber tubes due to helium generation as the boron carbide is irradiated. This methodology, as described in Sections 3.6 and 4.6 of the LTR starts with a thermal analysis to determine the temperature of the boron carbide during operation (LTR Section 3.6.3). Then, the helium release fraction is determined as a function of temperature using the design basis helium release fraction model shown in Figure 1 (LTR Section 3.6.3). Using the helium release fraction and absorber column dimensional data, a computer simulation is run to correlate pressure within the absorber tube to the average depletion of the tube (LTR Section 4.6). Based on this correlation, along with the allowable pressure limit of the tube, an average depletion limit for each absorber tube is established. This limit is then used to determine the mechanical depletion limit for the control rod (LTR Section 4.6).

There are several conservatisms in this methodology:

- Thermal analysis uses worst-case dimensions and maximum heat generation from the peak absorber tube axial location (LTR Section 3.6.3). By basing the thermal analysis, and therefore the helium release fraction, on this worst-case condition, it is assumed that all locations on the control rod wing have are at this worst-case condition. In reality, interior absorber tubes will be at a lower temperature and helium release, as will axial locations away from the top of the absorber section.
- The thermal analysis uses peak beginning-of-life heat generation rates, combined with maximum end-of-life crud build-up (LTR Section 3.6.3).
- The pressurization analysis correlating absorber tube internal pressure to average B-10 depletion considers worst-case capsule and absorber tube dimensions, maximum boron carbide swelling rates, and maximum absorber tube initial moisture content (LTR Section 4.6).
- The resulting 4-segment mechanical lifetime limits are greater than the $\frac{1}{4}$ segment nuclear limit. In reactor operation, the 4-segment average depletion will always be somewhat less than the peak $\frac{1}{4}$ -segment depletion. Therefore, the nuclear limit will always be limiting over the mechanical limit (LTR Section 4.6).

GEH completed a Post-Irradiation Examination (PIE) of an irradiated Marathon control rod in 2008. As part of this examination, pressure measurements were taken from two intact absorber tubes from one wing of the control rod.

The laboratory hot cell utilized is equipped with a gas collection system that is capable of measuring the pressure of the Marathon absorber tubes by puncturing the tube inside a sealed connection to gas sampling equipment. Using this apparatus, pressures were measured inside two absorber tubes of the Marathon control rod.

Table 3 shows the absorber tube pressures predicted by the pressurization methodology described above, which is at plant operating temperatures. These predicted pressures are scaled to room temperature pressures using the ideal gas law. The pressures measured by the test at room temperature are shown for comparison.

| Case | Predicted Pressure at Operating Temperature (psia) | Predicted Pressure at Room Temperature (psia) | Measured Pressure (psia) |
|-----------|--|---|--------------------------|
| Tube # 4 | [[| | |
| Tube # 11 | | |]] |

Table 3: Marathon Post-Irradiation Examination Absorber Tube Internal Pressures versus Predicted

As shown in Table 3, the actual measured pressures are less than the predicted pressures by a wide margin.

In summary, the methodology used by GEH to evaluate the pressurization of Marathon and Marathon-5S absorber tubes is significantly conservative. Results from irradiated test capsules, and from a destructive examination of an irradiated Marathon control rod suggest that the pressurization methodology, including the helium release fraction design basis, is significantly conservative. Therefore, it is concluded that the mechanical lifetime of the Marathon-5S control rod will exceed the nuclear lifetime.

References

Letter from GE to USNRC, "Response to Additional Questions on GE Marathon Control Rod Designs From November 26, 1990 Conference Call", February 20, 1991.